



Complex coacervation between proteins and polysaccharides for the encapsulation of active molecules

Jian Wang

► To cite this version:

Jian Wang. Complex coacervation between proteins and polysaccharides for the encapsulation of active molecules. Biochemistry, Molecular Biology. Université de Lyon, 2020. English. NNT : 2020LYSE1135 . tel-03840266

HAL Id: tel-03840266

<https://theses.hal.science/tel-03840266>

Submitted on 5 Nov 2022

HAL is a multi-disciplinary open access archive for the deposit and dissemination of scientific research documents, whether they are published or not. The documents may come from teaching and research institutions in France or abroad, or from public or private research centers.

L'archive ouverte pluridisciplinaire **HAL**, est destinée au dépôt et à la diffusion de documents scientifiques de niveau recherche, publiés ou non, émanant des établissements d'enseignement et de recherche français ou étrangers, des laboratoires publics ou privés.



N°d'ordre NNT : 2020LYSE1135

THESE de DOCTORAT DE L'UNIVERSITE DE LYON
opérée au sein de
l'Université Claude Bernard Lyon 1
Ecole Doctorale N° 205
(Ecole Doctorale Interdisciplinaire Sciences-Santé (EDISS))

Spécialité de doctorat : Biochimie
Discipline : Sciences des aliments

Soutenue publiquement le 10/09/2020, par :
Jian WANG

**Complex coacervation between proteins
and polysaccharides for the
encapsulation of active molecules**

Devant le jury composé de :

ANTON, Marc, Directeur de Recherche, INRA Angers-Nantes
SANCHEZ GONZALEZ, Laura, MCF, Université de Lorraine
BRIANCON, Stéphanie, Professeure, Université Lyon 1
CHIHIB, Nour-Eddine, Professeur, Université de Lille
GHARSALLAOUI, Adem, MCF, Université Lyon 1
DUMAS, Emilie, MCF, Université Lyon 1

Rapporteur
Rapporteuse
Examinatrice
Examineur
Directeur de thèse
Co-directrice de thèse

ABSTRACT

Complex coacervation between oppositely charged proteins and polysaccharides has drawn a lot of attention during last decades, which has been widely applied for encapsulating bioactive molecules in food, pharmaceutical and agricultural fields. The first four studies of this thesis focused on the complex coacervation between a classic pair of protein and polysaccharide, sodium caseinate (CAS) and low methoxyl pectin (LMP). The complexation behavior and the effect of pH, ionic strength and temperature were studied through isothermal titration calorimetry (ITC) in the first study. Two strategies for preparing emulsions, (i) stabilization by CAS/LMP complexes formed in advance and (ii) stabilization by layer-by-layer (LBL) method were compared in the second work. In addition, the effects of shearing and heating during spray-drying on CAS/LMP complexes were investigated. Finally, an essential oil compound (citral) was encapsulated in an emulsion stabilized by CAS/LMP complexes, dry microcapsules were obtained through spray-drying in the presence of maltodextrins and their antimicrobial activity was evaluated. Besides complex coacervation between CAS and LMP, lysozyme (LYS) was complexed with CAS as heteroprotein complex coacervates, and CAS-LMP mixtures as ternary complexes at pH 7 in the last two studies. Overall, model bioactive compounds including hydrophobic (citral) and hydrophilic (LYS) molecules were successfully encapsulated through complex coacervation.

Keywords: Complex coacervation, Sodium caseinate, LM Pectin, Encapsulation, Antimicrobials.

RÉSUMÉ

La coacervation complexe entre les protéines et les polysaccharides de charges opposées a attiré beaucoup d'attention au cours des dernières décennies, et a été largement appliquée pour l'encapsulation de molécules bioactives dans les domaines alimentaire, pharmaceutique et agricole. Les quatre premières études de cette thèse se sont concentrées sur la coacervation complexe entre deux biopolymères bien étudiés, le caséinate de sodium (CAS) et la pectine faiblement méthylée (LMP). Le déroulement de la complexation ainsi que l'effet du pH, de la force ionique et de la température ont été étudiés par titration calorimétrique isotherme (ITC). Deux stratégies pour préparer des émulsions, (i) la stabilisation par des complexes CAS/LMP formés à l'avance et (ii) la stabilisation par la méthode couche par couche (LBL), ont été ensuite comparées. De plus, les effets du cisaillement et du chauffage sur les propriétés des complexes pendant le séchage par atomisation ont été étudiés. Enfin, un composé d'huile essentielle (le citral) a été encapsulé dans des émulsions stabilisées par des complexes CAS/LMP, et des microcapsules ont été obtenues par séchage par atomisation de ces émulsions en présence de maltodextrines et leur activité antimicrobienne a été évaluée. Outre la coacervation complexe entre CAS et LMP, le lysozyme (LYS) a été complexé avec CAS sous forme de coacervats complexes hétéroprotéiques, ainsi que des mélanges CAS/LMP pour former des complexes ternaires à pH 7 dans les deux dernières études. Dans l'ensemble, des composés bioactifs modèles, hydrophobe (citral) et hydrophile (LYS), ont été encapsulés avec succès en utilisant la coacervation complexe.

Mots-clés : Coacervation complexe, Caséinate de sodium, Pectine faiblement méthylée, Encapsulation, Antimicrobiens.

PUBLICATIONS AND COMMUNICATIONS

Articles (Published)

Wang, J., Souihi, S., Amara, C. B., Dumas, E., & Gharsallaoui, A. (2019). Effect of drying and interfacial membrane composition on the antimicrobial activity of emulsified citral. *Food Chemistry*, 298, 125079.

Wang, J., Maoulida, F., Ben Amara, C., Ghnimi, S., Chihib, N. E., Dumas, E., & Gharsallaoui, A. (2019). Spray-drying of protein/polysaccharide complexes: dissociation of the effects of shearing and heating. *Food Chemistry*, 297, 124943.

Wang, J., Dumas, E., & Gharsallaoui, A. (2019). Low Methoxyl pectin / sodium caseinate complexing behavior studied by isothermal titration calorimetry. *Food Hydrocolloids*, 88, 163-169.

Wang, J., Souihi, S., Ben Amara, C., Dumas, E., & Gharsallaoui, A. (2018). Influence of low methoxyl pectin on the physicochemical properties of sodium caseinate-stabilized emulsions. *Journal of Food Process Engineering*, 41(8), e12906.

Articles (To be submitted)

Wang, J., Dumas, E., Ghnimi, S., & Gharsallaoui, A. Formation and properties of lysozyme-caseinate heteroprotein complexes.

Wang, J., Dumas, E., & Gharsallaoui, A. Formation and characterization of lysozyme-caseinate-pectin ternary complexes.

Oral communications

Wang, J., Maoulida, F., Ben Amara, C., Dumas, E., & Gharsallaoui, A. (2018). Spray-drying of protein/polysaccharide complexes: dissociation of the effects of shearing and dehydration. 10th International Conference on Water in Food, September 19-21, 2018, Prague (Czech).

Wang, J., Khelissa, S. O., Chihib, N. E., Dumas, E., & Gharsallaoui, A. (2018). Effect of drying and interfacial membrane composition on the antimicrobial activity of emulsified citral. 10th International Conference on Water in Food, September 19-21, 2018, Prague (Czech).

Wang, J., Dumas, E., & Gharsallaoui, A. (2018). Using complex coacervation of sodium caseinate for the development of antimicrobial materials: microcapsules and packaging films. 2^{ème} Conférence « Sécurité et Qualité des produits agroalimentaires – SQUAD² », April, 12-14, 2018, Tripoli (Liban).

Wang, J., Dumas, E., & Gharsallaoui, A. (2019). Formation of lysozyme-caseinate heteroprotein complexes for the encapsulation of lysozyme. 5th International Mediterranean Symposium on Medicinal and Aromatic Plants and 5th International Symposium on Pharmaceutical and Biomedical Sciences, April, 24-28, 2019, Cappadocia (Turkey).

Poster communications

Wang, J., Khelissa, S. O., Chihib, N. E., Dumas, E., & Gharsallaoui, A. (2018). Effect of drying and interfacial membrane composition on the antimicrobial activity of emulsified citral. 10th International Conference on Water in Food, September 19-21, 2018, Prague (Czech).

Wang, J., Dumas, E., & Gharsallaoui, A. (2019). Formation of lysozyme-caseinate heteroprotein complexes for the encapsulation of lysozyme by spray-drying. 33rd European Federation of Food Science and Technology (EFFoST), November 12-14, 2019, Rotterdam (The Netherlands).

ACKNOWLEDGEMENTS

I wish to take this opportunity to thank all those who have supported me in the completion of this study or helped me in any way during my living in France. First of all, I would like to express my deep and sincere gratitude to my supervisor, Dr. Adem Gharsallaoui, who not only provided me with fundamental advices and solid supports to conduct my research, but also supported me in all aspects of my life in France. I still remember that, four years ago, the first day I arrived in France, Adem helped me so much that I couldn't list. During these four years, without his support, the live in France will be difficult for me, especially for this special period of the epidemic. Of course, the success of this project would have been impossible without his encouragement, patience and experience, and it was really a pleasure to work with him.

I am so thankful to Dr. Emilie Dumas, not only for reviewing this thesis and giving me a lot of helpful advices, but also for her kindly guide during the microbiological researches. Besides, I would like to thank the rest of my thesis committee, namely, Dr. Marc Anton, Pr. Stéphanie Briançon, Pr. Nour-Eddine Chihib and Dr. Sanchez-Gonzalez Laura for accepting to evaluate my thesis. I would like also to express my sincere gratitude to all the professors and staff of the IUT Lyon 1 who accompanied me in these years, they are very kind to tolerate me not being able to speak French. I also acknowledge the help and kind cooperation of the other academic staff and especially Pr. Chihib and Dr. Khelissa from the University of Lille.

A special acknowledgement also goes to Mr. Wei Liao for his continued study throughout the whole project as well as the many interesting discussions. A sincere appreciation to my friends in my PhD period, Dr. Chedia Ben Amara, Dr. Olfa Loussaief, Dr. Yousra Abid, Dr. Juan Zamora Sillero and Mr. Jorge Macridachis Gonzalez, they helped me quickly integrate into the laboratory and provided technical assistance. Also, Mrs. Donia Zidi, Dr. Morad Mousazadeh and Mr. Faydi Maoulida, for the friendly discussions we had together. Many thanks to them for their kind help during the project. I would also like to send a heartfelt thanks to my other friends and colleagues for their support and help during my PhD study and also my life, especially Aimee, Arthur, Asma, Benjamin, Claudy, Elodie, Ghada, Ichrak, Illona, Justine, Keziban, Khaoula, Laura, Lynda, Mojtaba, Moslem, Paul, Rachel, Samuel, Tavani, Yoann and Yousra.

I gratefully acknowledge the financial support from CSC (China Scholarship Council).

Finally, for my dear family, without their support, I can't pursue my academic career, I hope I can continuously make them proud.

CONTENTS

INTRODUCTION.....	1
Organization of the thesis.....	3
CHAPTER 1 - LITERATURE REVIEW	4
1.1. Proteins and polysaccharides	4
1.1.1. Proteins	4
1.1.2. Polysaccharides	7
1.2. Complexation between proteins and polysaccharides.....	14
1.2.1. pH	17
1.2.2. Biopolymer ratio.....	18
1.2.3. Biopolymer concentration	19
1.2.4. Ionic strength	19
1.2.5. Temperature.....	19
1.2.6. Cross-linking	20
1.3. Encapsulated active molecules (core materials).....	20
1.3.1. Hydrophobic bioactive compounds	20
1.3.2. Hydrophilic bioactive compounds.....	23
1.4. Encapsulation forms and techniques	24
1.4.1. Emulsion based systems	25
1.4.2. Particle based systems	26
1.4.3. Gel based systems.....	27
1.4.4. Capsule based systems.....	27
1.5. Conclusion.....	28
References	29
Summary of Chapter 2	36
CHAPTER 2.....	37
Low Methoxyl pectin / sodium caseinate complexing behavior studied by isothermal titration calorimetry	37
2.1. Abstract	37
2.2. Introduction	37
2.3. Materials and methods	39
2.3.1. Materials	39
2.3.2. Solution preparation	39
2.3.3. Transmittance measurement	40
2.3.4. Zeta potential measurement.....	40
2.3.5. Isothermal titration calorimetry (ITC).....	40

2.3.6. Statistical analysis.....	41
2.4. Results and discussion.....	41
2.4.1. Phase diagrams of transmittance analysis	41
2.4.2. ζ -potential	43
2.4.3. Isothermal titration calorimetry results.....	44
2.5. Conclusion.....	48
References	50
Summary of Chapter 3	52
CHAPTER 3.....	53
Influence of Low Methoxyl pectin on the physicochemical properties of sodium caseinate-stabilized emulsions	53
3.1. Abstract	53
3.2. Introduction	53
3.3. Materials and methods	55
3.3.1. Materials	55
3.3.2. Preparation of complexes suspensions	55
3.3.3. Turbidity and UV-absorbance measurements	55
3.3.4. Protein surface hydrophobicity measurement	56
3.3.5. Emulsion preparation.....	56
3.3.6. Zeta potential measurement.....	57
3.3.7. Particle size distribution	57
3.3.8. Viscosity measurement.....	57
3.3.9. Emulsion stability measurement.....	57
3.3.10. Statistical analysis.....	58
3.4. Results and discussion.....	59
3.4.1. Turbidity of complexes suspensions.....	59
3.4.2. Zeta potential and dynamic viscosity of complexes.....	60
3.4.3. Effect of complexation on caseinate structure and surface hydrophobicity	61
3.4.4. Zeta potential and dynamic viscosity of caseinate/low methoxyl pectin-stabilized emulsions	62
3.4.5. Stability and particle size distribution of emulsions.....	65
3.5. Conclusion.....	69
References	70
Summary of Chapter 4	72
CHAPTER 4.....	73
Spray-drying of protein/polysaccharide complexes: Dissociation of the effects of shearing and heating	73

4.1. Abstract	73
4.2. Introduction	73
4.3. Materials and methods	75
4.3.1. Materials	75
4.3.2. Solution preparation	75
4.3.3. The atomization process	75
4.3.4. Heat treatment.....	76
4.3.5. Turbidity measurement.....	76
4.3.6. Particle size distribution	76
4.3.7. Zeta potential measurement.....	76
4.3.8. Measurement of surface hydrophobicity	77
4.3.9. Statistical analysis.....	77
4.4. Results and discussion.....	78
4.4.1. Effect of atomization on the properties of caseinate/pectin complexes	78
4.4.2. Effect of heat treatment on the properties of caseinate/pectin complexes	80
4.4.3. Combined effect of atomization and heat treatment on the properties of complexes	83
4.5. Conclusion.....	85
References	86
Summary of Chapter 5	88
CHAPTER 5.....	89
Effect of drying and interfacial membrane composition on the antimicrobial activity of emulsified citral.....	89
5.1. Abstract	89
5.2. Introduction	89
5.3. Materials and methods	91
5.3.1. Materials: chemicals and bacteria.....	91
5.3.2. Solution preparation	91
5.3.3. Emulsion preparation.....	92
5.3.4. Spray-drying process	92
5.3.5. ζ -potential measurement.....	92
5.3.6. Particle size distribution	93
5.3.7. Encapsulation Efficiency (EE)	93
5.3.8. Minimum inhibitory concentration (MIC)	93
5.3.9. Growth rate and lag time	94
5.3.10. Measurement of inhibition zone	94
5.3.11. Statistical analysis.....	94

5.4. Results and discussion.....	95
5.4.1. Physicochemical properties of emulsions.....	95
5.4.2. Properties of citral microcapsules.....	97
5.4.3. Antimicrobial activity assessments	98
5.4.4. Inhibition zone measurements	101
5.5. Conclusion.....	103
References	104
Summary of Chapter 6	107
CHAPTER 6.....	108
Formation and properties of lysozyme-caseinate heteroprotein complexes	108
6.1. Abstract	108
6.2. Introduction	108
6.3. Materials and methods	110
6.3.1. Materials	110
6.3.2. Preparation of stock solutions and heteroprotein complexes	110
6.3.3. Turbidity measurement.....	111
6.3.4. Zeta potential measurement.....	111
6.3.5. Particle size measurement	111
6.3.6. Isothermal titration calorimetry (ITC).....	111
6.3.7. Spray-drying and reconstitution of lysozyme/caseinate complexes.....	112
6.3.8. Lysozyme activity evaluation.....	112
6.3.9. Statistical analysis.....	113
6.4. Results and discussion.....	113
6.4.1. Properties of heteroprotein complexes in solution	113
6.4.2. Thermodynamics of CAS/LYS interactions.....	115
6.4.3. Lysozyme activity of CAS/LYS complexes.....	117
6.5. Conclusion.....	120
References	121
Summary of Chapter 7	123
CHAPTER 7.....	124
Formation and characterization of lysozyme-caseinate-pectin ternary complexes.....	124
7.1. Abstract	124
7.2. Introduction	124
7.3. Materials and methods	126
7.3.1. Materials	126
7.3.2. Ternary complexes preparation	127

7.3.3. Turbidity measurement.....	127
7.3.4. Zeta potential	127
7.3.5. Particle size distribution	127
7.3.6. Isothermal titration calorimetry (ITC).....	128
7.3.7. Lysozyme activity evaluation.....	128
7.3.8. Statistical analysis.....	129
7.4. Results and discussion.....	129
7.4.1. Turbidity of ternary complexes	129
7.4.2. Isothermal titration calorimetry (ITC).....	130
7.4.3. Zeta-potential of ternary complexes	131
7.4.4. Particle size of ternary complexes	132
7.4.5. Activity of ternary complexes	133
7.5. Conclusion.....	134
References	135
CHAPTER 8.....	137
GENERAL DISCUSSION, CONCLUSION AND PERSPECTIVES	137
8.1. General discussion and conclusion	137
8.2. Perspectives.....	140

INTRODUCTION

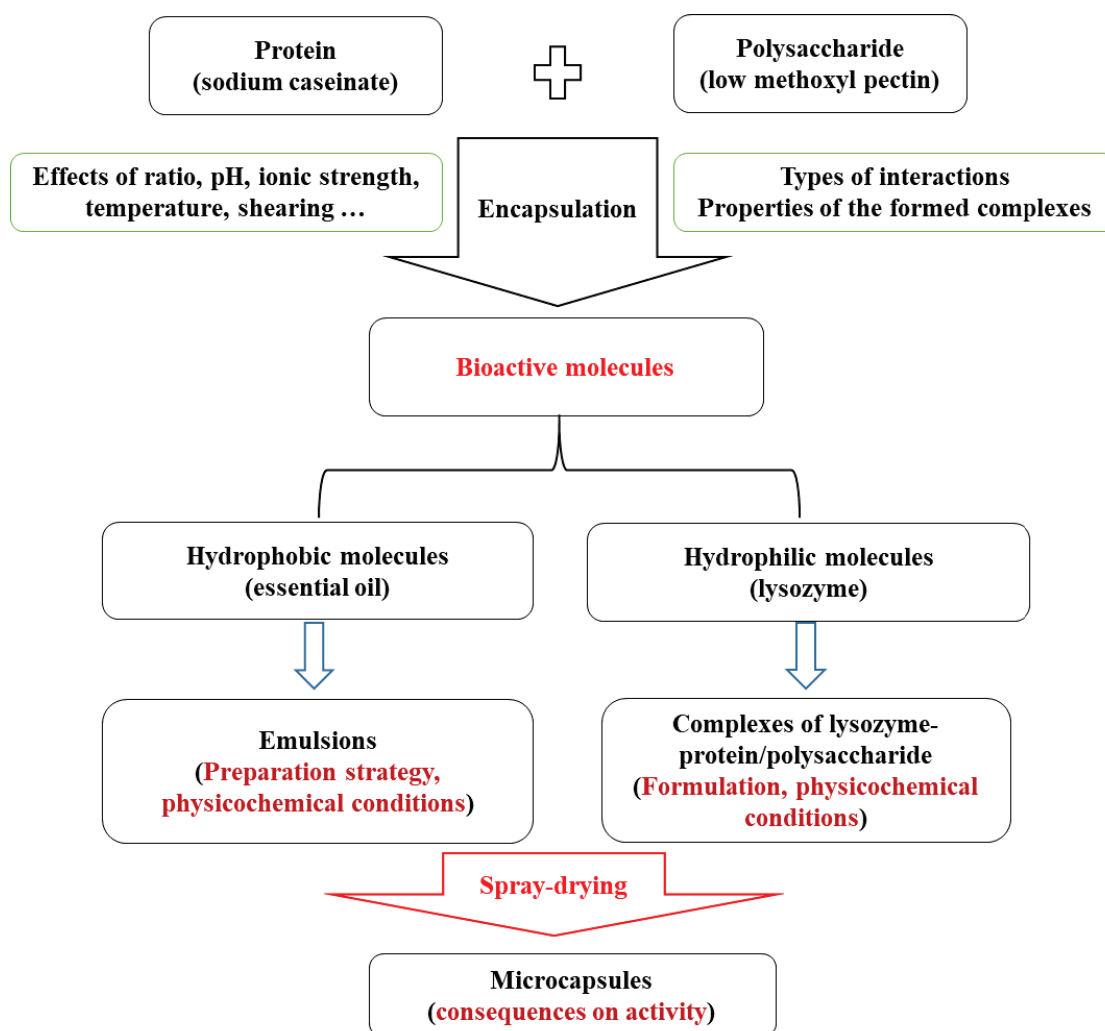
Proteins and polysaccharides are two natural major biopolymers, which are widely used in food industry due to their natural and source-rich features. Proteins and polysaccharides, as functional biopolymers, have various properties covering most of areas. In food industry, the surface activity and nutritional value of proteins are most valued. As well as proteins, polysaccharides mainly contribute to change the structure and textural properties of foods through their aggregation and gelation behavior. Mixtures of proteins and polysaccharides can be also applied in food industry to design multi-layered structures, form and stabilize food emulsions, form new food gels, encapsulate active molecules and, recover proteins from industrial by-products. Due to their huge industrial potential, the mixing behaviors of proteins and polysaccharides were massively studied during the last decades.

Basically, according to whether a protein can interact with a polysaccharide or not, the mixing process can be divided into complexation and non-complexation. The complexation between proteins and polysaccharides can form soluble complexes and insoluble complexes according to the solubility of the formed complexes. The non-complexation case can be due to co-solubility and thermodynamic incompatibility. The statuses described above can transform each other by changing pH, ionic strength and concentration. Complex coacervation is a physicochemical phenomenon caused by aggregation between two oppositely charged macromolecules. Since 1930, Bungenberg de Jong introduced the term “coacervation” for describing the liquid-liquid separate phase phenomenon (one colloid-rich phase in the bottom and one colloid-deficient phase in the top), the study about coacervation has never been stopped for these decades.

Encapsulation is a technique allowing to entrap active ingredients into liquid or solid matrices. The functions of encapsulation in food industry can be divided into two major parts: isolation and controlled release. Due to the properties of some materials such as vulnerability, incompatibility or sensitivity to external environment, the coating materials can be applied to isolate the core materials from external environment (air, oxygen, moisture, heat, light etc.) to reach purposes like protecting core material against losing functions by oxidation, evaporation, and masking unpleasant organoleptic properties. Release of the encapsulated molecules can be also controlled to optimize drug delivery, or prolong the shelf life of foods.

In this thesis, two biopolymers, sodium caseinate (protein) and low methoxyl pectin (polysaccharide), are used to encapsulate hydrophobic or hydrophilic active molecules. Firstly,

the interactions between sodium caseinate and low methoxyl pectin were explored in different conditions to study the effects of many parameters like biopolymer ratio, pH, ionic strength, temperature... After optimizing the complex coacervation process, the complexation behavior was applied for the encapsulation of hydrophobic and hydrophilic molecules. For the encapsulation of hydrophobic molecules, emulsions were prepared by different preparation strategies, and the consequences of the physicochemical properties were evaluated. Furthermore, an essential oil compound (citral) was used as a model for hydrophobic active molecules. For hydrophilic molecules, lysozyme was chosen to form heteroprotein coacervates (lysozyme, sodium caseinate), and ternary complexes (lysozyme, sodium caseinate, low methoxyl pectin). Finally, dry microcapsules were obtained through spray-drying, and the consequences of the process on the activity of encapsulated active molecules were evaluated. The following scheme gives the global strategy of this thesis:



Organization of the thesis

The aim of this thesis was to understand the nature of the interactions between proteins and polysaccharides in different conditions, and to apply the complexation between these two biopolymers to encapsulate bioactive molecules. **Chapter 1** is a literature review about the commonly used proteins, polysaccharides and their interactions, encapsulated molecules and encapsulation techniques. Chapters 2 to 7 are based on six articles that have been published or to be submitted to scientific journals, describing the main achievements obtained in this thesis. In details, **Chapter 2** describes the complexation behavior between sodium caseinate (CAS) and low methoxyl pectin (LMP) at different pHs, ionic strengths and temperatures, **Chapter 3** compares two different strategies for preparing emulsions by CAS and LMP, **Chapter 4** studies the effects of the two steps that constitute the spray-drying process (spraying and heating) on the properties of CAS/LMP complexes, **Chapter 5** presents the application of CAS/LMP complexes for the microencapsulation of citral and the evaluation of the antimicrobial activity of microcapsules, **Chapter 6** shows the potential applications of heteroprotein coacervation between CAS and lysozyme (LYS) for the encapsulation of lysozyme (LYS) by spray-drying, and **Chapter 7** investigates the interactions in the ternary complexes formed by LYS, CAS and LMP, and its consequences on LYS enzymatic activity.

Finally, **Chapter 8** reports a general discussion and states the conclusions and perspectives.

CHAPTER 1 - LITERATURE REVIEW

1.1. Proteins and polysaccharides

Proteins and polysaccharides are the two major biopolymers in nature, which are widely used in food industry due to their natural and source-rich features (Fig. 1.1). Proteins and polysaccharides, as functional biomaterials, have various properties covering most of areas. In food industry, the surface activity and nutritional value of proteins are most valued. As well as proteins, polysaccharides mainly contribute to change the structure and textural properties of foods mainly through their thickening and gelation behaviors. Mixtures of proteins and polysaccharides are proposed to modify and enhance their functional properties and applied in food industry such as micro- and nano-encapsulation processes, the design of multi-layered structures, the formation and stabilization of food emulsions, the formation of new food gels and the recovery of proteins from industrial by-products. Due to their huge industrial potential, the mixing behavior of proteins and polysaccharides were massively studied for the last decades.

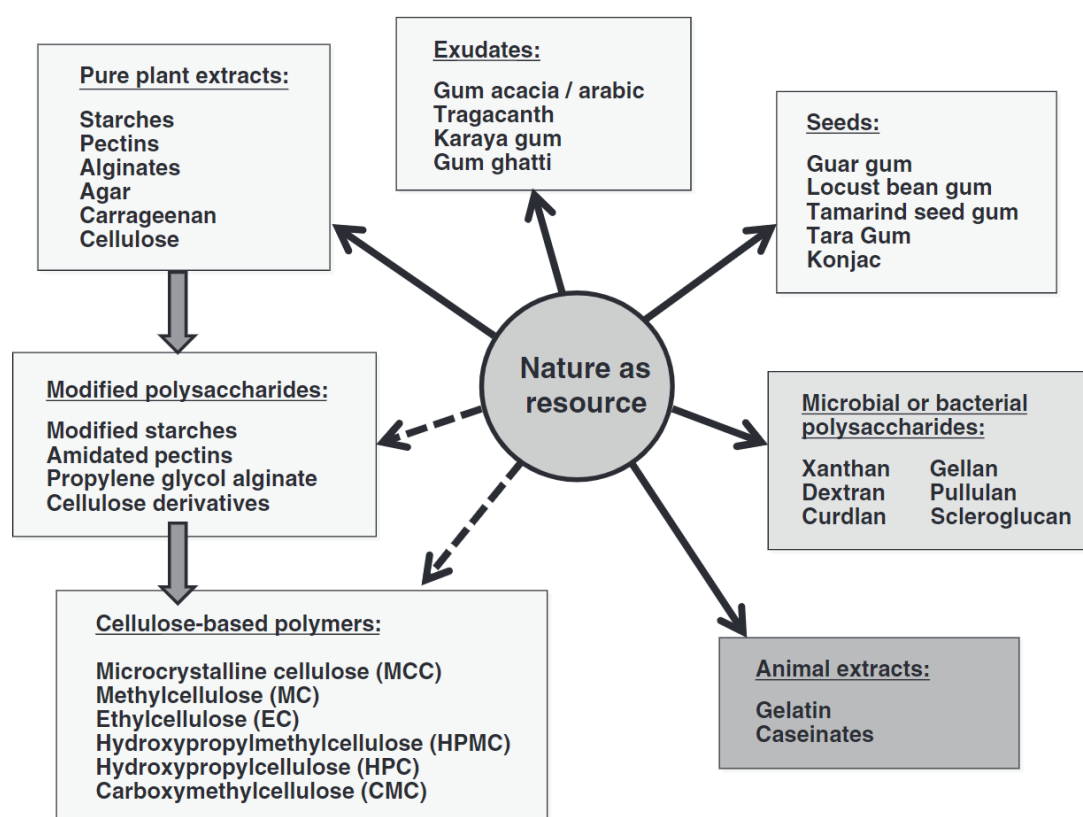


Figure 1.1. Nature sourced polysaccharides and proteins ([Wüstenberg, 2015](#)).

1.1.1. Proteins

Proteins are the most common biomacromolecules in nature, which consist of folded

linear polymers made from peptide bond linked amino acids. They play several vital functions in all biological processes, including the function as macronutrients that maintain the growth of body tissues. As listed in [Table 1.1.](#), the proteins frequently used in the food industry are mostly derived from milk, egg, legume, animal, etc. These proteins are the most frequently mentioned in the research studies concerning hydrogels and nano/microencapsulation due to their commercial availability, high nutritional value, and excellent functional properties. In addition, they are also used in the formation of complex coacervates with several polysaccharides under different conditions, which will be discussed in section 1.2. The most frequently studied proteins are listed in [Table 1.1.](#)

Table 1.1. Frequently proteins used in food industry.

Protein name		Structure	pI	Molecular weight (kDa)
Milk proteins	Sodium caseinate	α_{s1} -casein	4.95	23.6
		α_{s2} -casein	5.25	25.3
		β -casein	5.15	~24
		κ -casein	5.60	~19
	Whey proteins	α -lactalbumin	4.2-4.5	14.2
		β -lactoglobulin	4.8-5.1	18.3
		bovine serum albumin	4.7	66.5
		lactoferrin	7.9-8.7	~80
Legume proteins	Soy proteins	glycinin	4.9	180-210
		β -conglycinin	4.6	140-180
	Pea proteins	vicilin	5.7	150-250
		legumin	5.0-5.3	300-400
Egg proteins	lysozyme		11	14.3
	ovalbumin		4.5-4.7	42.7
	ovotransferrin		6	77.9
Gelatin	gelatin A		7-9.5	15-250
	gelatin B		4.7-5.5	90-300

1.1.1.1. Milk Proteins

Milk proteins consist of two major families of proteins, caseins and whey proteins. Caseins are composed of α_{s1} -, α_{s2} -, β -, and κ -caseins. Caseins usually exist in form of a sodium salt as sodium caseinate (made by adding sodium hydroxide to acid caseins). These four proteins have a strong tendency to associate with each other to form supramolecular aggregates ([Surh et al., 2006](#)). Due to the flexible random coil structure of caseinate, it has good

emulsifying properties and thermal stability, which makes casein as the most commonly used milk protein in food industry ([Glab & Boratynski, 2017](#)).

Whey proteins are globular proteins derived from milk during cheese-making and casein manufacture in dairy industry. It is a complex mixture of globular proteins such as α -lactalbumin (14.2 kDa), β -lactoglobulin (18.3 kDa, containing 160 amino acids), bovine serum albumin (66 kDa, longest single-chain protein), immunoglobulins (thermolabile mixture of proteins) and also several other protein/peptide components comprising lactoperoxidase, lysozyme, and lactoferrin. Complex coacervation between different polysaccharides and whey proteins are extensively studied for the encapsulation of bioactive compounds ([Ghasemi et al., 2018](#); [Sedaghat Doost et al., 2019](#); [Tavares & Zapata Noreña, 2019](#); [Zhang et al., 2019](#)), as well as whey protein's components like bovine serum albumin ([Maldonado et al., 2017](#)), β -lactoglobulin ([Shamsara et al., 2017](#)), lysozyme ([Diarrassouba et al., 2015](#)) and lactoferrin ([Liu et al., 2018](#)).

1.1.1.2. Legume Proteins

Legume proteins are the most typical representative of plant proteins. Due to the rich source and high protein content, legume proteins are considered as an ideal alternative to animal proteins to meet the growing demand in food industry. Besides being used as nutraceutical ingredients, legume proteins also possess other functionalities, like emulsifying and film forming properties. Due to the superior functionalities of legume proteins, they can play an important role for the encapsulation of bioactive materials. In addition, the emulsifying and encapsulating properties can be enhanced by combination with polysaccharides ([Sharif et al., 2018](#)). According to the sedimentation coefficients, legume proteins can be subdivided into 2S, 7S, 11S and even 15S fractions ([Tang, 2019](#)). The albumins in legume proteins are mainly present in the 2S form, while the 7S, 11S or 15S fractions generally correspond to the globulins. The ratio between globulins/albumins can vary based on species and the methods of production ([Karaca et al., 2011](#)), which can further result in differences in the structure and functionality of legume proteins ([Kimura et al., 2008](#)).

Pea proteins and soy proteins are two major legume proteins, which are intensively studied due to their widespread characteristics and good functionalities ([Burger & Zhang, 2019](#); [Tang, 2019](#)). Pea proteins consist of 65–80% globulins and 10–20% albumins. The globulins in pea proteins have two main fractions, legumin (pI 5–6) and vicilin (pI 4–6), which belong to the 11S and 7S seed storage protein classes, respectively ([Burger & Zhang, 2019](#)). Soy proteins mainly consist of albumins and 50–90% of globulins. Glycinin and β -conglycinin are two

dominant globulins in soy proteins, which are, in the literature, also named as 11S and 7S, respectively ([Tang, 2019](#)).

1.1.1.3. Egg Proteins

Egg proteins are important ingredients in the food industry due to their abundant nutritive values and various functional properties, distributed almost equally in egg white and egg yolk. Egg yolk proteins can be divided into two main fractions as granules and plasma after centrifugation. Compared to egg yolk proteins, egg white proteins have much better emulsifying and foaming abilities, which can be influenced by combination of egg yolk proteins or polysaccharides ([Li et al., 2019](#); [Niu et al., 2015](#)). Egg white proteins are composed of more than 70 proteins based on proteomics analysis ([Wang et al., 2012](#)), while the major ones are ovalbumin (~54%), ovotransferrin (~12%), ovomucoid (~11%), ovomucin (~3.5%) and lysozyme (~3.4%) ([Wang et al., 2019a](#)). Among these major egg white proteins, lysozyme has received much more attention due to its antimicrobial activity and high isoelectric point (pI~11), which make the encapsulation of lysozyme by combination with other anionic biopolymers scientifically interesting.

1.1.1.4. Gelatin

Gelatin, is a heat-denatured collagen extracted from bovine, porcine or fish skin. According to the gelatin extraction process, gelatin is commercially divided into two types: type A gelatin (pI 7–9) is extracted through the acid hydrolysis, while type B (pI 4.7–5.5) is extracted by alkaline hydrolysis ([Ahmad et al., 2017](#)). The lower isoelectric point of type B gelatin is due to its greater proportion of carboxylic groups caused by alkaline hydrolysis of asparagine and glutamine to aspartate and glutamate ([Young et al., 2005](#)). Besides these two types of commercial gelatin, gelatin can be easily modified to cationized gelatin by introducing amine residues to the carboxyl groups of gelatin or anionized gelatin by converting amino groups of gelatin into carboxyl groups ([Mahmoudi Saber, 2019](#); [Young et al., 2005](#)). Due to the good functional properties of gelatin in terms of biocompatibility, biodegradability, low antigenicity, film-forming capacity and easily modified ability, gelatin has been widely applied in food, pharmaceutical and cosmetic industries as carrier for the encapsulation of active molecules ([Etxabide et al., 2017](#); [Madkhali et al., 2019](#); [Young et al., 2005](#)).

1.1.2. Polysaccharides

Polysaccharides are carbohydrate molecules comprising long chains of monosaccharides linked by glycosidic bonds which are generally amorphous in nature.

Polysaccharides are largely found in various resources like plant, microbial, algal and animal ones. They have a large number of reactive functional groups, variable chemical composition, and different ranges of molecular weight, which define their diversity in property and in structure. Depending on their structure and monosaccharide units, they have different physical and chemical properties. Different derivatives of polysaccharides can be prepared by chemically modifying the various reactive groups present on their molecular chains. Among so many polysaccharides, pectin, alginate, cellulose derivatives, chitosan and polysaccharide gums (like carrageenan, tragacanth, gellan etc.) are widely studied in complex coacervation of polysaccharides and proteins.

1.1.2.1. Pectin

Pectin is a kind of anionic and linear polysaccharide which universally exists in the cell wall of all terrestrial plants. Commercially, pectin is mainly sourced from apple pomace, citrus peel and sugar beet. Chemically, pectin is mainly composed of α -1,4-glycosidic bonded D-galacturonic acid esterified with methyl or acetyl groups ([Fig. 1.2](#)). The degree of esterification (DE) is an important index that influences various properties of pectin and can be defined as the percentage of esterified carboxyl groups (mainly methyl esterified). Based on DE, there are two different classes of pectin *i.e.* high methoxyl pectin (HMP) (DE > 50%) and low methoxyl pectin (LMP) (DE < 50%). HMP can form gels under acidic conditions (pH 2.5-3.5) in the presence of high sugar concentrations, while LMP requires less sugar to form gels, and can form gels in a wider range of pH (from 2.6 to 7.0) ([Wang et al., 2019b](#)). Besides DE, the distribution of methyl and acetyl residues along the pectin chain and other modifications involve replacement of methyl groups with amide groups which can also affect the properties of pectin.

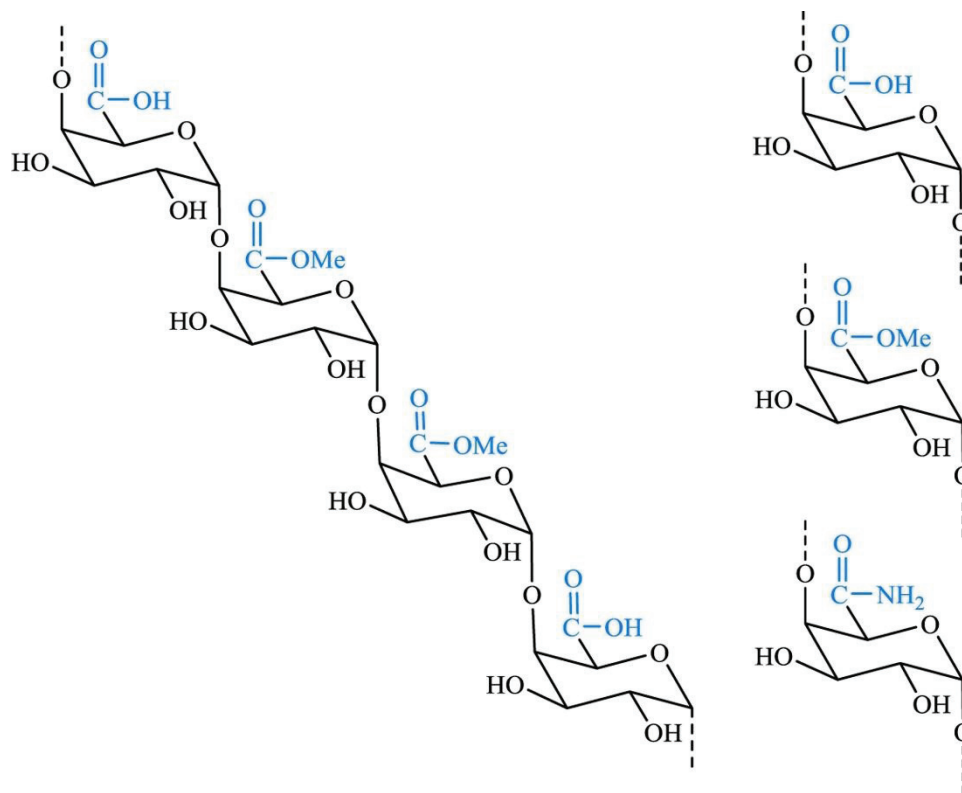


Figure 1.2. Chemical structure of pectin ([Mohamed et al., 2020](#)).

Pectin, as a typical food grade additive, is not digested in an upper gastrointestinal tract but completely absorbed in the colon ([Liu et al., 2003](#)), which make it suitable for the encapsulation and release control of bioactive compounds. In addition, DE and other indexes of pectin vary according to the source and extraction methods of pectin, which further influence pectin potential applications ([Marić et al., 2018](#)). Due to its widespread availability and diversity, pectin is extensively studied and used as wall material to encapsulate bioactive compounds with different methods ([Rehman et al., 2019](#)).

1.1.2.2. Alginate

Alginate is a linear and anionic polysaccharide derived from brown seaweed. This biopolymer is composed of alternating blocks of α -1,4-L-guluronic acid (G) and β -1,4-D-manuronic acid units (M) ([Fig. 1.3](#)). Only the G-blocks of alginate are believed to participate in dimeric association with multivalent cations (e.g., Ca^{2+}) to form hydrogels ([George & Abraham, 2006](#)). Besides hydrogels induced by multivalent cations, alginate can form acid gels at pH below the pK_a value of the uronic acid residues. These gels have been proposed to be stabilized by intermolecular hydrogen bonds ([Yang et al., 2011](#)). The composition (*i.e.*, M/G ratio), sequence, G-block length, and molecular weight are responsible for the heterogeneity of the physicochemical properties of alginate ([Lee & Mooney, 2012](#)).

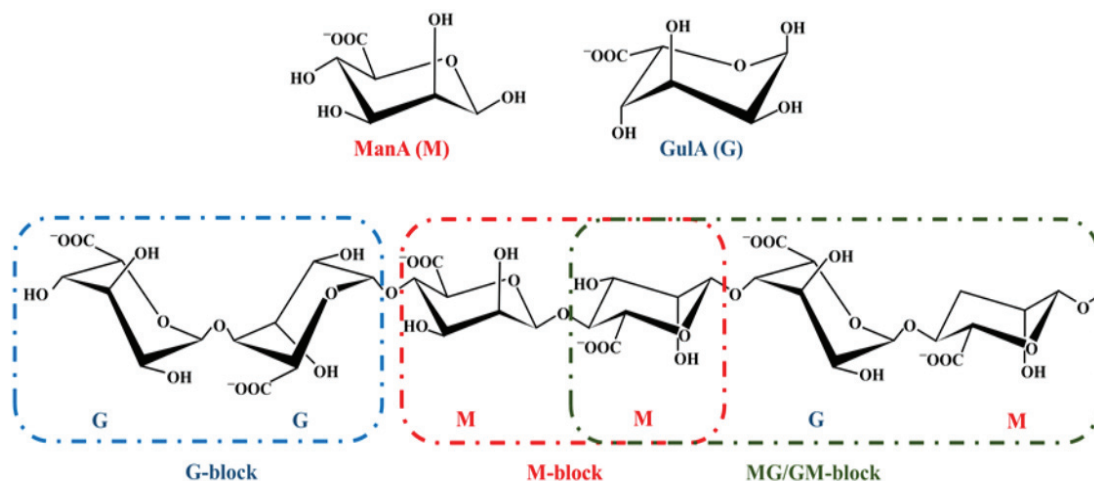


Figure 1.3. Chemical structure of alginate. The alginate monomers β -D-mannuronic acid (ManA; M) and α -L-guluronic acid (GulA; G), as well as an alginate chain illustrating linkage conformation and block composition ([Martau et al., 2019](#)).

According to the properties required for a given application, alginate is available from various sources. Although alginate can be produced by bacterial sources, it is commercially available from brown algae in form of salt, typically as sodium alginate. The biodegradability, low toxicity, chemical versatility of alginate and its special property to form hydrogel in aqueous media by addition of multivalent cations make this biopolymer more and more used in food industry ([Guo et al., 2019](#)).

1.1.2.3. Cellulose

Cellulose, a natural polymer, is considered as the most renewable and abundant polysaccharide. Biochemically, cellulose, an organic compound with the formula $(C_6H_{10}O_5)_n$, is a straight carbohydrate polymer chain consisting of β -1,4-glucosidic linkages ([Fig. 1.4](#)). It is biosynthesized by several living organisms such as sea animals, different plants, bacteria, and fungi. Whereas, pure cellulose showed bad mechanical properties and limited solubility in water and other common solvents. To improve the properties of cellulose, chemical, physical or biochemical modifications by reacting with hydroxy groups on its backbone (such as esterification, etherification, crosslinking, grafting etc.) were commonly used ([Pang et al., 2019](#)). Among many kinds of cellulose derivatives, the most extensively studied ones are cellulose acetate (CA), methyl cellulose (MC), ethyl cellulose (EC), hydroxyethyl cellulose (HEC), hydroxypropyl cellulose (HPC), and carboxymethyl cellulose (CMC). They are water soluble and widely used for binding, stabilizing, thickening, encapsulation, and film-forming ([Shishir et al., 2018](#)). Besides that, recently, cellulose nanocrystals (CNC) and cellulose nanofibrils (CNF) are yielded by chemical and mechanical treatments of cellulose fibrils ([Fig.](#)

1.4), which may readily bind drugs, proteins, and nanoparticles to develop vehicles, encompassing hydrogels, aerogels, films, coatings, capsules, and membranes, for the delivery of a broad range of bioactive compounds ([Sheikhi et al., 2019](#)).

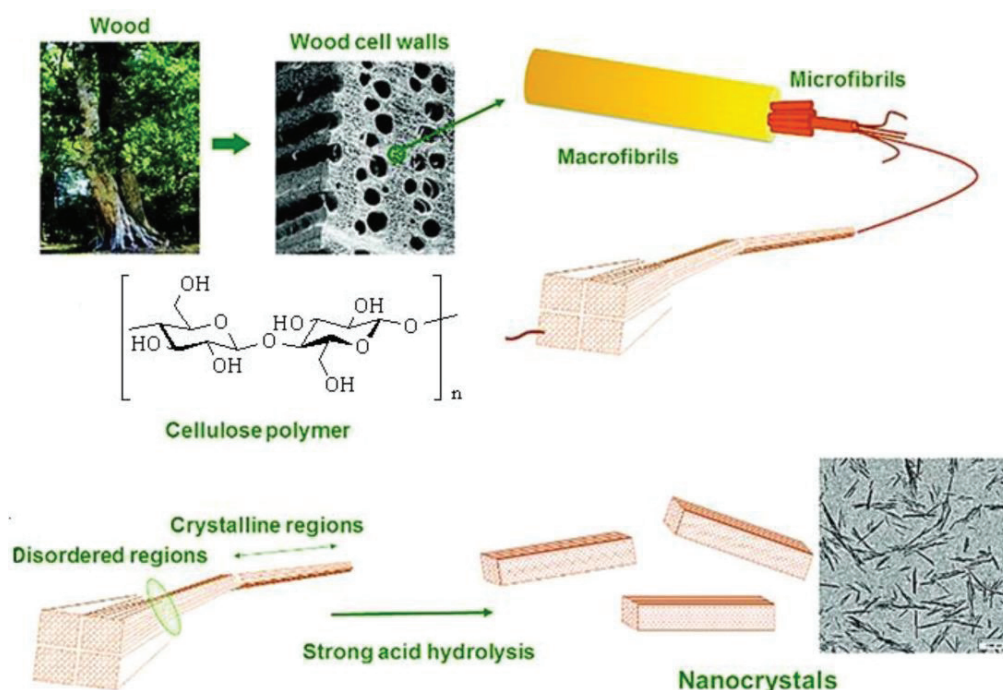


Figure 1.4. The source and chemical structure of cellulose polymer and production of cellulose nanocrystals ([Nasrollahzadeh et al., 2020](#)).

1.1.2.4. Chitosan

Chitosan, as one of few natural cationic polysaccharides, is the second most abundant natural biopolymer after cellulose. Chemically, chitosan is the deacetylated form of chitin, obtained by adding aqueous alkali to chitin at a temperature up to 160 °C to remove the N-acetyl groups of chitins as shown in [Fig. 1.5](#) ([Schmitz et al., 2019](#)). The resulting deacetylated chitin is composed of β -1,4-D-glucosamine and N-acetyl-D-glucosamine varying in degree of deacetylation. Unlike chitin, chitosan is slightly soluble in acidic medium, besides, it has non-toxic, biodegradable, biocompatible, film-forming, antioxidant and antibacterial properties ([Grande-Tovar et al., 2018](#)). Due to its special cationic nature and excellent functionality, chitosan has been intensively studied to cooperate with other anionic biopolymers for the encapsulation and delivery of bioactive compounds ([Yuan et al., 2017](#)).

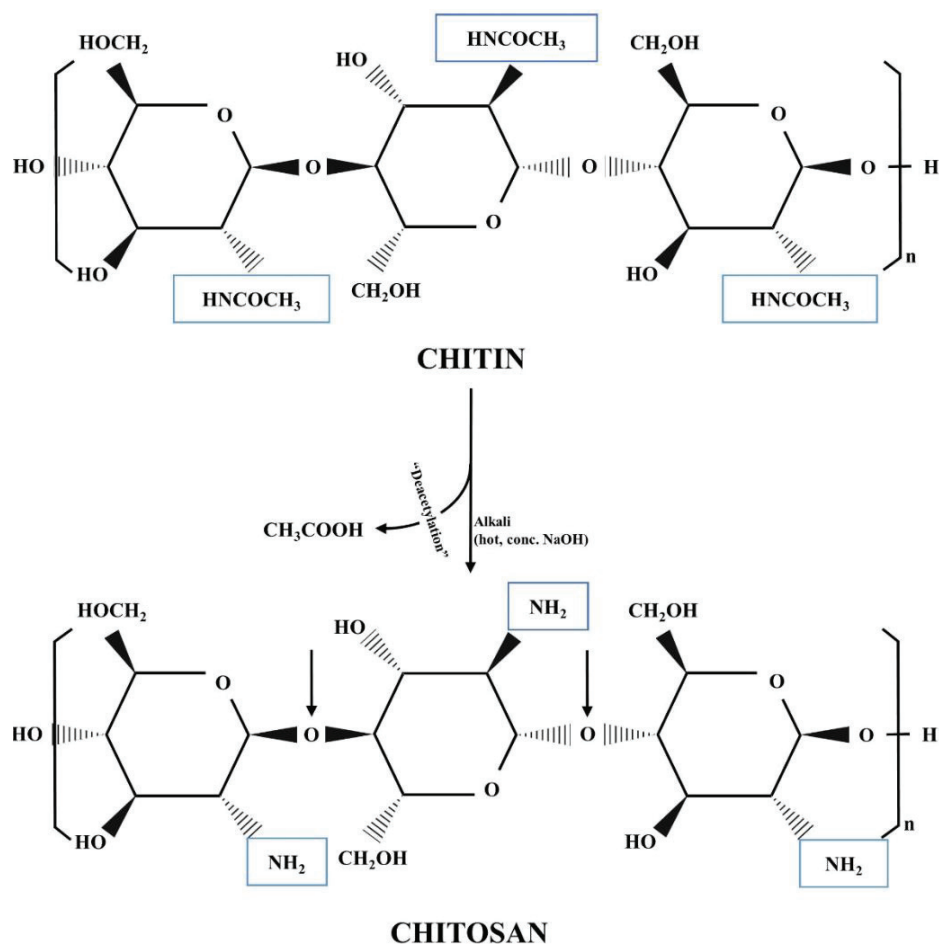


Figure 1.5. Chitosan production from chitin and chemical structure of chitin and chitosan ([Martau et al., 2019](#)).

1.1.2.5. Gums

Gum is referred to a kind of water-soluble polysaccharides which can interact with water to form viscous solutions, emulsions or gels ([Tahir et al., 2019](#)). Natural gum polysaccharides are classified into different groups relying upon their source namely bacterial polysaccharides (gellan gum, xanthan gum...), botanicals (guar gum, locust bean gum...), tree gums (Arabic gum, tragacanth...) and seaweed polysaccharides (carrageenan, agar...) ([Ahmad et al., 2019](#)). The most common gums used in encapsulation systems are commercially available gums (Arabic, guar, gellan, karaya, konjac, locust bean, tamarind, tragacanth, and xanthan) ([Fig. 1.6](#)) ([Tahir et al., 2019](#)). Their desirable properties, such as low cost, biocompatibility, biodegradability, availability and ease of use have led to their extremely large and broad applications in formation of excellent vehicles for active molecules, also controlling the rate of diffusion of bioactive compounds ([Ahmad et al., 2019](#)).

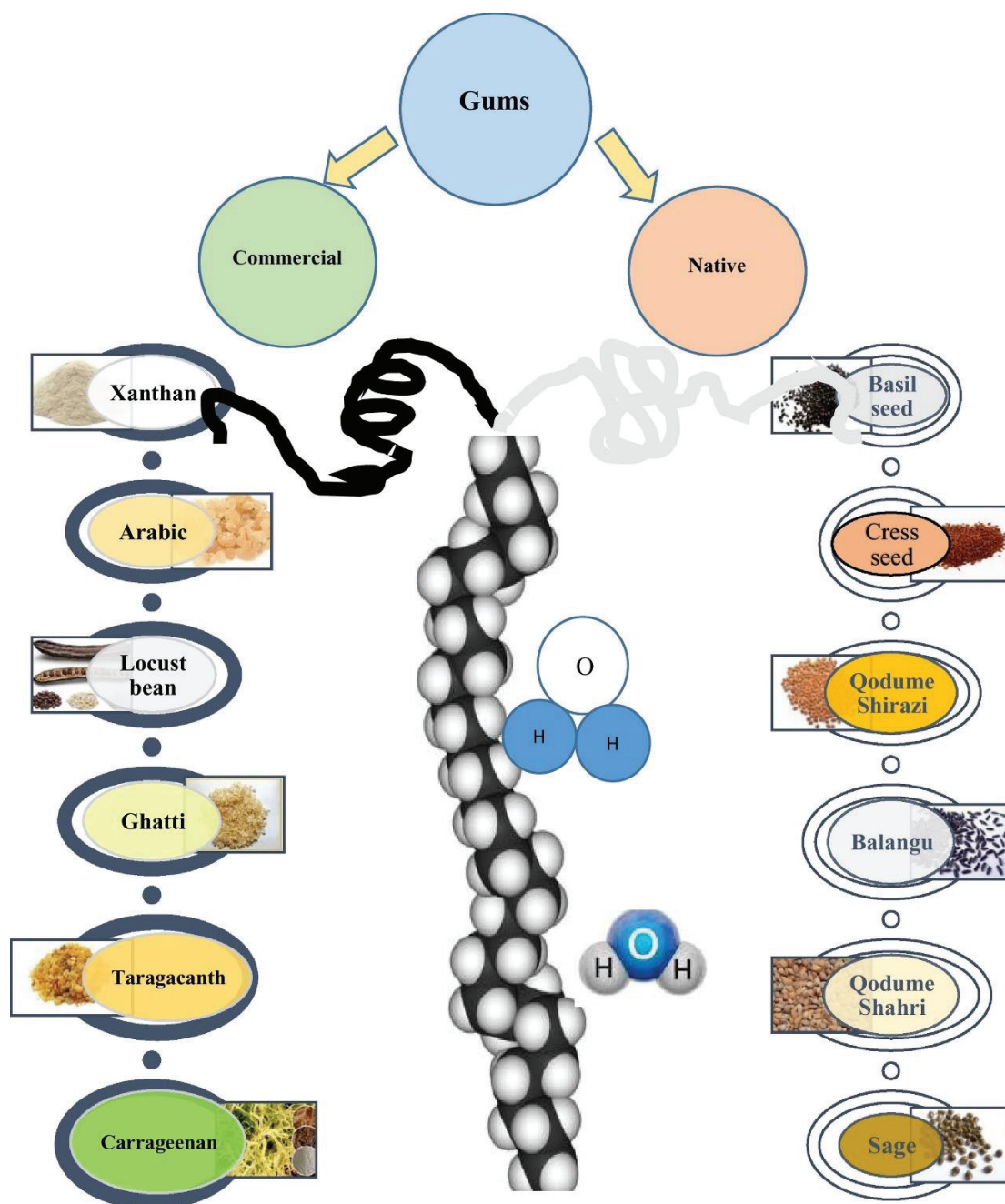


Figure 1.6. Classification of gums into commercial and native groups ([Taheri & Jafari, 2019](#)).

1.1.2.6. Dextrin

Dextrin, as a kind of starch hydrolysate, is a mixture of polysaccharides consist of α -1,4- and α -1,6-glycosidic bonded D-glucose. Dextrose equivalency (DE) is an index of the degree of hydrolysis which means the percent of reducing power compared to anhydrous D-glucose (dextrose). The DE value of D-glucose is 100, and for native starch, the DE value is 0. Maltodextrin is referred to dextrin having DE value of less than 20. Maltodextrin is widely used in food and pharmaceutical field as a carrier material for encapsulation of bioactive compounds due to its highly water solubility, low viscosity and safety. In addition, maltodextrin, as a carrier

material, has good compatibility with other biopolymers mentioned above for the encapsulation of bioactive compounds, which can further reduce the oxygen permeability of the wall matrix to protect encapsulated bioactive molecules and enhance the bioactive retention, especially in spray-drying process ([Karaca et al., 2013](#); [Rajabi et al., 2015](#); [Wang et al., 2019c](#)).

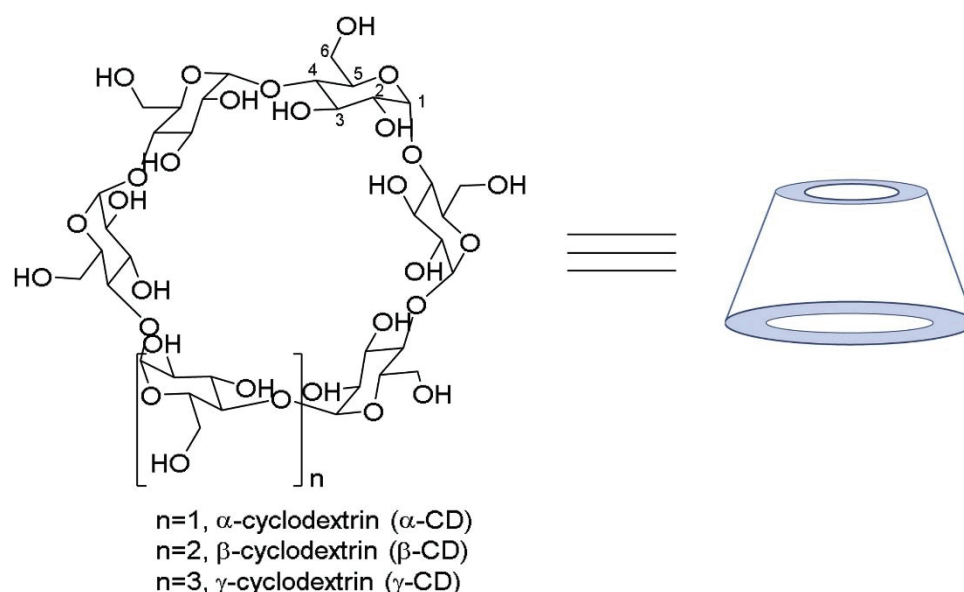


Figure 1.7. The structure and conformation of Cyclodextrins ([Gidwani & Vyas, 2015](#)).

Cyclodextrins are a kind of cyclic dextrins prepared by enzymatic hydrolysis of starch with the action of cyclodextrin glycosyltransferase ([Li et al., 2020](#)). Chemically, cyclodextrins are cyclic oligosaccharides containing 6, 7 and 8 α -1,4-linked D-glucopyranose units, which are called α -, β - and γ -cyclodextrins, respectively ([Fig. 1.7](#)). Structurally, cyclodextrins are truncated cone shape molecules, with a hydrophobic cavity inside and a hydrophilic external surface ([Gidwani & Vyas, 2015](#)). Therefore, inclusion complexes can be formed by cyclodextrins to load hydrophobic molecules. Combined with their relatively low cost, low immunogenicity and low toxicity, cyclodextrins are widely used in foods, cosmetics, pharmaceuticals and agrochemicals ([Garrido et al., 2018](#)). Due to the best aptitude for inclusion of drug molecules but the lowest aqueous solubility of β -cyclodextrin among α -, β - and γ -cyclodextrins, different derivatives of β -cyclodextrin are fabricated to improve its solubility such as methyl- and hydroxypropyl- and sulfobutyl ether- β -cyclodextrin ([Duchene & Bochot, 2016](#)).

1.2. Complexation between proteins and polysaccharides

Complexation between polysaccharides and proteins mostly initiates from the electrostatic interactions between different oppositely charged biomacromolecules. In most

cases, positive charges are from proteins and negative charges are carried by polysaccharides. However, chitosan, covalent chitosan derivatives and quaternary ammonium salts of cellulose ethers, which are cationic polysaccharides, can be combined with negatively-charged proteins. Mainly driven by electrostatic force, oppositely-charged proteins and polysaccharides can form soluble complexes, or the soluble complexes further aggregate to decrease the free energy of the system until their size and surface properties provide route to insolubilization, subsequently leading to coacervation. By changing the pH and ionic strength of solution, soluble and insoluble complexes can result in co-solubility of proteins and polysaccharides at low concentrations or thermodynamic incompatibility at high concentrations, as shown in [Fig. 1.8](#) ([Rodríguez Patino & Pilosof, 2011](#)).

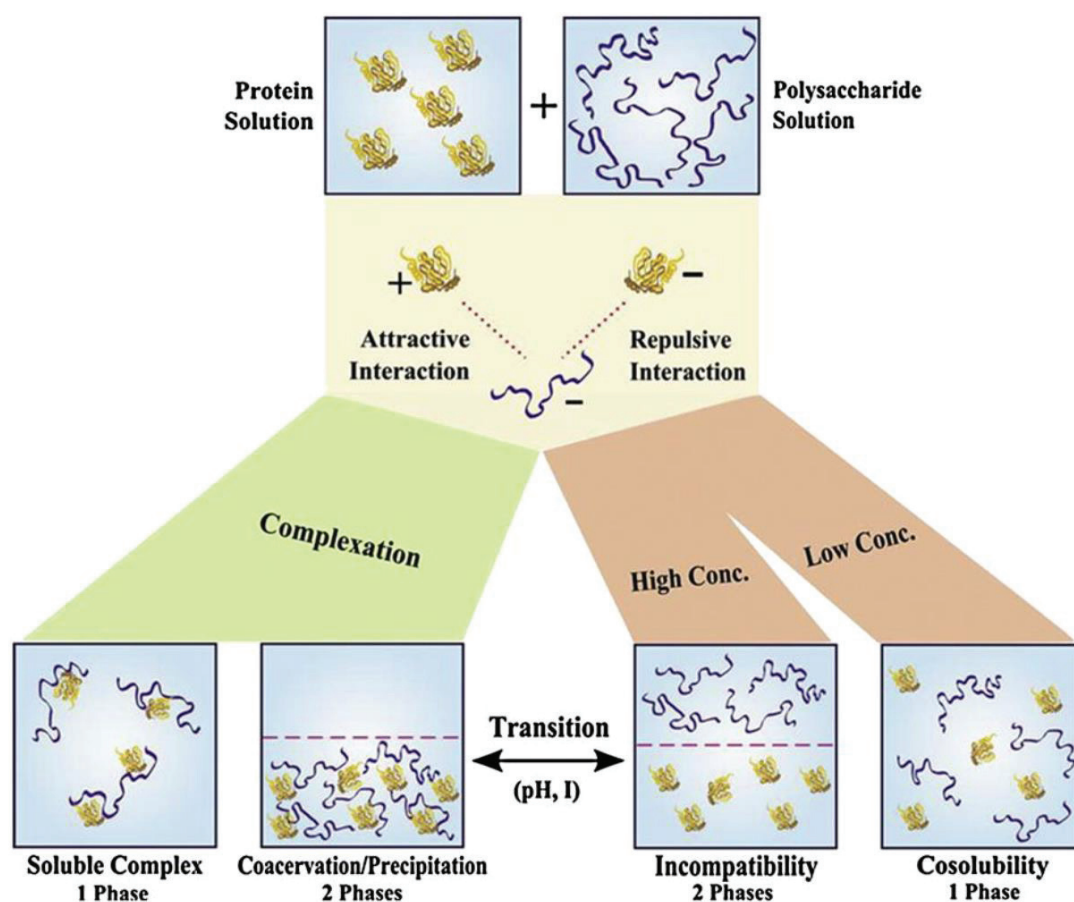


Figure 1.8. Different types of interactions (soluble complexes, insoluble complexes, co-solubility and thermodynamic incompatibility) between proteins and polysaccharides in aqueous solutions ([Matalanis et al., 2011](#)).

The complex coacervation between polysaccharides and proteins is influenced by many important factors such as protein to polysaccharide ratio, pH, ionic strength (salt concentration), total polymer concentration, and molecular weight of the polysaccharides and proteins ([Fig. 1.9](#)). Some other factors such as the flexibility, the charge density, the stirring, the pressure or

the temperature have also been shown to influence the coacervate formation. In this review, the factors of complexation behavior will be divided in two parts: intrinsic factors and extrinsic factors. The intrinsic factors are the characteristics of the proteins and the polysaccharides, such as isoelectric point of the protein, pK_a value of the polysaccharide, molecular weight and charge density of both protein and polysaccharide, chain length of polysaccharide, and presence and distribution of side branches in polysaccharide chain. The extrinsic factors include solvent properties (like pH, temperature, ionic strength, concentration) and mixing conditions (such as mixing ratio, shear processing). Depending on all these factors, proteins and polysaccharides can interact to form soluble or insoluble complexes (coacervation). To form good complexes, a proper pair of protein and polysaccharide should be chosen firstly. According to the main driving forces for complexation as electrostatic force, the chosen biopolymers should carry opposite charges under the mixing conditions.

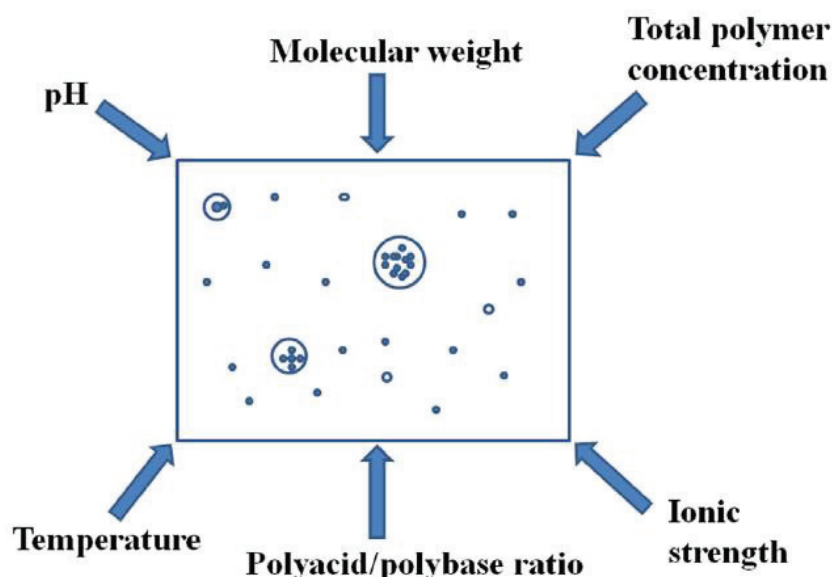


Figure 1.9. Physicochemical factors of complexation behavior ([Schmitt & Turgeon, 2011](#)).

Isothermal titration calorimeter (ITC) is a well-suited technique for studying the complexation between two biopolymers due to its calorimetric methodology for the direct measurement of the enthalpy change (ΔH), which reflects the heat generated or absorbed upon the interactions between two macromolecules. During the experiment, a titration curve can be generated based on the heat released or taken up in each titration. Through applying an adequate model to fit the titration curve, the stoichiometry of the interactions (N), the affinity constant (K) and the entropy change (ΔS) can be extracted. Furthermore, the Gibbs free energy (ΔG) can be calculated from the entropy (ΔS) and the enthalpy change (ΔH). The effect of experimental parameters on the complexation of proteins and polysaccharides can be evaluated by changing the studied factors through ITC tests as reported by [Kayitmazer \(2017\)](#). Therefore, a further

detailed review of the factors affecting the complexation between proteins and polysaccharides is given in the following sections.

1.2.1. pH

Among all the extrinsic factors of complexation between proteins and polysaccharides, pH can be the most important one, because pH has a direct impact on the degree of ionization of the functional groups of proteins (amino groups) and polysaccharides (carboxyl groups). With increasing the pH, the zeta potential value of both proteins and polysaccharides change from positive to negative due to the deprotonation of functional groups. For proteins, the electrical charge is depended on the presence of different amino acids in the protein molecules and their mode of ionization at different pH ranges. In detail, proteins possess positive charge when the solution pH is below their isoelectric point (pI) and become negatively charged as soon as the solution pH is improved above their pIs, which is caused by deprotonation of amino groups. For polysaccharides, due to the presence of acidic groups (mostly as carboxyl groups) on the polysaccharide chain, most of polysaccharides will be negatively-charged at wide pH ranges, and known as anionic polysaccharides. When an anionic polysaccharide solution is mixed with a protein solution and pH is reduced below pI of the protein, electrostatic attraction causes the complexation between protein and polysaccharide molecules.

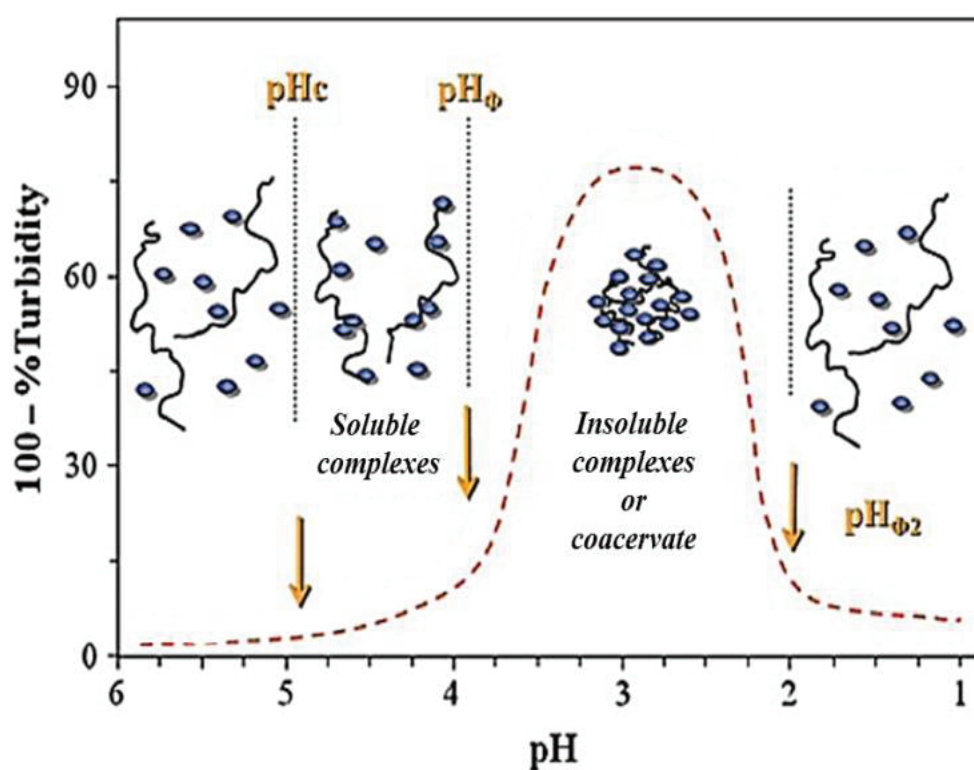


Figure 1.10. Schematic diagram of pH induced transitions of biopolymers' mixtures (proteins as circles; polysaccharides as coils) ([Weinbreck et al., 2003](#)).

Turbidity measurement is a commonly used method to monitor the structural evolution of protein/polysaccharide complexes. During the pH induced turbidity evolution, there are three critical pHs denoted the transition in the structure evolution, as follow: the first critical pH (pH_c) denoted the formation of soluble complexes from co-soluble mixture solution; the second critical pH ($pH_{\phi 1}$) denoted the formation of insoluble complexes from soluble complexes; the third critical pH ($pH_{\phi 2}$) denoted the dissociation of insoluble complexes. Furthermore, when the charge of insoluble complexes becomes neutral, the particle size will reach maximum at a pH, defined as pH_{opt} or pH_{max} . For example, the turbidity evolution of protein ($pI = 4.5$)/anionic polysaccharide ($pK_a = 2$) complexes as a function of solution pH is shown in [Fig. 1.10](#).

The ITC measurement is widely applied to corroborate the effect of pH on the complexation between proteins and polysaccharides. The ITC tests between pea protein isolate and pectin were performed at three pHs (pH 6, 5.5 and 3.5) ([Lan et al., 2020](#)). Quite low enthalpy change was shown at pH 5.5 and pH 6.0, due to weak electrostatic interactions between the two biopolymers. On the contrary, the exothermic titration profiles and regular peak decrease were presented at pH 3.5, because of the nonspecific electrostatic interactions between pectin chains and PPI molecules.

1.2.2. Biopolymer ratio

Besides pH, the surface charge of protein/polysaccharide complexes is depended on the biopolymer ratio between oppositely-charged proteins and polysaccharides, which significantly influences the amount and the intensity of formed complexes. Basically, at a fixed pH, the formation of insoluble complexes will reach maximum at charge ratio 1:1, which indicates that the complexes are neutrally charged. This optimum ratio will shift with the change of pH, due to the surface charge change of each biopolymer as a function of pH. Therefore, the optimum conditions for complex coacervation can be deduced by calculating the strength of electrostatic interactions (SEI) through the multiplication of ζ -potential values of individual biopolymer at each pH and each mixing ratio. Furthermore, the binding saturation ratios of protein/polysaccharide can be detected through ITC test, as no endothermic and/or exothermic signal detected during the titration process. [Ru et al. \(2012\)](#) studied the effect of protein/polysaccharide ratio on the coacervation between bovine serum albumin/pectin, and found that increasing BSA/pectin ratio from 1:1 to 10:1 favors the formation of BSA/pectin coacervates, as indicated by the increase in $pH_{\phi 1}$ and the decrease in $pH_{\phi 2}$, but further increase of BSA/pectin ratio to 20:1 has no effect on $pH_{\phi 1}$ value. Similar results were found in another research, higher pH_c and $pH_{\phi 1}$ were archived when pea protein isolate/pectin mixing ratio was

increased from 1:1 to 20:1 ([Lan et al., 2020](#)).

1.2.3. Biopolymer concentration

The effect of the total biopolymer concentration on the complexation varies depending on the used biopolymers. For the complex coacervation of whey proteins and gum Arabic, increasing the total biopolymer concentration favors the release of more counterions in solution, which screen the charges of the biopolymers, suppressing coacervation, and increasing the solubility of the coacervates ([Weinbreck et al., 2003](#)). The concentration change of biopolymers will also cause the transition of the form of protein/polysaccharide mixtures. As mentioned in [Fig. 1.8](#), when protein and polysaccharide carry the same charges, at low concentration, protein and polysaccharide are co-soluble in the solution; however, with increasing biopolymers' concentration over a critical value, protein and polysaccharide will separate into two phases, as one phase rich in protein, the other phase rich in polysaccharide, which is called thermodynamic incompatibility.

1.2.4. Ionic strength

The ionic strength, or salt concentration in the solution, has a direct impact on the formation of protein/polysaccharide complexes, because the main driving forces in the complexation between the two biopolymers are electrostatic interactions. In general, with the increase of ionic strength in the solution, there is a dissociating effect of coacervate complexes, until a critical salt concentration, the complexation will be suppressed. In details, lower pH_c , $\text{pH}_{\phi 1}$ and pH_{opt} can be observed with the increase of ionic strength ([Chai et al., 2014](#); [Ru et al., 2012](#); [Yuan et al., 2013](#)). This indicates that the addition of salt can screen out the electrostatic interactions. However, lower pH is favored to the strength of electrostatic interactions in most cases, due to the increase in positive charges of proteins by protonation, consequently the electrostatic barrier can be broken to form complexes. On the other hand, at low salt concentration, an enhancement effect of ionic strength on complexation is observed in some researches ([Li et al., 2017](#); [Xiong et al., 2017](#)), which is explained as the result of the promotional effect on the solubility of polymers (coiling of the molecule) ([Weinbreck et al., 2003](#); [Xiong et al., 2017](#)).

1.2.5. Temperature

Temperature is an important factor for the complexation between proteins and polysaccharides. Firstly, temperature has an impact on the structure of proteins, which involves the disruption and possible destruction of both the secondary and tertiary structures, depending

on the thermal stability of the studied protein ([Setiowati et al., 2020](#)). As a result, increasing temperature can cause the exposure of hydrophobic groups in protein, which further affects the hydrophobic interactions with other biopolymers. Secondly, besides hydrophobic interactions, temperature has also an effect on hydrogen bonding. As temperature increases, hydrogen bonding will break apart. Finally, due to the unfolding of biopolymers with change of temperature, more charged groups in the biopolymers can be exposed, especially for some biopolymers like pectin or gelatin which can form gel with change of temperature ([Jones & McClements, 2011](#)). This could also affect the electrostatic interactions between the two biopolymers.

1.2.6. Cross-linking

Besides non-covalent forces, the binding force between biopolymers can be further enhanced by covalent forces. The most common used methods are through Maillard reaction between proteins and polysaccharides ([Nooshkam & Varidi, 2020](#)), or addition of cross-linkers like glutaraldehyde and transglutaminase. For a Maillard reaction, the presence of lysine in proteins is crucial for reacting with polysaccharides under the heat treatment with a suitable low humidity for over several hours. The resulted Maillard protein–polysaccharide conjugates could possess higher oxidative and thermal stability compared to conventional emulsifiers ([Zha et al., 2019](#)). However, the Maillard reaction could also generate some harmful compounds ([Gentile, 2020](#)). Similarly, using chemical cross-linkers could improve the mechanical properties of protein-polysaccharide conjugates, but most of the reagents used for cross linking have undesirable effects and may exert toxic reactions ([Oryan et al., 2018](#)).

1.3. Encapsulated active molecules (core materials)

The core materials are referred to the encapsulated compounds covered by wall materials, as they are vulnerable, incompatible or harmful to external environment. According to the core material is hydrophobic or hydrophilic, the encapsulation process will be different. Therefore, a brief overview of a number of representative hydrophobic and hydrophilic bioactive compounds in the food industry is given in the next sections.

1.3.1. Hydrophobic bioactive compounds

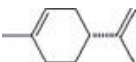
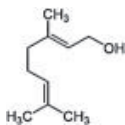
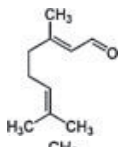
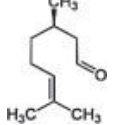
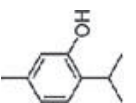
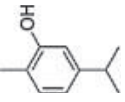
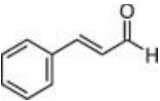
Typically, hydrophobic bioactive components are encapsulated by mixing them with surfactants like proteins, lipids in food applications in aqueous phase, to be converted into colloidal dispersions, as emulsions. The hydrophobic food bioactive compounds mainly include

essential oils, water-insoluble vitamins, carotenoids and phenolic compounds ([Rezaei et al., 2019](#)).

1.3.1.1. Essential oils

Essential oils are secondary metabolites of aromatic plants which are characterized by a strong odor. Due to the broad spectrum in biological activity (antibacterial, antifungal, antiviral and pest-repelling) of essential oils, they have drawn a lot of attention and the application of essential oils has been involved in many fields including agriculture, food and medicine.

Table 1.2. Frequently used components of essential oils ([El Asbahani et al., 2015](#)).

EO components	CAS number	Molecular structure	Chemical formula	Molecular weight	Boiling point °C	Refractive index (20 °C)	Relative density g/mL (20 °C)	Plant source
D-Limonene	5989-27-5		C ₁₀ H ₁₆	136.23	175.4	1.473	0.842	<i>Citrus limon</i>
Geraniol	106-24-1		C ₁₀ H ₁₈ O	154.25	229.5	1.474	0.879	<i>Pelargonium graveolens</i>
Citral	5392-40-5		C ₁₀ H ₁₆ O	152.23	229	1.488	0.888	<i>Aloysia citrodora</i>
Citronellal	5949-05-3		C ₁₀ H ₁₈ O	154.25	201–207	1.446	0.851	<i>Cymbopogon citratus</i>
Thymol	89-83-8		C ₁₀ H ₁₄ O	150.22	233	–	0.965	<i>Thymus vulgaris</i>
Carvacrol	499-75-2		C ₁₀ H ₁₄ O	150.22	237.7	1.522	0.977	<i>Thymus maroccanus</i>
Cinnamaldehyde	104-55-2		C ₉ H ₈ O	132.16	248–250	1.621	1.05	<i>Cinnamomum Zeylanicum</i>

The chemical composition of essential oils is complex, which has over 100 different terpenic compounds, mainly classified in two groups: hydrocarbon terpenes (isoprenes) and

terpenoids (isoprenoids) ([El Asbahani et al., 2015](#)). Hydrocarbon terpenes are the major constituents and consist of monoterpenes and sesquiterpenes. Terpenoids are different oxygenated derivatives of hydrocarbon terpenes such as phenols, aldehydes, lactones, esters, ketones, phenol ethers and alcohols ([Bakkali et al., 2008](#)). In general, essential oils are unstable due to their volatile and chemically active nature. Therefore, there is a growing interest in the encapsulation of essential oils to overcome the degradation and volatilization. As shown in [Table 1.2](#), the representative chemical compounds of essential oils are organized by [El Asbahani et al. \(2015\)](#) as follow.

1.3.1.2. Water-insoluble vitamins

Vitamins are bioactive compounds that are essential for maintaining the daily life of human being because they are unable to be obtained by self-synthesis in our bodies. Hence, sufficient quantities of vitamins have to be provided through outside supply. Among all kinds of vitamins, vitamins A, D, E and K are categorized as water-insoluble, which are partially sensitive to heat, light or oxidation. Therefore, during processing, transportation and storage, the efficiency of vitamins will be inevitably lost. Under these circumstances, encapsulation of these water-insoluble vitamins is a good solution to preserve their efficiency. For example, vitamin D3 was encapsulated in composite gels of whey protein isolate and lotus root amylopectin ([Liu et al., 2020](#)), in carboxymethyl chitosan/soy protein complex nanoparticles ([Teng et al., 2013](#)), in pickering emulsions stabilized by nanofibrillated mangosteen cellulose ([Winuprasith et al., 2018](#)); similar as vitamins A ([Fahami & Fathi, 2018](#)), E ([Ziani et al., 2012](#)) and K ([Wang et al., 2015](#)).

1.3.1.3. Carotenoids

Carotenoids are a kind of lipophilic pigments which have health benefits (antioxidant ([Stinco et al., 2016](#)), anti-cancer ([Saini et al., 2018](#)), anti-cardiac ([Zeng et al., 2019](#)), anti-inflammatory ([Kaulmann & Bohn, 2014](#))) but can't be synthesized by humans and other animals. There are over 1100 known carotenoids. Based on the presence or absence of oxygen in chemical structure, carotenoids can be categorized into two classes, carotenes (pure hydrocarbon) and xanthophylls (with oxygen). Like most bioactive compounds, carotenoids are sensitive to external stresses like oxygen, light and heat, which limited the application of carotenoids in food and pharmaceuticals. Encapsulation of carotenoids is widely studied ([Rehman et al., 2020](#)), typically for β -carotene and lutein, utilized to replace synthetic yellow colorants and nutraceutical ingredients in functional foods, supplements, and pharmaceutical products due to the strong antioxidant capacity ([Fu et al., 2019](#); [Steiner et al., 2018](#)).

1.3.1.4. Phenolic compounds

Phenolic compounds are secondary metabolites existing in all vascular plants that have at least one aromatic ring hydroxyl-substituted. The most typical phenolic compounds are flavonoids (including anthocyanins, flavonols, flavanones), tannins (or proanthocyanidins) and phenolic acids (like caffeic acid, chlorogenic acid, ferulic acid) ([Jia et al., 2016](#)). Phenolic compounds are widely used in the food industry due to their antibacterial and antioxidant properties. However, they are unstable in the presence of heat and light and mostly have a low bioavailability because of their poor solubility ([Faridi Esfanjani et al., 2018](#)). In addition, the bitter taste of many phenolic compounds (such as flavanones or flavanols) also limits their application in the food industry ([Munin & Edwards-Levy, 2011](#)). Therefore, encapsulation of phenolic compounds could be a good solution to overcome these problems, which has been widely reported in other reviews ([Faridi Esfanjani et al., 2016](#); [Jia et al., 2016](#)).

1.3.2. Hydrophilic bioactive compounds

Compared to hydrophobic bioactive compounds, hydrophilic ones are less challenging for encapsulation in various forms like tablets or capsules in pharmaceutical field ([Aditya et al., 2017](#)). Most of time, hydrophilic bioactive compounds can easily be mixed with wall material and dehydrated. However, for some cases, Water in Oil in Water (W/O/W) emulsions can also be prepared for improving the stability of emulsion, or Water in Oil (W/O) emulsions can also be prepared for the application in non-aqueous matrices.

1.3.2.1. Enzymes

Enzymes are a kind of proteins that are functional as biocatalysts in biotechnological processes spanning from food, cosmetic, and pharmaceutical field to environmental and biomass treatments. Most enzymes are either hydrophilic or amphiphilic. The stability of enzymes, like most proteins, is the consequence of a subtle balance of forces, which can be disrupted with changing the environment. This in turn, causes loss of the structure and bioactivity ([Valledeperas et al., 2019](#)). The encapsulation of enzymes can prevent or reduce such losses and significantly increase the stability, which benefits the commercial applications, including improving their storage and handling, increasing their activity, and controlling their release. For example, enzymes like pectinases incorporated into polymeric matrices, show greater activity even after repeated use in fruit juice system ([Ephrem et al., 2018](#)). Lysozyme, as a natural antimicrobial agent, has been frequently encapsulated to enhance its ability of controlling spoilage and pathogenic microorganisms ([Lopes et al., 2019](#); [Wu et al., 2019](#); [Xu et](#)

[al., 2019](#)).

1.3.2.2. Water-soluble vitamins

Water-soluble vitamins include vitamin B group and vitamin C. Most of water-soluble vitamins are chemically unstable, unstable within the gastrointestinal tract, and need targeted delivery. Consequently, encapsulation is required to improve their chemical stability in foods, to keep bioactivity within the gastrointestinal tract and to be targeted delivered. For example, alginate/chitosan nanoparticles were used for the encapsulation and controlled release of vitamin B₂ ([Azevedo et al., 2014](#)). What's more, the dynamic release of vitamin B₂ from calcium alginate and chitosan multilayered beads in simulated gastrointestinal conditions was studied ([Bajpai & Tankhiwale, 2006](#)). In addition, vitamin B₁₂ was investigated to be encapsulated in different carriers for targeted delivery ([Maiorova et al., 2019](#); [Matos et al., 2015](#)). Vitamin C was encapsulated in cellulose-based film, to generate an advanced and eco-friendly wound dressing device ([Voss et al., 2018](#)).

1.3.2.3. Water-soluble polyphenols

Polyphenols are a part of the phenolic compounds which are characterized by the presence of large multiples of phenol structural units. They exist as an integral part of both human and animal diets which possess a high spectrum of biological activities, including antioxidant, anti-inflammatory, antibacterial, and antiviral functions ([Fang & Bhandari, 2010](#)). Most of polyphenols are slightly soluble in water, and the solubility will be improved by transforming to the form of glycosides. However, the water-soluble polyphenols are still sensitive to oxidation, temperature, pH or light. Therefore, to prevent them from coming into contact with other substances that promote their degradation, a wide range of technologies have been developed to encapsulate polyphenols, including spray-drying, coacervation, emulsions, liposomes, nanoparticles, freeze-drying, co-crystallization and yeast encapsulation ([Fang & Bhandari, 2010](#); [Lu et al., 2016](#)).

1.4. Encapsulation forms and techniques

Complex coacervation has recently obtained special attention for encapsulation applications ([Eghbal & Choudhary, 2018](#)). In past few decades, the research work reported has focused on the synthesis and characterization of new biopolymer systems for encapsulating various active agents ([Đorđević et al., 2014](#)). Among these coacervates, proteins and polysaccharides are the most commonly paired in complex coacervation ([de Kruif et al., 2004](#)).

Therefore, different types of delivery systems based on protein–polysaccharide complex coacervation are designed and synthesized and a huge number of publications are reported in the field of encapsulation ([Devi et al., 2017](#)). According to the morphology of the encapsulated product, the final products can be classified in emulsions, gels, particles and capsules. Depending on the size of the encapsulated products, they can be further classified as micro scale (microemulsions, microcapsules, microparticles...), submicron scale and nano scale (nano-emulsions, nano-capsules, nanoparticles...). Typically, micro scale is in the range of 1 μm to 1000 μm ; whereas nano scale is typical less than 0.2 μm , submicron scale is between the two (0.2 to 1 μm). Particle with size larger than 1000 μm are called macroparticles.

1.4.1. Emulsion based systems

An emulsion is a mixture of two immiscible liquids, typically water and oil, formed under the function of amphiphilic surfactant ([Mwangi et al., 2020](#)). All emulsions are thermodynamically unstable and eventually phase-separate via coalescence, creaming/sedimentation, flocculation, or Ostwald ripening ([McClements, 2007](#)). To delay the thermodynamically favorable phase separation, proteins as amphiphilic emulsifiers are used to lower the interfacial tension thus kinetically stabilizing the emulsions. Polysaccharides, as thickening agents, may also be used to modify the viscosity of the aqueous phase. To apply protein–polysaccharide coacervation to stabilize emulsions, there are two strategies: one called “layer-by-layer” strategy (the addition of charged polysaccharide to a primary protein stabilized emulsion); the other strategy is sometimes termed as “mixed emulsions” (the addition of protein–polysaccharide complex coacervates in aqueous solution and subsequently homogenization) ([Fig. 1.11](#)).

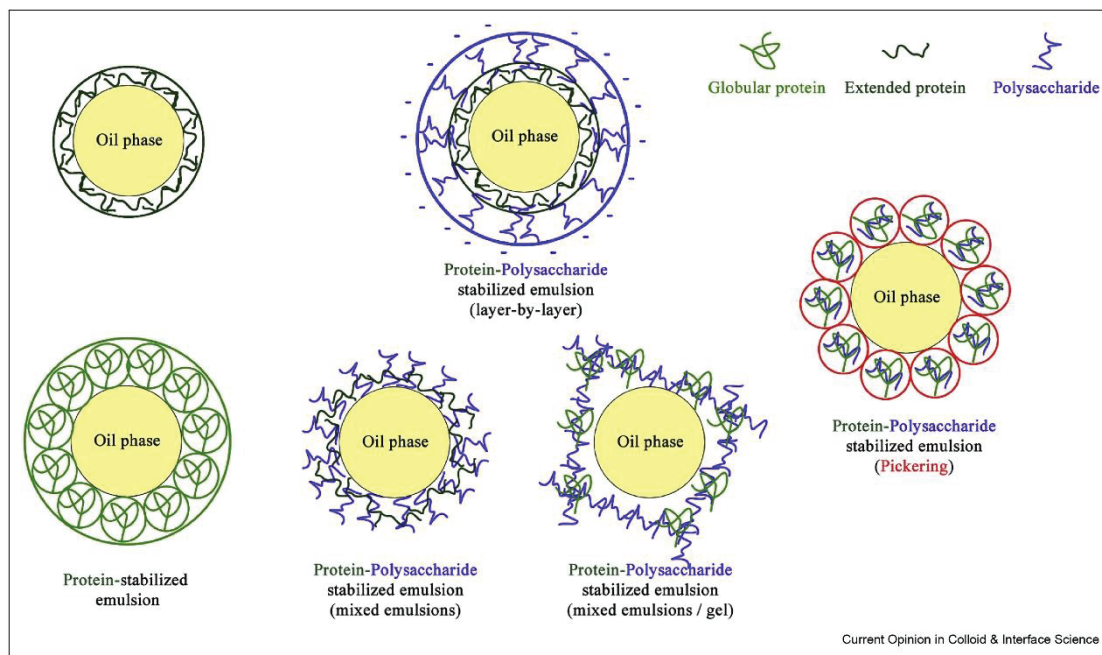


Figure 1.11. Schematic overview of protein and protein–polysaccharide stabilization of oil droplets in an oil–water emulsion ([Gentile, 2020](#)).

The techniques for emulsion preparation are diverse, including homogenization, high pressure homogenization, microfluidization, ultrasonication, membrane emulsification ([Jiang et al., 2020](#)). Among these techniques, homogenization is the most common one, due to its low cost and simplicity. However, this technique can only prepare coarse emulsions. For preparing nanoemulsion, other techniques like high homogenization and microfluidization should be further applied. These techniques normally need more energy input, which easily cause temperature increase in the operation process. Therefore, cooling system should be further induced, like the cold-water bath during ultrasonication.

1.4.2. Particle based systems

Particles in aqueous solution can be referred to emulsion droplets, when hydrophobic molecules are encapsulated, which has been mentioned in the last section. Besides that, particles also include the hydrophilic molecules encapsulating ones. Particles, mainly as microparticles or nanoparticles, have been largely prepared by biopolymers. Many protein-polysaccharide complex nanoparticles such as gelatin-cellulose composites, albumin-glycol chitosan composites, oxidized corn starch-gelatin composites and gelatin-sodium carboxymethyl nanocellulose composites are being used for drug delivery ([Verma et al., 2020](#)). In addition, some bioactive proteins like lysozyme, lactoferrin and insulin can form nanoparticles with oppositely-charged polysaccharides by electrostatic complexation ([Il'ina et al., 2016](#); [Wong et al., 2018](#)). Nanoparticles from biopolymers can be prepared by different approaches including

solvent evaporation, salting-out, thermal denaturation, dialysis and supercritical fluid technology ([Nimesh, 2013](#)).

1.4.3. Gel based systems

Biopolymer gels are composed of colloidal particles formed by biopolymers like proteins and polysaccharides, which have a three-dimensional network of biopolymers that trap a high fraction of water ([McClements, 2017](#)). According to the external dimensions of gels, these delivery systems are classified into nanogels, microgels and macrogels ([Milcovich et al., 2017](#)). All types of gels can be used to encapsulate, protect, and release bioactive compounds ([Zhang et al., 2015](#)). Basically, these gels can be fabricated from water-soluble food-grade proteins (such as collagen and gelatin) and polysaccharides (such as starch, alginate and agarose) through non-covalent bonds (such as electrostatic interactions, hydrogen bonds or hydrophobic interactions) and/or covalent bonds (such as disulfide bonds) ([Liu et al., 2018](#)). Some bioactive proteins or antimicrobial peptides complexed with polymer gels can be related to enhanced antimicrobial effects, increased stability and reduced toxicity ([Fig. 1.12](#)) ([Borro et al., 2020](#); [Darge et al., 2019](#); [McClements, 2018](#)).

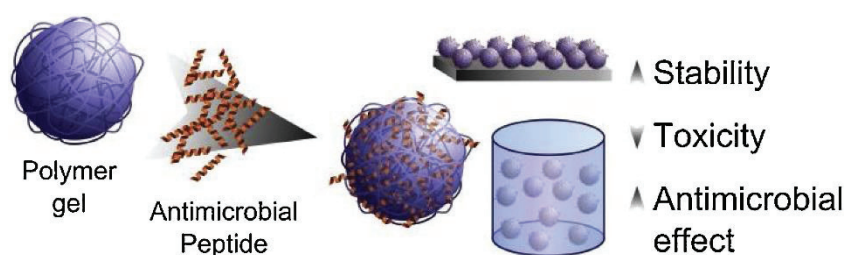


Figure 1.12. Schematic illustration of the use of gels and related systems as carriers for antimicrobial peptides ([Borro et al., 2020](#)).

Gels can be formed through polymerization techniques, including bulk, solution, and suspension polymerization ([Ahmed, 2015](#)). Briefly, gels are self-enssembled through different kinds of initiators inducing the formation of bonds between biopolymer chains. The initiators could be changes in environmental conditions, such as pH, ionic strength, temperature, light and enzyme activity ([Zhang et al., 2015](#)).

1.4.4. Capsule based systems

A capsule is composed of an interior core (active compounds) and an exterior shell (biopolymers). The core of capsules can withhold either liquid (hydrophobic compounds) or solid (hydrophilic compounds). Capsules have been extensively applied for drug delivery and food and agriculture industry. For storage convenience, the liquid encapsulated forms

mentioned above need to be transformed to a solid state.

For preparing capsules, drying techniques are necessary, including oven drying, vacuum drying, spray-drying, freeze-drying and spray-chilling. In general, drying techniques with spray process (spray-drying, spray-chilling) can yield nearly spherical particles of 5–50 μm size, whereas drying techniques without spray process (oven drying, vacuum drying and freeze-drying) produce a dried lump that must be ground to a powder form by mechanical disintegration. During this grinding process, some capsules break down and a portion of the core may get leached out. This core material that comes to the surface of the capsule and is exposed to the external environment is more prone to degradation (oxidation). In principle, thermally sensitive materials should be applied with low temperature drying techniques (freeze-drying and spray chilling) in order to minimize degradation by heat. Among these techniques, freeze-drying and spray-drying are two most commonly employed drying techniques ([Timilsena et al., 2019](#)). Overall, spray-drying is the preferable method due to ease of scale up and low cost, compared with freeze-drying, for materials that are not temperature sensitive.

1.5. Conclusion

As reviewed above, proteins and polysaccharides are ideal natural materials which can be applied in many fields, especially for encapsulation application as wall materials, due to their diversity and richness. Complex coacervation of proteins and polysaccharides has drawn much attention during the last years. As a result, the factors which affect the formation of protein/polysaccharide complexes are extensively studied. Understanding the mechanisms of these factors could be helpful for designing controlled-release delivery systems. Meanwhile, as core materials, the bioactive molecules were reviewed by dividing into two classes, hydrophobic and hydrophilic molecules. Finally, the encapsulation forms and their related techniques were discussed separately, mainly based on the properties of the formed protein/polysaccharide complexes.

References

- Aditya, N. P., Espinosa, Y. G., & Norton, I. T. (2017). Encapsulation systems for the delivery of hydrophilic nutraceuticals: Food application. *Biotechnology Advances*, 35(4), 450-457.
- Ahmad, S., Ahmad, M., Manzoor, K., Purwar, R., & Ikram, S. (2019). A review on latest innovations in natural gums based hydrogels: Preparations & applications. *International Journal of Biological Macromolecules*, 136, 870-890.
- Ahmad, T., Ismail, A., Ahmad, S. A., Khalil, K. A., Kumar, Y., Adeyemi, K. D., & Sazili, A. Q. (2017). Recent advances on the role of process variables affecting gelatin yield and characteristics with special reference to enzymatic extraction: A review. *Food Hydrocolloids*, 63, 85-96.
- Ahmed, E. M. (2015). Hydrogel: Preparation, characterization, and applications: A review. *Journal of Advanced Research*, 6(2), 105-121.
- Azevedo, M. A., Bourbon, A. I., Vicente, A. A., & Cerqueira, M. A. (2014). Alginate/chitosan nanoparticles for encapsulation and controlled release of vitamin B2. *International Journal of Biological Macromolecules*, 71, 141-146.
- Bajpai, S. K., & Tankhiwale, R. (2006). Investigation of dynamic release of vitamin B2 from calcium alginate/chitosan multilayered beads: Part II. *Reactive and Functional Polymers*, 66(12), 1565-1574.
- Bakkali, F., Averbeck, S., Averbeck, D., & Idaomar, M. (2008). Biological effects of essential oils--a review. *Food and Chemical Toxicology*, 46(2), 446-475.
- Borro, B. C., Nordstrom, R., & Malmsten, M. (2020). Microgels and hydrogels as delivery systems for antimicrobial peptides. *Colloids and Surfaces B: Biointerfaces*, 187, 110835.
- Burger, T. G., & Zhang, Y. (2019). Recent progress in the utilization of pea protein as an emulsifier for food applications. *Trends in Food Science & Technology*, 86, 25-33.
- Chai, C., Lee, J., & Huang, Q. (2014). The effect of ionic strength on the rheology of pH-induced bovine serum albumin/ κ -carrageenan coacervates. *LWT - Food Science and Technology*, 59(1), 356-360.
- Darge, H. F., Andrgie, A. T., Tsai, H. C., & Lai, J. Y. (2019). Polysaccharide and polypeptide based injectable thermo-sensitive hydrogels for local biomedical applications. *International Journal of Biological Macromolecules*, 133, 545-563.
- de Kruif, C. G., Weinbreck, F., & de Vries, R. (2004). Complex coacervation of proteins and anionic polysaccharides. *Current Opinion in Colloid & Interface Science*, 9(5), 340-349.
- Devi, N., Sarmah, M., Khatun, B., & Maji, T. K. (2017). Encapsulation of active ingredients in polysaccharide-protein complex coacervates. *Advances in Colloid and Interface Science*, 239, 136-145.
- Diarrassouba, F., Remondetto, G., Garrait, G., Alvarez, P., Beyssac, E., & Subirade, M. (2015). Self-assembly of beta-lactoglobulin and egg white lysozyme as a potential carrier for nutraceuticals. *Food Chemistry*, 173, 203-209.
- Đorđević, V., Balanč, B., Belščak-Cvitanović, A., Lević, S., Trifković, K., Kalušević, A., Kostić, I., Komes, D., Bugarski, B., & Nedović, V. (2014). Trends in Encapsulation Technologies for Delivery of Food Bioactive Compounds. *Food Engineering Reviews*, 7(4), 452-490.
- Duchene, D., & Bochot, A. (2016). Thirty years with cyclodextrins. *International Journal of Pharmaceutics*, 514(1), 58-72.
- Eghbal, N., & Choudhary, R. (2018). Complex coacervation: Encapsulation and controlled release of active agents in food systems. *LWT - Food Science and Technology*, 90, 254-264.
- El Asbahani, A., Miladi, K., Badri, W., Sala, M., Ait Addi, E. H., Casabianca, H., El Mousadik, A., Hartmann, D., Jilale, A., Renaud, F. N., & Elaissari, A. (2015). Essential oils: from extraction to encapsulation. *International Journal of Pharmaceutics*, 483(1-2), 220-243.

- Ephrem, E., Najjar, A., Charcosset, C., & Greige-Gerges, H. (2018). Encapsulation of natural active compounds, enzymes, and probiotics for fruit juice fortification, preservation, and processing: An overview. *Journal of Functional Foods*, 48, 65-84.
- Etxabide, A., Uranga, J., Guerrero, P., & de la Caba, K. (2017). Development of active gelatin films by means of valorisation of food processing waste: A review. *Food Hydrocolloids*, 68, 192-198.
- Fahami, A., & Fathi, M. (2018). Development of cress seed mucilage/PVA nanofibers as a novel carrier for vitamin A delivery. *Food Hydrocolloids*, 81, 31-38.
- Fang, Z., & Bhandari, B. (2010). Encapsulation of polyphenols – a review. *Trends in Food Science & Technology*, 21(10), 510-523.
- Faridi Esfanjani, A., & Jafari, S. M. (2016). Biopolymer nano-particles and natural nano-carriers for nano-encapsulation of phenolic compounds. *Colloids and Surfaces B: Biointerfaces*, 146, 532-543.
- Faridi Esfanjani, Afshin., Assadpour, E., & Jafari, S. M. (2018). Improving the bioavailability of phenolic compounds by loading them within lipid-based nanocarriers. *Trends in Food Science & Technology*, 76, 56-66.
- Fu, D., Deng, S., McClements, D. J., Zhou, L., Zou, L., Yi, J., Liu, C., & Liu, W. (2019). Encapsulation of β -carotene in wheat gluten nanoparticle-xanthan gum-stabilized Pickering emulsions: Enhancement of carotenoid stability and bioaccessibility. *Food Hydrocolloids*, 89, 80-89.
- Garrido, E., Cerqueira, A. S., Chavarria, D., Silva, T., Borges, F., & Garrido, J. (2018). Microencapsulation of caffeic acid phenethyl ester and caffeic acid phenethyl amide by inclusion in hydroxypropyl-beta-cyclodextrin. *Food Chemistry*, 254, 260-265.
- Gentile, L. (2020). Protein-polysaccharide interactions and aggregates in food formulations. *Current Opinion in Colloid & Interface Science*, 48, 18-27.
- George, M., & Abraham, T. E. (2006). Polyionic hydrocolloids for the intestinal delivery of protein drugs: alginate and chitosan--a review. *Journal of Controlled Release*, 114(1), 1-14.
- Ghasemi, S., Jafari, S. M., Assadpour, E., & Khomeiri, M. (2018). Nanoencapsulation of d-limonene within nanocarriers produced by pectin-whey protein complexes. *Food Hydrocolloids*, 77, 152-162.
- Gidwani, B., & Vyas, A. (2015). A Comprehensive Review on Cyclodextrin-Based Carriers for Delivery of Chemotherapeutic Cytotoxic Anticancer Drugs. *Biomed Research International*, 2015, 198268.
- Glab, T. K., & Boratynski, J. (2017). Potential of Casein as a Carrier for Biologically Active Agents. *Topics in Current Chemistry*, 375(4), 71.
- Grande-Tovar, C. D., Chaves-Lopez, C., Serio, A., Rossi, C., & Paparella, A. (2018). Chitosan coatings enriched with essential oils: Effects on fungi involved in fruit decay and mechanisms of action. *Trends in Food Science & Technology*, 78, 61-71.
- Guo, L., Goff, H. D., Xu, F., Liu, F., Ma, J., Chen, M., & Zhong, F. (2019). The effect of sodium alginate on nutrient digestion and metabolic responses during both in vitro and in vivo digestion process. *Food Hydrocolloids*, 105304.
- Il'ina, A. V., Kurek, D. V., Zubareva, A. A., Il'in, M. M., Mestechkina, N. M., & Varlamov, V. P. (2016). Preparation and characterization of biopolymer nanoparticles based on lactoferrin-polysaccharide complexes. *Reactive and Functional Polymers*, 102, 33-38.
- Jia, Z., Dumont, M.-J., & Orsat, V. (2016). Encapsulation of phenolic compounds present in plants using protein matrices. *Food Bioscience*, 15, 87-104.
- Jiang, T., Liao, W., & Charcosset, C. (2020). Recent advances in encapsulation of curcumin in nanoemulsions: A review of encapsulation technologies, bioaccessibility and applications. *Food Research International*, 132, 109035.
- Jones, O. G., & McClements, D. J. (2011). Recent progress in biopolymer nanoparticle and microparticle formation by heat-treating electrostatic protein-polysaccharide complexes.

- Advances in Colloid and Interface Science*, 167(1-2), 49-62.
- Karaca, A. C., Low, N., & Nickerson, M. (2011). Emulsifying properties of chickpea, faba bean, lentil and pea proteins produced by isoelectric precipitation and salt extraction. *Food Research International*, 44(9), 2742-2750.
- Karaca, A. C., Nickerson, M., & Low, N. H. (2013). Microcapsule production employing chickpea or lentil protein isolates and maltodextrin: physicochemical properties and oxidative protection of encapsulated flaxseed oil. *Food Chemistry*, 139(1-4), 448-457.
- Kaulmann, A., & Bohn, T. (2014). Carotenoids, inflammation, and oxidative stress--implications of cellular signaling pathways and relation to chronic disease prevention. *Nutrition Research*, 34(11), 907-929.
- Kayitmazer, A. B. (2017). Thermodynamics of complex coacervation. *Advances in Colloid and Interface Science*, 239, 169-177.
- Kimura, A., Fukuda, T., Zhang, M., Motoyama, S., Maruyama, N., & Utsumi, S. (2008). Comparison of physicochemical properties of 7S and 11S globulins from pea, fava bean, cowpea, and French bean with those of soybean-French bean 7S globulin exhibits excellent properties. *Journal of Agricultural and Food Chemistry*, 56, 10273-10279.
- Lan, Y., Ohm, J.-B., Chen, B., & Rao, J. (2020). Phase behavior, thermodynamic and microstructure of concentrated pea protein isolate-pectin mixture: Effect of pH, biopolymer ratio and pectin charge density. *Food Hydrocolloids*, 101, 105556.
- Lee, K. Y., & Mooney, D. J. (2012). Alginate: properties and biomedical applications. *Progress in Polymer Science*, 37(1), 106-126.
- Li, X., Hua, Y., Chen, Y., Kong, X., & Zhang, C. (2017). Two-step complex behavior between Bowman-Birk protease inhibitor and κ -carrageenan: Effect of protein concentration, ionic strength and temperature. *Food Hydrocolloids*, 62, 1-9.
- Li, X., Li, J., Chang, C., Wang, C., Zhang, M., Su, Y., & Yang, Y. (2019). Foaming characterization of fresh egg white proteins as a function of different proportions of egg yolk fractions. *Food Hydrocolloids*, 90, 118-125.
- Li, Z., Feng, Y., Li, Z., Gu, Z., Chen, S., Hong, Y., Cheng, L., & Li, C. (2020). Inclusion of tributyrin during enzymatic synthesis of cyclodextrins by β -cyclodextrin glycosyltransferase from *Bacillus circulans*. *Food Hydrocolloids*, 99, 105336.
- Liu, F., Zhang, S., Li, J., McClements, D. J., & Liu, X. (2018). Recent development of lactoferrin-based vehicles for the delivery of bioactive compounds: Complexes, emulsions, and nanoparticles. *Trends in Food Science & Technology*, 79, 67-77.
- Liu, K., Kong, X. L., Li, Q. M., Zhang, H. L., Zha, X. Q., & Luo, J. P. (2020). Stability and bioavailability of vitamin D3 encapsulated in composite gels of whey protein isolate and lotus root amylopectin. *Carbohydrate Polymers*, 227, 115337.
- Liu, L., Fishman, M. L., Kost, J., & Hicks, K. B. (2003). Pectin-based systems for colon-specific drug delivery via oral route. *Biomaterials*, 24(19), 3333-3343.
- Lopes, N. A., Barreto Pinilla, C. M., & Brandelli, A. (2019). Antimicrobial activity of lysozyme-nisin co-encapsulated in liposomes coated with polysaccharides. *Food Hydrocolloids*, 93, 1-9.
- Lu, W., Kelly, A. L., & Miao, S. (2016). Emulsion-based encapsulation and delivery systems for polyphenols. *Trends in Food Science & Technology*, 47, 1-9.
- Madkhali, O., Mekhail, G., & Wettig, S. D. (2019). Modified gelatin nanoparticles for gene delivery. *International Journal of Pharmaceutics*, 554, 224-234.
- Mahmoudi Saber, M. (2019). Strategies for surface modification of gelatin-based nanoparticles. *Colloids and Surfaces B: Biointerfaces*, 183, 110407.
- Maiorova, L. A., Erokhina, S. I., Pisani, M., Barucca, G., Marcaccio, M., Koifman, O. I., Salmikov, D. S., Gromova, O. A., Astolfi, P., Ricci, V., & Erokhin, V. (2019). Encapsulation of vitamin B12 into nanoengineered capsules and soft matter nanosystems for targeted delivery. *Colloids and Surfaces B: Biointerfaces*, 182, 110366.
- Maldonado, L., Sadeghi, R., & Kokini, J. (2017). Nanoparticulation of bovine serum albumin

- and poly-d-lysine through complex coacervation and encapsulation of curcumin. *Colloids and Surfaces B: Biointerfaces*, 159, 759-769.
- Marić, M., Grassino, A. N., Zhu, Z., Barba, F. J., Brnčić, M., & Rimac Brnčić, S. (2018). An overview of the traditional and innovative approaches for pectin extraction from plant food wastes and by-products: Ultrasound-, microwaves-, and enzyme-assisted extraction. *Trends in Food Science & Technology*, 76, 28-37.
- Martau, G. A., Mihai, M., & Vodnar, D. C. (2019). The Use of Chitosan, Alginate, and Pectin in the Biomedical and Food Sector-Biocompatibility, Bioadhesiveness, and Biodegradability. *Polymers (Basel)*, 11(11).
- Matalanis, A., Jones, O. G., & McClements, D. J. (2011). Structured biopolymer-based delivery systems for encapsulation, protection, and release of lipophilic compounds. *Food Hydrocolloids*, 25(8), 1865-1880.
- Matos, M., Gutiérrez, G., Iglesias, O., Coca, J., & Pazos, C. (2015). Enhancing encapsulation efficiency of food-grade double emulsions containing resveratrol or vitamin B12 by membrane emulsification. *Journal of Food Engineering*, 166, 212-220.
- McClements, D. J. (2007). Critical review of techniques and methodologies for characterization of emulsion stability. *Critical Reviews in Food Science and Nutrition*, 47(7), 611-649.
- McClements, D. J. (2017). Designing biopolymer microgels to encapsulate, protect and deliver bioactive components: Physicochemical aspects. *Advances in Colloid and Interface Science*, 240, 31-59.
- McClements, D. J. (2018). Encapsulation, protection, and delivery of bioactive proteins and peptides using nanoparticle and microparticle systems: A review. *Advances in Colloid and Interface Science*, 253, 1-22.
- Milcovich, G., Lettieri, S., Antunes, F. E., Medronho, B., Fonseca, A. C., Coelho, J. F. J., Marizza, P., Perrone, F., Farra, R., Dapas, B., Grassi, G., Grassi, M., & Giordani, S. (2017). Recent advances in smart biotechnology: Hydrogels and nanocarriers for tailored bioactive molecules depot. *Advances in Colloid and Interface Science*, 249, 163-180.
- Mohamed, S. A. A., El-Sakhawy, M., & El-Sakhawy, M. A. (2020). Polysaccharides, Protein and Lipid -Based Natural Edible Films in Food Packaging: A Review. *Carbohydrate Polymers*, 238, 116178.
- Munin, A., & Edwards-Levy, F. (2011). Encapsulation of natural polyphenolic compounds; a review. *Pharmaceutics*, 3(4), 793-829.
- Mwangi, W. W., Lim, H. P., Low, L. E., Tey, B. T., & Chan, E. S. (2020). Food-grade Pickering emulsions for encapsulation and delivery of bioactives. *Trends in Food Science & Technology*, 100, 320-332.
- Nasrollahzadeh, M., Shafiei, N., Nezafat, Z., Soheili Bidgoli, N. S., & Soleimani, F. (2020). Recent progresses in the application of cellulose, starch, alginate, gum, pectin, chitin and chitosan based (nano)catalysts in sustainable and selective oxidation reactions: A review. *Carbohydrate Polymers*, 116353.
- Nimesh, S. (2013). 2 - Methods of nanoparticle preparation. In S. Nimesh (Ed.), *Gene Therapy*, (pp. 13-42): Woodhead Publishing.
- Niu, F., Zhou, J., Niu, D., Wang, C., Liu, Y., Su, Y., & Yang, Y. (2015). Synergistic effects of ovalbumin/gum arabic complexes on the stability of emulsions exposed to environmental stress. *Food Hydrocolloids*, 47, 14-20.
- Nooshkam, M., & Varidi, M. (2020). Maillard conjugate-based delivery systems for the encapsulation, protection, and controlled release of nutraceuticals and food bioactive ingredients: A review. *Food Hydrocolloids*, 100, 105389.
- Oryan, A., Kamali, A., Moshiri, A., Baharvand, H., & Daemi, H. (2018). Chemical crosslinking of biopolymeric scaffolds: Current knowledge and future directions of crosslinked engineered bone scaffolds. *International Journal of Biological Macromolecules*, 107(Pt A), 678-688.

- Pang, L., Gao, Z., Feng, H., Wang, S., & Wang, Q. (2019). Cellulose based materials for controlled release formulations of agrochemicals: A review of modifications and applications. *Journal of Controlled Release*, 316, 105-115.
- Rajabi, H., Ghorbani, M., Jafari, S. M., Sadeghi Mahoonak, A., & Rajabzadeh, G. (2015). Retention of saffron bioactive components by spray drying encapsulation using maltodextrin, gum Arabic and gelatin as wall materials. *Food Hydrocolloids*, 51, 327-337.
- Rehman, A., Ahmad, T., Aadil, R. M., Spotti, M. J., Bakry, A. M., Khan, I. M., Zhao, L., Riaz, T., & Tong, Q. (2019). Pectin polymers as wall materials for the nano-encapsulation of bioactive compounds. *Trends in Food Science & Technology*, 90, 35-46.
- Rehman, A., Tong, Q., Jafari, S. M., Assadpour, E., Shehzad, Q., Aadil, R. M., Iqbal, M. W., Rashed, M. M. A., Mushtaq, B. S., & Ashraf, W. (2020). Carotenoid-loaded nanocarriers: A comprehensive review. *Advances in Colloid and Interface Science*, 275, 102048.
- Rezaei, A., Fathi, M., & Jafari, S. M. (2019). Nanoencapsulation of hydrophobic and low-soluble food bioactive compounds within different nanocarriers. *Food Hydrocolloids*, 88, 146-162.
- Rodríguez Patino, J. M., & Pilosof, A. M. R. (2011). Protein-polysaccharide interactions at fluid interfaces. *Food Hydrocolloids*, 25(8), 1925-1937.
- Ru, Q., Wang, Y., Lee, J., Ding, Y., & Huang, Q. (2012). Turbidity and rheological properties of bovine serum albumin/pectin coacervates: Effect of salt concentration and initial protein/polysaccharide ratio. *Carbohydrate Polymers*, 88(3), 838-846.
- Saini, R. K., Moon, S. H., Gansukh, E., & Keum, Y.-S. (2018). An efficient one-step scheme for the purification of major xanthophyll carotenoids from lettuce, and assessment of their comparative anticancer potential. *Food Chemistry*, 266, 56-65.
- Schmitt, C., & Turgeon, S. L. (2011). Protein/polysaccharide complexes and coacervates in food systems. *Advances in Colloid and Interface Science*, 167(1-2), 63-70.
- Schmitz, Auza, Koberidze, Rasche, Fischer, & Bortesi. (2019). Conversion of Chitin to Defined Chitosan Oligomers: Current Status and Future Prospects. *Marine Drugs*, 17(8), 452.
- Sedaghat Doost, A., Nikbakht Nasrabadi, M., Kassozi, V., Dewettinck, K., Stevens, C. V., & Van der Meeren, P. (2019). Pickering stabilization of thymol through green emulsification using soluble fraction of almond gum – Whey protein isolate nano-complexes. *Food Hydrocolloids*, 88, 218-227.
- Setiowati, A. D., Wijaya, W., & Van der Meeren, P. (2020). Whey protein-polysaccharide conjugates obtained via dry heat treatment to improve the heat stability of whey protein stabilized emulsions. *Trends in Food Science & Technology*, 98, 150-161.
- Shamsara, O., Jafari, S. M., & Muhidinov, Z. K. (2017). Development of double layered emulsion droplets with pectin/ β -lactoglobulin complex for bioactive delivery purposes. *Journal of Molecular Liquids*, 243, 144-150.
- Sharif, H. R., Williams, P. A., Sharif, M. K., Abbas, S., Majeed, H., Masamba, K. G., Safdar, W., & Zhong, F. (2018). Current progress in the utilization of native and modified legume proteins as emulsifiers and encapsulants – A review. *Food Hydrocolloids*, 76, 2-16.
- Sheikhi, A., Hayashi, J., Eichenbaum, J., Gutin, M., Kuntjoro, N., Khorsandi, D., & Khademhosseini, A. (2019). Recent advances in nanoengineering cellulose for cargo delivery. *Journal of Controlled Release*, 294, 53-76.
- Shishir, M. R. I., Xie, L., Sun, C., Zheng, X., & Chen, W. (2018). Advances in micro and nano-encapsulation of bioactive compounds using biopolymer and lipid-based transporters. *Trends in Food Science & Technology*, 78, 34-60.
- Steiner, B. M., McClements, D. J., & Davidov-Pardo, G. (2018). Encapsulation systems for lutein: A review. *Trends in Food Science & Technology*, 82, 71-81.
- Stinco, C. M., Escudero-Gilete, M. L., Heredia, F. J., Vicario, I. M., & Melendez-Martinez, A.

- J. (2016). Multivariate analyses of a wide selection of orange varieties based on carotenoid contents, color and in vitro antioxidant capacity. *Food Research International*, 90, 194-204.
- Surh, J., Decker, E., & McClements, D. (2006). Influence of pH and pectin type on properties and stability of sodium-caseinate stabilized oil-in-water emulsions. *Food Hydrocolloids*, 20(5), 607-618.
- Taheri, A., & Jafari, S. M. (2019). Gum-based nanocarriers for the protection and delivery of food bioactive compounds. *Advances in Colloid and Interface Science*, 269, 277-295.
- Tahir, H. E., Xiaobo, Z., Mahunu, G. K., Arslan, M., Abdalhai, M., & Zhihua, L. (2019). Recent developments in gum edible coating applications for fruits and vegetables preservation: A review. *Carbohydrate Polymers*, 224, 115141.
- Tang, C.-H. (2019). Nanostructured soy proteins: Fabrication and applications as delivery systems for bioactives (a review). *Food Hydrocolloids*, 91, 92-116.
- Tavares, L., & Zapata Noreña, C. P. (2019). Encapsulation of garlic extract using complex coacervation with whey protein isolate and chitosan as wall materials followed by spray drying. *Food Hydrocolloids*, 89, 360-369.
- Teng, Z., Luo, Y., & Wang, Q. (2013). Carboxymethyl chitosan-soy protein complex nanoparticles for the encapsulation and controlled release of vitamin D(3). *Food Chemistry*, 141(1), 524-532.
- Timilsena, Y. P., Akanbi, T. O., Khalid, N., Adhikari, B., & Barrow, C. J. (2019). Complex coacervation: Principles, mechanisms and applications in microencapsulation. *International Journal of Biological Macromolecules*, 121, 1276-1286.
- Valdeperas, M., Salis, A., Barauskas, J., Tiberg, F., Arnebrant, T., Razumas, V., Monduzzi, M., & Nylander, T. (2019). Enzyme encapsulation in nanostructured self-assembled structures: Toward biofunctional supramolecular assemblies. *Current Opinion in Colloid & Interface Science*, 44, 130-142.
- Verma, M. L., Dhanya, B. S., Sukriti, Rani, V., Thakur, M., Jeslin, J., & Kushwaha, R. (2020). Carbohydrate and protein based biopolymeric nanoparticles: Current status and biotechnological applications. *International Journal of Biological Macromolecules*, 154, 390-412.
- Voss, G. T., Gualarte, M. S., Vogt, A. G., Giongo, J. L., Vaucher, R. A., Echenique, J. V. Z., Soares, M. P., Luchese, C., Wilhelm, E. A., & Fajardo, A. R. (2018). Polysaccharide-based film loaded with vitamin C and propolis: A promising device to accelerate diabetic wound healing. *International Journal of Pharmaceutics*, 552(1-2), 340-351.
- Wang, B., Vongsivut, J., Adhikari, B., & Barrow, C. J. (2015). Microencapsulation of tuna oil fortified with the multiple lipophilic ingredients vitamins A, D3, E, K2, curcumin and coenzyme Q10. *Journal of Functional Foods*, 19, 893-901.
- Wang, C., Li, J., Li, X., Chang, C., Zhang, M., Gu, L., Su, Y., & Yang, Y. (2019a). Emulsifying properties of glycation or glycation-heat modified egg white protein. *Food Research International*, 119, 227-235.
- Wang, J., Liang, Y., Omana, D. A., Kav, N. N., & Wu, J. (2012). Proteomics analysis of egg white proteins from different egg varieties. *Journal of Agriculture and Food Chemistry*, 60(1), 272-282.
- Wang, J., Maoulida, F., Ben Amara, C., Ghnimi, S., Chihib, N. E., Dumas, E., & Gharsallaoui, A. (2019b). Spray-drying of protein/polysaccharide complexes: Dissociation of the effects of shearing and heating. *Food Chemistry*, 297, 124943.
- Wang, J., Oussama Khelissa, S., Chihib, N.-E., Dumas, E., & Gharsallaoui, A. (2019c). Effect of drying and interfacial membrane composition on the antimicrobial activity of emulsified citral. *Food Chemistry*, 298, 125079.
- Weinbreck, F., De Vries, R., Schrooyen, P., & De Kruif, C. G. (2003). Complex coacervation of whey proteins and gum Arabic. *Biomacromolecules*, 4(2), 293-303.
- Winuprasith, T., Khomein, P., Mitbumrung, W., Supphantharika, M., Nitithamyong, A., &

- McClements, D. J. (2018). Encapsulation of vitamin D3 in pickering emulsions stabilized by nanofibrillated mangosteen cellulose: Impact on in vitro digestion and bioaccessibility. *Food Hydrocolloids*, 83, 153-164.
- Wong, C. Y., Al-Salami, H., & Dass, C. R. (2018). Microparticles, microcapsules and microspheres: A review of recent developments and prospects for oral delivery of insulin. *International Journal of Pharmaceutics*, 537(1-2), 223-244.
- Wu, T., Jiang, Q., Wu, D., Hu, Y., Chen, S., Ding, T., Ye, X., Liu, D., & Chen, J. (2019). What is new in lysozyme research and its application in food industry? A review. *Food Chemistry*, 274, 698-709.
- Wüstenberg, T. (2015). General overview of food hydrocolloids. *Cellulose and cellulose derivatives in the food industry*. Wüstenberg T (ed). Wiley-VCH, Weinheim, Germany, 1-68.
- Xiong, W., Ren, C., Tian, M., Yang, X., Li, J., & Li, B. (2017). Complex coacervation of ovalbumin-carboxymethylcellulose assessed by isothermal titration calorimeter and rheology: Effect of ionic strength and charge density of polysaccharide. *Food Hydrocolloids*, 73, 41-50.
- Xu, W., Zhu, D., Li, Z., Luo, D., Hang, L., Jing, J., & Shah, B. R. (2019). Controlled release of lysozyme based core/shells structured alginate beads with CaCO₃ microparticles using Pickering emulsion template and in situ gelation. *Colloids and Surfaces B: Biointerfaces*, 183, 110410.
- Yang, J.-S., Xie, Y.-J., & He, W. (2011). Research progress on chemical modification of alginate: A review. *Carbohydrate Polymers*, 84(1), 33-39.
- Young, S., Wong, M., Tabata, Y., & Mikos, A. G. (2005). Gelatin as a delivery vehicle for the controlled release of bioactive molecules. *Journal of Controlled Release*, 109(1-3), 256-274.
- Yuan, Y., Kong, Z.-Y., Sun, Y.-E., Zeng, Q.-Z., & Yang, X.-Q. (2017). Complex coacervation of soy protein with chitosan: Constructing antioxidant microcapsule for algal oil delivery. *LWT - Food Science and Technology*, 75, 171-179.
- Yuan, Y., Wan, Z.-L., Yin, S.-W., Teng, Z., Yang, X.-Q., Qi, J.-R., & Wang, X.-Y. (2013). Formation and dynamic interfacial adsorption of glycinin/chitosan soluble complex at acidic pH: Relationship to mixed emulsion stability. *Food Hydrocolloids*, 31(1), 85-93.
- Zeng, J., Zhao, J., Dong, B., Cai, X., Jiang, J., Xue, R., Yao, F., Dong, Y., & Liu, C. (2019). Lycopene protects against pressure overload-induced cardiac hypertrophy by attenuating oxidative stress. *Journal of Nutritional Biochemistry*, 66, 70-78.
- Zha, F., Dong, S., Rao, J., & Chen, B. (2019). Pea protein isolate-gum Arabic Maillard conjugates improves physical and oxidative stability of oil-in-water emulsions. *Food Chemistry*, 285, 130-138.
- Zhang, H., Fan, Q., Li, D., Chen, X., & Liang, L. (2019). Impact of gum Arabic on the partition and stability of resveratrol in sunflower oil emulsions stabilized by whey protein isolate. *Colloids and Surfaces B: Biointerfaces*, 181, 749-755.
- Zhang, Z., Zhang, R., Chen, L., Tong, Q., & McClements, D. J. (2015). Designing hydrogel particles for controlled or targeted release of lipophilic bioactive agents in the gastrointestinal tract. *European Polymer Journal*, 72, 698-716.
- Ziani, K., Fang, Y., & McClements, D. J. (2012). Encapsulation of functional lipophilic components in surfactant-based colloidal delivery systems: Vitamin E, vitamin D, and lemon oil. *Food Chemistry*, 134(2), 1106-1112.

Summary of Chapter 2

Complexation of pectin and sodium caseinate was frequently studied and applied for preparing gels, emulsions and films. However, there is a lack of information on the effect of ionic strength, pH and temperature on the interactions between sodium caseinate and low methoxyl pectin at the molecular level.

The complexation behavior between sodium caseinate and low methoxyl pectin in solution at different conditions was studied by isothermal titration calorimetry and the results were published in “*Food Hydrocolloids*”. Insoluble complexes, soluble complexes and co-soluble biopolymers were formed at pH 3, 5 and 7, respectively. The bonding forces between these two biopolymers were mainly electrostatic, which could be weakened with the increase of ionic strength *via* the formation of an electrostatic shield. In addition, the electrostatic attraction bonded to insoluble complexes at pH 3 was stronger than that bonded to the soluble complexes at pH 5. Meanwhile, temperature has a significant impact on the interactions between these two biopolymers. Higher temperature promotes the interaction by changing the biopolymers’ structure to expose more binding sites. Through these results, we have now a better understanding of the formation of CAS/LMP complexes in solution.

CHAPTER 2

Low Methoxyl pectin / sodium caseinate complexing behavior studied by isothermal titration calorimetry

Wang, Jian, Emilie Dumas, and Adem Gharsallaoui

Food Hydrocolloids, 2019. 88: p. 163-169.

2.1. Abstract

The formation of Low Methoxyl pectin (LMP) / sodium caseinate (CAS) complexes was studied at different pHs by measuring transmittance, phase separation and ζ -potential. At the different tested CAS/LMP ratios, insoluble complexes, soluble complexes and biopolymer solutions were formed at pH 3.0, 5.0 and 7.0, respectively. In order to study the interactions between CAS and LMP in these three different conditions, isothermal titration calorimetry (ITC) was used. The results showed that there were no significant interactions at pH 7.0 while electrostatic interactions were predominant in both soluble and insoluble complexes. The electrostatic interactions in insoluble complexes were much stronger than in soluble complexes. The effect of ionic strength and temperature on the formation of insoluble complexes at pH 3.0 was also studied by ITC. The presence of sodium chloride was shown to inhibit the electrostatic interactions until a threshold CAS/LMP ratio, and high temperature favored the attractive interactions between CAS and LMP. The data obtained in this study should allow efficient development of encapsulation systems by complex coacervation.

2.2. Introduction

Proteins and polysaccharides are natural biodegradable biopolymers, available from renewable resources, and compatible with other food ingredients. In the food industry, proteins are commonly used as emulsifiers in the stabilization of oil/water emulsions, and also as foaming agents. Most polysaccharides can be used as thickening agents and also for their water-holding properties. Their interactions can also be carefully tailored for protein and polysaccharide separation / purification purposes ([Happi Emaga et al., 2012](#); [Xu et al., 2011](#)), in the design of biopolymer adhesives and edible films ([Wang et al., 2007](#)) and controlled delivery applications ([Schmitt & Turgeon, 2011](#)). A better understanding of biopolymer

interactions and factors/conditions leading to their phase behavior could increase their usefulness for tailoring food structure or in the development of more high value applications (e.g., capsules and films).

Pectin is a typical food-grade polysaccharide which is widely used in food products. It is a main component of plant cell wall, commonly extracted from citrus peel and apple pomace. Pectin is composed by a chain of α -(1-4)-linked D-galacturonic acid and methoxylated carboxylic acid residues. According to the degree of esterification, it can be classified as high-methylated (HM) or low-methylated (LM). Sodium caseinate (CAS) is made by adding sodium hydroxide to acid caseins, which are milk proteins that contain α_{s1} -, α_{s2} -, β -, and κ -casein molecules. Due to the different physicochemical properties of these four protein fractions, these caseins are readily adsorbed at the oil/water interfaces but they have different adsorption behaviors at the droplet surface ([Ye et al., 2011](#)). As many literary works reported, sodium caseinate has many good properties for preparing gels, foams, emulsions and films ([Dickinson, 2006](#); [Fabra et al., 2008](#)).

Complexation of pectin and sodium caseinate was studied these last years and applied for preparing gels, emulsions and films. For example, in our previous works, we studied complex coacervation and interactions between LM pectin and sodium caseinate in order to prepare composite edible films at different physicochemical conditions ([Eghbal et al., 2017](#); [Eghbal et al., 2016](#)). [Matia-Merino et al. \(2004\)](#) studied the effect of LM pectin and calcium ions on the rheology and the microstructure of sodium caseinate gels. The stability of emulsions according to the type of pectin and to pH was also studied ([Surh et al., 2006](#)). Diffusing wave spectroscopy was used to study dynamics of interactions between HM pectin and sodium caseinate-stabilized emulsions ([Liu et al., 2007](#)). Pectin was purified from apple pomace juice using sodium caseinate and isothermal titration calorimetry was used to characterize their binding at acid pH ([Happi Emaga et al., 2012](#)). Electrostatic interactions between pectin and sodium caseinate were studied for preparing stabilized conjugated linoleic acid emulsions ([Cheng & McClements, 2016](#)). According to the most published works, the main binding force for complexation of pectin and sodium caseinate in acid conditions is electrostatic. Formation of pectin - sodium caseinate complexes is highly dependent on pH. In fact, at acid pH, pectin and sodium caseinate carry opposite charges. At higher pH, both pectin and sodium caseinate carry negative charges, electrostatic repulsions happen and inhibit the formation of complexes. Depending on the electrostatic interactions between pectin and sodium caseinate, soluble and insoluble complexes can be formed. Despite these numerous studies, the influence of others parameters still need to be investigated to have a better understanding on their influence on the interactions between

LMP and CAS.

In our previous studies, these same two biopolymers (CAS and LMP) were used to develop edible films under different pH conditions. The mechanical and physicochemical properties of these films were then evaluated. Thus, to complete these two works, the aim of this study was to investigate the effects of ionic strength and temperature on the interactions between LMP and CAS at the molecular level. In this goal, CAS/LMP complexes were first prepared at various protein to polysaccharide ratios and at pH ranging from 3.0 to 7.0. The effect of CAS/LMP ratio and pH on the turbidity and zeta potential was investigated. Then, soluble and insoluble complexes of LMP-CAS and their solutions were formed to study the interactions at different temperatures and NaCl concentrations by isothermal titration calorimetry (ITC) tests. This knowledge should optimize the usage of LMP-CAS complexes in several applications such as encapsulation of active molecules or edible packaging films development.

2.3. Materials and methods

2.3.1. Materials

Low methoxyl pectin (LMP) (Unipectine™ OF 305 C SB, degree of esterification from 22% to 28% and degree of acetylation from 20% to 23%) was purchased from Cargill (Baupre, France). Carbohydrate and ash contents of LMP powder were respectively 81.21% and 6.05%. Sodium caseinate (CAS) powder was purchased from Fisher Scientific (United Kingdom). Protein content in CAS determined by the Kjeldahl method was 93.20% (nitrogen conversion factor N=6.38). Ash content of CAS was about 5.14%. Analytical grade sodium chloride (NaCl), imidazole (C₃H₄N₂), acetic acid, sodium hydroxide (NaOH), and hydrochloric acid (HCl), were purchased from Sigma-Aldrich Chimie (St Quentin Fallavier, France). All the solutions were prepared in distilled water.

2.3.2. Solution preparation

Imidazole-acetate buffer solutions (5 mM) were prepared by dispersing weighed amounts of imidazole and acetic acid into distilled water and then adjusting the pH to 3.0, 3.5, 4.0, 4.5, 5.0, 5.5, 6.0, 6.5, or 7.0. According to the ratio between LMP and CAS, concentrated stock solutions of LMP (20 g/L) and CAS (10 g/L) were prepared by dispersing powders in imidazole-acetate buffer (5 mM, pH unadjusted) and stirred for at least 3 h with a magnetic stirrer to make sure them totally soluble. The pH was then adjusted by using HCl (1.0 M) or NaOH (1.0 M) during the process of diluting. Biopolymer mixtures containing different

CAS/LMP ratios (0.5, 1.0, 2.5, 5.0) were prepared by mixing different ratios of the concentrated stock solutions with imidazole-acetate buffer at the suitable pH. The resulting mixtures were mixed for 1 min and their pH was adjusted again.

2.3.3. Transmittance measurement

According to the method described by [Fioramonti et al. \(2014\)](#), transmittance measurements were performed at each ratio of CAS/LMP solutions over a pH range of 3.0 - 7.0 by a UV/Vis spectrophotometer (Jenway 3705, Villepinte, France) at 850 nm using plastic cuvettes (1 cm path length). Before the test, all the solutions were mixed for 10 min and their pH was checked again. Then, test tubes were filled with the different samples and stored at room temperature for exactly 20 min. Digital photos were taken using a 16-megapixel camera.

2.3.4. Zeta potential measurement

The zeta potential (ζ -potential) of CAS/LMP solutions was determined using a Zetasizer NanoZS90 (Malvern Instruments, Malvern, UK). The samples were diluted (0.5% (w/w)) with imidazole-acetate buffer at the corresponding pH. The mean ζ -potential (ZP) values (\pm SD (standard deviation)) were obtained from the instrument.

2.3.5. Isothermal titration calorimetry (ITC)

The energetics of the interactions between CAS and LMP were measured using an isothermal titration calorimeter (VP-ITC) from MicroCal (Malvern Instruments, Northampton, MA) with a reaction cell volume of 1.4214 mL. All the solutions of LMP and CAS were prepared by using the same buffer (5 mM imidazole-acetate buffer, Milli-Q water). For the preparation of solutions containing 50 mM or 100 mM NaCl, weighted amounts of NaCl were added to each biopolymer solution. The obtained solutions were dialyzed against buffer having the same ionic strength and pH (50 mM or 100 mM NaCl; pH: 3.0) through 500 Da membranes until ionic and pH balance. All solutions were degassed under stirring for 5-10 min before being loaded. LMP solution (0.5 g/L) was loaded into the calorimetric cell, equilibrated at 15, 25, 35, 45, 55, or 65 °C, according to the test temperature, and titrated by adding 2 μ L initial injection and 28 successive 10 μ L injections of CAS (5.0 g/L) while continuously stirring the mixture at 307 rpm. Each injection lasted 20 s, and there was an interval of 200 s between two successive injections. To study the effect of ionic strength, various concentrations of NaCl (0 mM, 50 mM, 100 mM) were used and all the other parameters of the titration were maintained unchanged (concentration, temperature, titration conditions). All the solutions were maintained under dialysis before the test to avoid buffer mismatch, and control tests were done by replacing the

LMP solution by buffer in the sample cell. Control titrations were performed to obtain the heat of dilution by injecting the CAS solution into imidazole-acetate buffer, so corrected raw data was acquired by subtracting the heat of dilution data from the raw data. Data analysis was performed with Origin 7.0 software. The Gibbs free energy was calculated from the equation $\Delta G = \Delta H - T\Delta S$. Measurements were carried out in triplicate, and the results are reported as the mean and standard deviation.

2.3.6. Statistical analysis

All assays were measured at least in triplicate. Means and standard deviations were calculated and differences between means were determined with Fishers Least Significant Difference (LSD) test at $p < 0.05$ significance level (Statgraphics Centurion XV).

2.4. Results and discussion

2.4.1. Phase diagrams of transmittance analysis

It is generally reported in the literature that electrostatic attractions are the main driving force in the formation of complexes between proteins and polysaccharides ([Schmitt & Turgeon, 2011](#)). The charge density of each biopolymer, which plays an important role in the electrostatic complexes formation, is strongly dependent on the suspension pH. With pH changing, complexation appears as a two-step process and can be assessed by transmittance (T%) measurement ([Fioramonti et al., 2014](#)) as shown in [Fig. 2.1](#). Two pH-induced transitions were identified by drawing the tangent lines in the T% vs. pH curves, between the areas determined by their inflection points. From right to left, there are two turning points and three regions. The first turning point is called pH_c and indicates the start of soluble complexes formation, the second turning point is called pH_ϕ and indicates the end of the soluble complexes formation ([Fioramonti et al., 2014](#)), which can be confirmed by the optical images, as shown in [Fig. 2.1](#). When solvent pH is above pH_c , the protein and polysaccharide charges are both negative, and consequently they are co-soluble. However, when solvent pH is between pH_c and pH_ϕ , protein and polysaccharide molecules form soluble complexes. By decreasing the solvent pH below pH_ϕ , coacervation takes place.

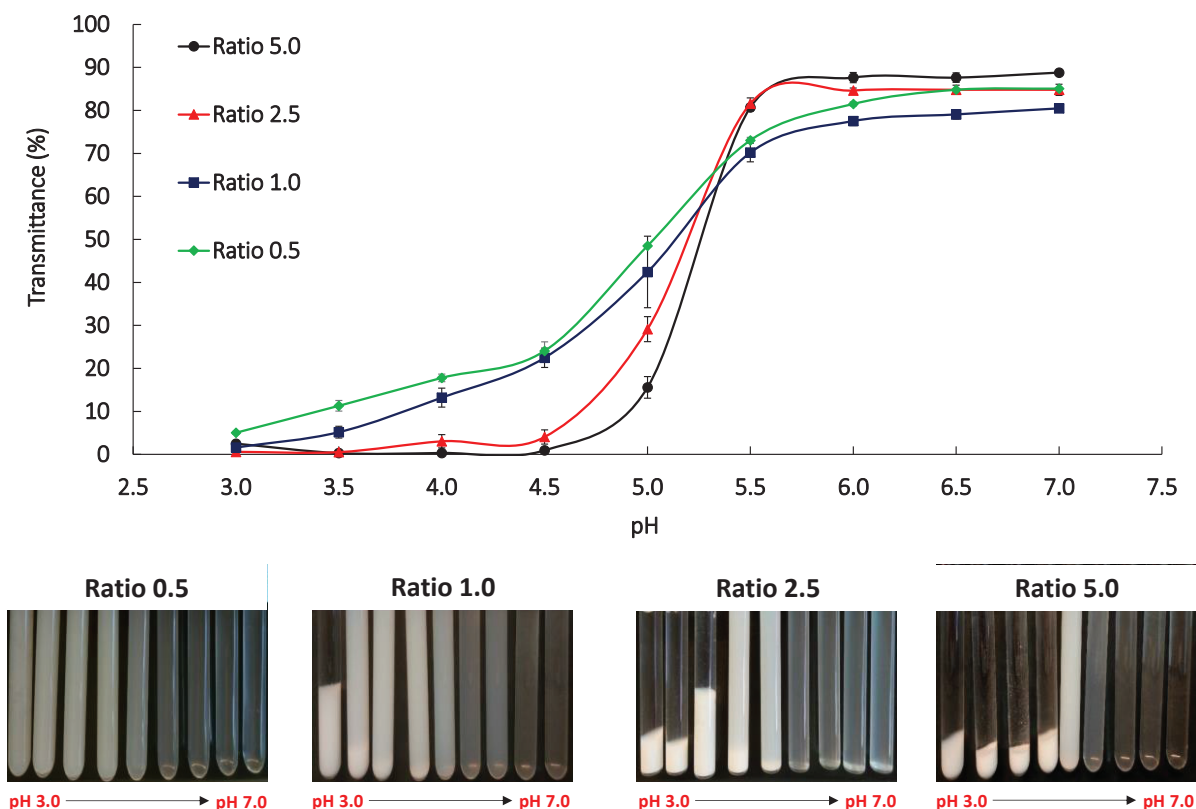


Figure 2.1. Transmittance (%) at 850 nm and photographs of CAS/LMP suspensions at different pHs (3.0 to 7.0) and CAS/LMP ratios (0.5 to 5.0) (Imidazole-acetate buffer (5 mM); temperature: 25 °C; NaCl: 0 mM). For all ratios, CAS was kept constant (5.0 g/L) and LMP was changed from 10.0 g/L (ratio 0.5) to 1.0 g/L (ratio 5.0).

Fig. 2.1 shows that the four mixing ratios possess the same value of pH_c (~ 5.5), whereas the visual aspects of tubes showed that the coacervation happened from pH 4.5 at ratio 5.0, from pH 4.0 at ratio 2.5, from pH 3.0 at ratio 1.0, and no phase separation at ratio 0.5, which allowed to obtain 4 different values of pH_ϕ at these 4 ratios. It can be concluded that mixing ratio will not change pH_c , but can change pH_ϕ . Similar conclusions were reported by other researches ([Lv et al., 2014](#); [Sara Ghorbani Gorji, 2014](#)). Indeed, supported by the hypothesis that soluble complexes are formed between a single polysaccharide and a given amount of protein, when the concentration of CAS is constant, LMP negative-charged groups become in excess at pH_c because of the limited positively-charged patches in CAS molecules. So the value of pH_c depends on the concentration of CAS, rather than the concentration of LMP. However, at pH_ϕ , there will be enough positively-charged CAS groups able to combine with LMP.

The isoelectric point (pI) of CAS is about 4.6 ([Cheng & McClements, 2016](#); [Eghbal et al., 2016](#)) which is between pH_c (~ 5.5) and pH_ϕ (< 4.5) whatever the studied CAS/LMP ratio. When pH is above the protein isoelectric point, some moieties of CAS molecules still carry positive

charges, and these positively charged patches can interact with negatively charged polysaccharides to form complexes ([Eghbal et al., 2017](#)), which could explain the fact that pH_c was above the protein pI.

According to [Fig. 2.1](#). in the region corresponding to the formation of soluble complexes (between pH_ϕ and pH_c), phase separation can also be observed, which means that some insoluble complexes were formed in this region. From pH 5.0, the amount of insoluble complexes increased when pH decreased. This can indicate that the maximum amount of soluble complexes was reached at pH 5.0. When the CAS/LMP ratio was decreased from 5.0 to 0.5, the region of soluble complexes has expanded, because the pH_ϕ decreased as explained above which is similar to the results presented in another study concerning the formation of soluble complexes formed by glycinin and chitosan ([Yuan et al., 2013](#)).

2.4.2. ζ -potential

Four different ratios of CAS/LMP complexes (5.0, 2.5, 1.0, and 0.5) were prepared and their ζ -potential was measured ([Fig. 2.2](#)). When pH was above 5.0, the ζ -potential of the four ratios complexes was more negative than -30 mV. The mixtures can be considered as stable solutions in these conditions, which is consistent with the transmittance results ([Fig. 2.1](#)). In fact, according to [Eghbal et al. \(2016\)](#), the number of LMP negatively charges significantly increases when the pH increased due to the deprotonation of carboxyl groups. However, CAS has two opposite charges on one side and the other of the pI (~ 4.6).

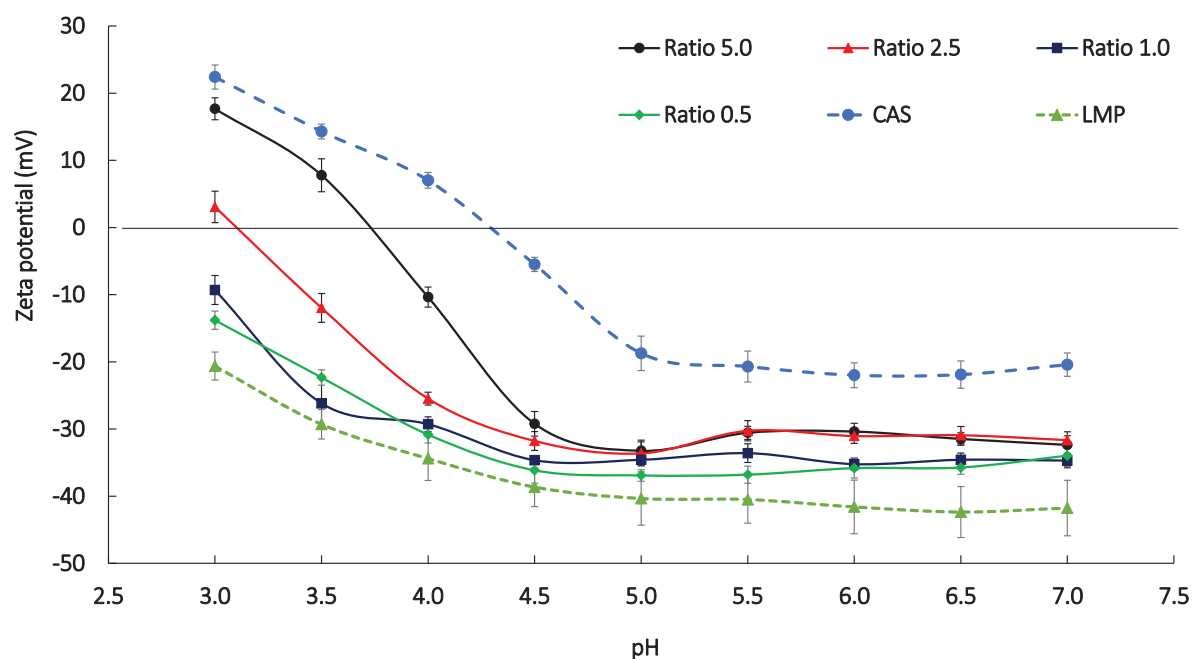


Figure 2.2. ζ -potential of CAS/LMP suspensions at different pHs (3.0 to 7.0) and CAS/LMP

ratios (0.5 to 5.0) (Imidazole-acetate buffer (5 mM); temperature: 25 °C; NaCl: 0 mM). For all ratios, CAS was kept constant (5.0 g/L) and LMP was changed from 10.0 g/L (ratio 0.5) to 1.0 g/L (ratio 5.0).

At pH 3.0, because of the oppositely charged LMP and CAS, with changing the CAS/LMP ratio, the charge of complexes was negative (ratio 0.5 and 1.0), almost neutral (ratio 2.5), and positive (ratio 5.0). When pH decreased from 7.0 to 5.0, ζ -potential didn't change significantly and stayed at about -30 mV. From pH 4.5, ζ -potential increased rapidly with pH decreasing. The turning point is closed to the isoelectric point of CAS (pI~4.6). This result shows that ζ -potential changed more dramatically when two biopolymers oppositely charged form complexes. However, for two biopolymers that carry the same charge (pH > 5.0), ζ -potential was not almost changed. Because of the negatively charged LMP, when the mixing ratio of CAS/LMP decreased, the value of ζ -potential also decreased.

When the ζ -potential of complexes was close to zero, which means that the charge of complexes was almost electrically neutral, coacervation is maximized, as it is shown in [Fig. 2.1](#). With decreasing the ratio of CAS/LMP, the isoelectric point of complexes shifts toward lower pH values. This result could be explained by the increase of the amount of LMP forming consequently more negatively charged complexes. These negatively charged complexes need more protons to reach a neutral state. All soluble complexes at the four studied ratios are formed when the net charge was fairly high (the values of ζ -potential were about -20 mV), which indicate that electrostatic interactions are quite strong. With decreasing the net charge of complexes by decreasing the pH, complex coacervation occurs leading to phase separation.

2.4.3. Isothermal titration calorimetry results

Isothermal titration calorimetry (ITC) is a direct way to measure the heat change during molecular interactions in biological and non-biological systems at a constant temperature. ITC was widely used to study the type and magnitude of energies involved in the interactions between proteins and polysaccharides ([Chang et al., 2016](#); [Happi Emaga et al., 2012](#); [Xiong et al., 2016](#)). CAS and LMP solutions prepared at pH 3.0, pH 5.0 and pH 7.0 were chosen to perform ITC tests at 25 °C in order to study the energetics of interactions in insoluble complexes, soluble complexes and co-soluble biopolymers, respectively. After that, the effects of ionic strength and temperature were also studied.

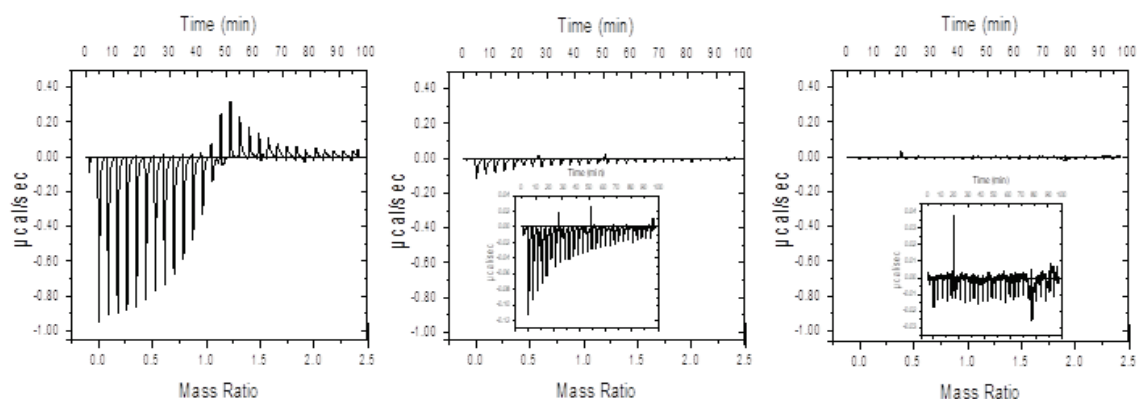


Figure 2.3. ITC titration graphs of CAS/LMP at pH 3.0 (left), pH 5.0 (middle) and pH 7.0 (right) (Imidazole-acetate buffer (5 mM); temperature: 25 °C; NaCl: 0 mM). LMP solution (0.5 g/L) was loaded in the calorimetric cell and CAS solution (5.0 g/L) was loaded in the syringe.

The raw data of ITC tests at pH 3.0, pH 5.0 and pH 7.0 are shown in Fig. 2.3. Heat flow versus time profiles were achieved by injecting progressively 5.0 g/L CAS solution into a reaction cell containing 0.5 g/L LMP solution at 25 °C. The enthalpy changes (ΔH) per gram of CAS versus CAS/LMP mass ratio were obtained by software. In this study, we used mass unit rather than molecular unit, because both CAS and LMP are high molecular weight polymers. At pH 3.0 (Fig. 2.3), the titration was exothermic and the released heat for each injection decreased regularly, which indicates that LMP chains in the reaction cell are interacting with injected CAS molecules and the resulted interactions were less and less strong until the CAS/LMP mass ratio reached 1.0. Above this ratio, the enthalpy became positive, which means that the titration became endothermic and the absorbed heat decreased until the enthalpy reached values close to zero. This phenomenon can be caused by the structure rearrangement from aggregates to coacervates, as previously shown by Happi Emaga *et al.* (2012). At pH 5.0 (Fig. 2.3), the whole process was exothermic, but compared to the released heat values obtained at pH 3.0, the released heat values at pH 5.0 were quite low. This result could indicate that the driving force for the interactions between CAS and LMP was weaker at pH 5.0 than at pH 3.0. Taken together, results from Fig. 2.1-2.3 indicate that the interactions into insoluble complexes are stronger than into soluble complexes. At pH 7.0, ITC test showed that there was no heat exchange during the injection process, just like control test (injection of CAS into buffer, data not shown). That means that at pH 7.0, CAS and LMP were just co-soluble and there were no significant interactions between them. The enthalpy change (ΔH) versus CAS/LMP mass ratio at the three studied pHs is shown in Fig. 2.4. The driving force between CAS and LMP at pH 3.0 was much stronger than that at pH 5.0 or pH 7.0, so pH 3.0 was chosen for the following ITC tests.

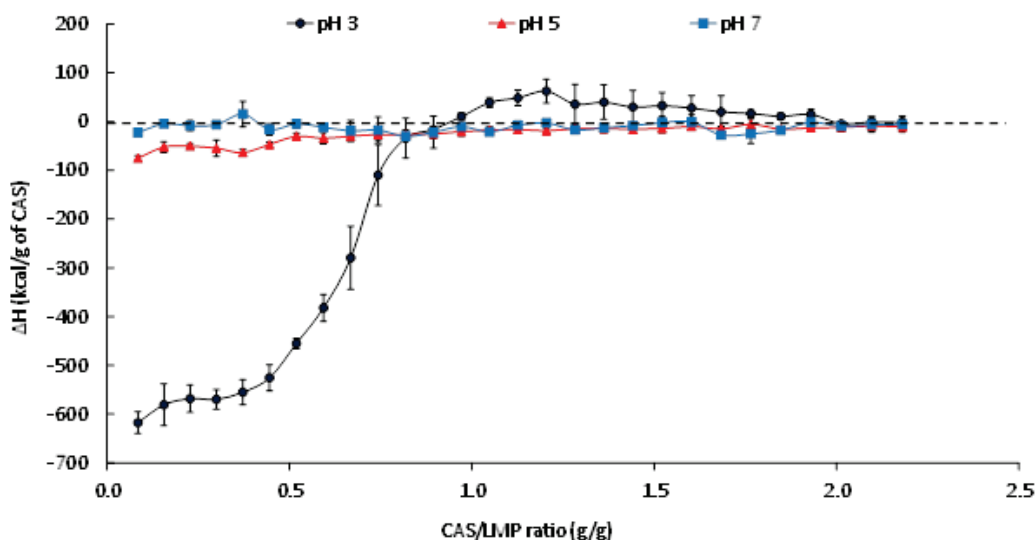


Figure 2.4. Enthalpy change (ΔH) versus CAS/LMP ratio when 5.0 g/L CAS solution is injected into a reaction cell containing 0.5 g/L LMP solution at pH 3.0, 5.0 and 7.0 (Imidazole-acetate buffer (5 mM); temperature: 25 °C; NaCl: 0 mM).

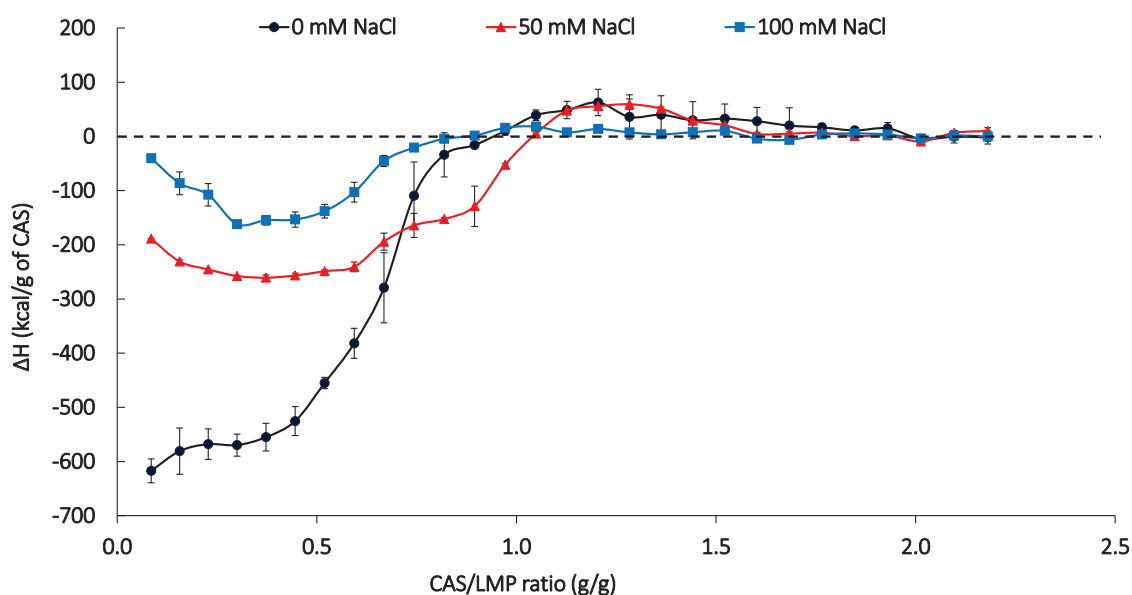


Figure 2.5. Enthalpy change (ΔH) versus CAS/LMP ratio when 5.0 g/L CAS solution is injected into a reaction cell containing 0.5 g/L LMP solution at pH 3.0 at different concentrations of NaCl (Imidazole-acetate buffer (5 mM); temperature: 25 °C; NaCl: from 0 mM to 100 mM).

As shown in Fig. 2.5, when NaCl concentration increased, the enthalpy change became smaller until a CAS/LMP ratio of about 1.0 (the saturation point). In addition, during the first 4-5 injections, the enthalpy change increased gradually and then decreased in the same way as the titration without NaCl. This may be due to the formation of an ionic screen preventing

interactions between the two biopolymers. Increasing the ratio results in breaking this screen and making interactions possible. This assumption seems plausible, especially since the decline in the curve is clearer in the presence of 100 mM NaCl as in the presence of 50 mM NaCl. According to Fig. 2.5, we can conclude that the ionic strength affects the intensity of interactions but not the saturation point and consequently all the interactions in the three studied NaCl concentrations ended at a CAS/LMP ratio of 1.0. In fact, NaCl would inhibit the binding interactions at the whole process until LMP chains became saturated with CAS as other authors reported (Xiong et al., 2017).

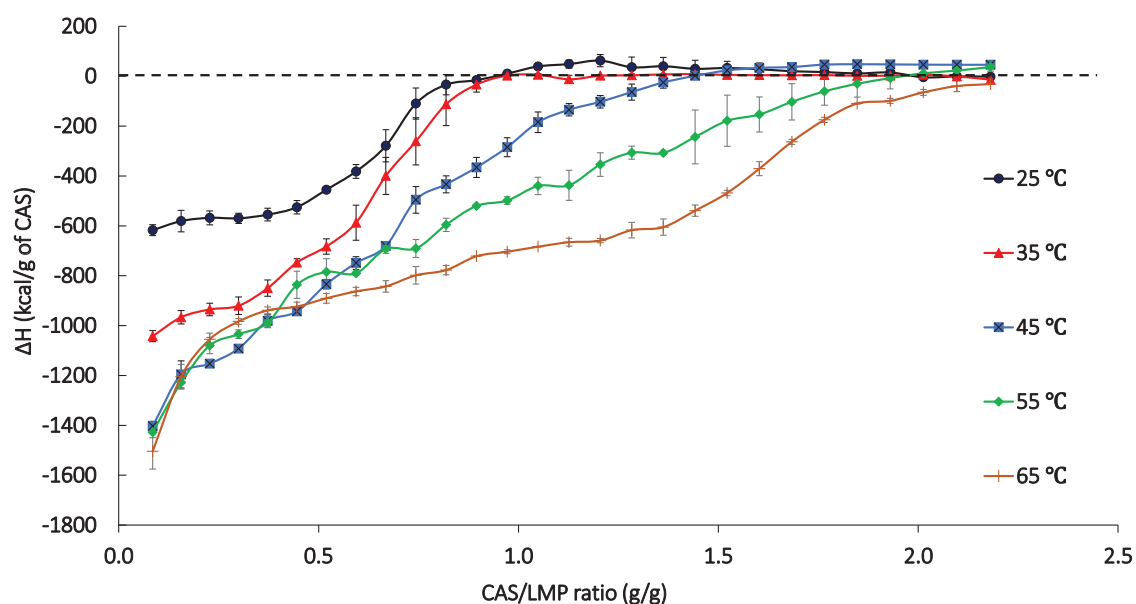


Figure 2.6. Enthalpy change (ΔH) versus CAS/LMP ratio when 5.0 g/L CAS solution is injected into a reaction cell containing 0.5 g/L LMP solution at different temperatures (Imidazole-acetate buffer (5 mM); temperature: from 25 °C to 65 °C; NaCl: 0 mM).

To study the effect of temperature on the binding interactions between CAS and LMP, ITC tests were performed at different temperatures (25 °C; 35 °C; 45 °C; 55 °C; 65 °C) by keeping all the other parameters unchanged. As shown in Fig. 2.6, with the increase of temperature from 25 °C to 65 °C, the saturation point of binding interactions increased from CAS/LMP ratio 1.0 to 2.0, and the enthalpy change also increased. It is known that the driving force of interactions between proteins and polysaccharides, at pH values below the pI of the protein, includes mainly electrostatic forces, but also hydrophobic interactions, Van der Waals forces and hydrogen bonds. The present results showed that the interaction between CAS and LMP was a spontaneous reaction ($\Delta G < 0$) and the main driving force was electrostatic in most of cases because ΔH was negative and ΔS was positive, as shown in Table 2.1 (binding parameters got from the curve fitted with “one set of sites”). Combined with the results

presented in Fig. 2.6, these parameters indicate that when the temperature was increased, enthalpy change (ΔH) (absolute value) increased while entropy change (ΔS), binding constant (K), and Gibbs free energy change (ΔG) (absolute value) decreased. In fact, low temperature favors hydrogen bonding while high temperature favors hydrophobic interactions (Csermely, Palotai, & Nussinov, 2010; Ross & Rekharsky, 1996). In the present study, high temperature was shown to favor the enthalpy change but was not favorable to the entropy change. This result indicate that hydrophobic interactions cannot be neglected during the formation of insoluble complexes.

Table 2.1. List of thermodynamic binding parameters for CAS-LMP interactions at 25 - 65 °C.

T (°C)	K(M ⁻¹)	ΔH (kcal/g)	ΔS (kcal/g/deg)	ΔG (kcal/g)
25	1.08E6±7.61E5	-621.2±32.81	25.2	-8134.6
35	1.51E5±3.54E4	-1008±24.21	20.1	-7201.8
45	4.14E4±1.10E4	-1358±69.42	16.8	-6702.9
55	1.01E4±4.69E3	-1576±317.2	13.9	-6137.3
65	8.79E3±4.51E3	-1577±251.2	12.9	-5939.1

Concerning the application of the biopolymer system studied in this work, the obtained results can be used to optimize the encapsulation processes of active molecules. For example, for the encapsulation of hydrophobic molecules such as essential oils, CAS-stabilized emulsions can be formed and oil/water interfaces could be reinforced by an additional layer of LMP *via* attractive interactions. Knowledge of the nature and intensity of these interactions in different physicochemical conditions should allow to better stabilize the encapsulated active molecules but also to control their release kinetics. In addition, if these emulsions are intended to be converted into powder, the study of the effect of temperature on the interactions between the two biopolymers seems to be interesting.

2.5. Conclusion

Through testing the transmittance and ζ -potential, this study tried to explain how LMP and CAS form complexes and how pH, ionic strength and temperature affect significantly the

interactions between LMP and CAS. Under the four tested CAS/LMP ratios (0.5, 1.0, 2.5, and 5.0), insoluble complexes, soluble complexes and co-soluble biopolymers were formed at different pH and the three corresponding zones have been delimited. At three typical pHs (3.0, 5.0 and 7.0), ITC tests were performed to study the interactions that can take place in each zone. The results showed that there were no significant interactions between the two biopolymers when they are co-soluble as is the case at pH 7.0. However, these results have shown that electrostatic interactions are the most important under conditions that lead to the formation of soluble and insoluble complexes. The intensity of the electrostatic interactions that leads to the formation of insoluble complexes was stronger than that of the electrostatic interactions involved in the formation of soluble complexes. After that, the effect of ionic strength and temperature on the intensity of binding interactions was also studied by ITC tests. The results showed that the presence of NaCl would form an ionic screen allowing to prevent the electrostatic interactions up to a certain CAS/LMP threshold ratio. Higher temperatures were shown to favor the enthalpic contribution which was related to the dissociation of LMP.

References

- Chang, C., Wang, T., Hu, Q., & Luo, Y. (2017). Zein/caseinate/pectin complex nanoparticles: Formation and characterization. *International Journal of Biological Macromolecules*, 104, 117-124.
- Chang, Y., Hu, Y., & McClements, D. J. (2016). Competitive adsorption and displacement of anionic polysaccharides (fucoidan and gum arabic) on the surface of protein-coated lipid droplets. *Food Hydrocolloids*, 52, 820-826.
- Cheng, W. & McClements, D. J. (2016). Biopolymer-stabilized conjugated linoleic acid (CLA) oil-in-water emulsions: Impact of electrostatic interactions on formation and stability of pectin-caseinate-coated lipid droplets. *Colloids and Surfaces A: Physicochemical and Engineering Aspects*, 511, 172-179.
- Csermely, P., Palotai, R., & Nussinov, R. (2010). Induced fit, conformational selection and independent dynamic segments: an extended view of binding events. *Trends in Biochemical Sciences*, 35(10), 539–546.
- Devi, N., Sarmah, M., Khatun, B., & Maji, T. K. (2017). Encapsulation of active ingredients in polysaccharide-protein complex coacervates. *Advances in Colloid Interface Science*, 239, 136-145.
- Dickinson, E. (2006). Structure formation in casein-based gels, foams, and emulsions. *Colloids and Surfaces A: Physicochemical and Engineering Aspects*, 288(1-3), 3-11.
- Eghbal, N., Degraeve, P., Oulahal, N., Yarmand, M. S., Mousavi, M. E., & Gharsallaoui, A. (2017). Low methoxyl pectin/sodium caseinate interactions and composite film formation at neutral pH. *Food Hydrocolloids*, 69, 132-140.
- Eghbal, N., Yarmand, M. S., Mousavi, M., Degraeve, P., Oulahal, N., & Gharsallaoui, A. (2016). Complex coacervation for the development of composite edible films based on LM pectin and sodium caseinate. *Carbohydrate Polymers*, 151, 947-956.
- Fabra, M. J., Talens, P., & Chiralt, A. (2008). Tensile properties and water vapor permeability of sodium caseinate films containing oleic acid–beeswax mixtures. *Journal of Food Engineering*, 85(3), 393-400.
- Fioramonti, S. A., Perez, A. A., Aringoli, E. E., Rubiolo, A. C., & Santiago, L. G. (2014). Design and characterization of soluble biopolymer complexes produced by electrostatic self-assembly of a whey protein isolate and sodium alginate. *Food Hydrocolloids*, 35, 129-136.
- Gorji, S. G., Gorji, E. G., & Mohammadifar, M. A. (2014). Characterisation of gum tragacanth (*Astragalus gossypinus*)/sodium caseinate complex coacervation as a function of pH in an aqueous medium. *Food Hydrocolloids*, 34(34), 161-168.
- Happi Emaga, T., Garna, H., Paquot, M., & Deleu, M. (2012). Purification of pectin from apple pomace juice by using sodium caseinate and characterisation of their binding by isothermal titration calorimetry. *Food Hydrocolloids*, 29(1), 211-218.
- Hassan, B., Chatha, S. A. S., Hussain, A. I., Zia, K. M., & Akhtar, N. (2018). Recent advances on polysaccharides, lipids and protein based edible films and coatings: A review. *International Journal of Biological Macromolecules*, 109, 1095-1107.

- Li, Q., & Zhao, Z. (2017). Formation of lactoferrin/sodium caseinate complexes and their adsorption behaviour at the air/water interface. *Food Chemistry*, 232, 697-703.
- Liu, J., Corredig, M., & Alexander, M. (2007). A diffusing wave spectroscopy study of the dynamics of interactions between high methoxyl pectin and sodium caseinate emulsions during acidification. *Colloids and Surfaces B: Biointerfaces*, 59(2), 164-170.
- Lv, Y., Yang, F., Li, X., Zhang, X., & Abbas, S. (2014). Formation of heat-resistant nanocapsules of jasmine essential oil via gelatin/gum arabic based complex coacervation. *Food Hydrocolloids*, 35, 305-314.
- Matia-Merino, L., Lau, K., & Dickinson, E. (2004). Effects of low-methoxyl amidated pectin and ionic calcium on rheology and microstructure of acid-induced sodium caseinate gels. *Food Hydrocolloids*, 18(2), 271-281.
- Ross, P. D. & Rekharsky, M. V. (1996). Thermodynamics of hydrogen bond and hydrophobic interactions in cyclodextrin complexes. *Biophysical Journal*, 71(4), 2144-2154.
- Schmitt, C. & Turgeon, S. L. (2011). Protein/polysaccharide complexes and coacervates in food systems. *Advances in Colloid Interface Science*, 167(1-2), 63-70.
- Surh, J., Decker, E., & McClements, D. (2006). Influence of pH and pectin type on properties and stability of sodium-caseinate stabilized oil-in-water emulsions. *Food Hydrocolloids*, 20(5), 607-618.
- Wang, L. Z., Liu, L., Holmes, J., Kerry, J. F., & Kerry, J. P. (2007). Assessment of film-forming potential and properties of protein and polysaccharide-based biopolymer films. *International Journal of Food Science & Technology*, 42(9), 1128-1138.
- Xiong, W., Ren, C., Jin, W., Tian, J., Wang, Y., Shah, B. R., Li, J., & Li, B. (2016). Ovalbumin-chitosan complex coacervation: Phase behavior, thermodynamic and rheological properties. *Food Hydrocolloids*, 61, 895-902.
- Xiong, W., Ren, C., Tian, M., Yang, X., Li, J., & Li, B. (2017). Complex coacervation of ovalbumin-carboxymethylcellulose assessed by isothermal titration calorimeter and rheology: Effect of ionic strength and charge density of polysaccharide. *Food Hydrocolloids*, 73, 41-50.
- Xu, Y., Mazzawi, M., Chen, K., Sun, L., & Dubin, P. L. (2011). Protein purification by polyelectrolyte coacervation: influence of protein charge anisotropy on selectivity. *Biomacromolecules*, 12(5), 1512-1522.
- Ye, A., Gilliland, J., & Singh, H. (2011). Thermal treatment to form a complex surface layer of sodium caseinate and gum arabic on oil-water interfaces. *Food Hydrocolloids*, 25(7), 1677-1686.
- Yuan, Y., Wan, Z.-L., Yin, S.-W., Teng, Z., Yang, X.-Q., Qi, J.-R., & Wang, X.-Y. (2013). Formation and dynamic interfacial adsorption of glycinin/chitosan soluble complex at acidic pH: Relationship to mixed emulsion stability. *Food Hydrocolloids*, 31(1), 85-93.

Summary of Chapter 3

For applying complex coacervation between CAS and LMP to encapsulate hydrophobic compounds, the formation of oil-in-water (O/W) emulsions is the first step. Then, the O/W emulsions can be stabilized by CAS/LMP complexes (complexes-stabilized emulsion) or by CAS followed by addition of the second LMP layer (Layer-by-layer (LBL)-stabilized emulsion). The aim of this work was to compare the two strategies of emulsion preparation in order to understand the effect on the interactions between the molecules and the impact on the stability of the emulsion. According to the present study, CAS can strongly bind with LMP at pH 3.0. The physicochemical properties of CAS/LMP complexes at different ratios were further studied at this pH, and the two kinds of O/W emulsions formed at this pH were compared by measuring zeta potential, dynamic viscosity, serum index, and particle size distribution. This study is presented as a scientific article published in “*Journal of Food Process Engineering*”.

CHAPTER 3

Influence of Low Methoxyl pectin on the physicochemical properties of sodium caseinate-stabilized emulsions

Wang Jian, Sondes Souihi, Chedia Ben Amara, Emilie Dumas, and Adem Gharsallaoui

Journal of Food Process Engineering, 2018. 41(8): p. e12906

3.1. Abstract

Two strategies of emulsion preparation, stabilization by sodium caseinate (CAS) / Low Methoxyl pectin (LMP) complexes formed in advance, and stabilization by the layer-by-layer (LBL) method, were compared. In aqueous solution, at a constant CAS concentration (5 g/L), the gradual addition of LMP resulted in an increase in turbidity of the solution caused by the increasing formation of insoluble complexes. The zeta potential change showed that the interactions are mainly due to an electrostatic mechanism. The spectrofluorometric studies as well as the spectroscopic analysis in the UV-visible region have shown that the interactions with LMP caused a change in the secondary and tertiary structures of the protein. Then, these complexes were used for stabilizing Oil / Water emulsions. The emulsions stabilized by complexes formed in advance and layer-by-layer method were characterized by measuring zeta potential, dynamic viscosity, serum index, and particle size distribution. The results showed that, at low LMP concentrations, complexes-stabilized emulsions were more stable than LBL-stabilized ones, while at high LMP concentrations, LBL-stabilized emulsions showed better stability.

3.2. Introduction

Oil-in-water (O/W) emulsions are widely used in food industry. Food products such as milk, mayonnaise, and chocolate, among others, are examples of O/W emulsions. O/W emulsions also can be used to encapsulate functional hydrophobic molecules such as essential oils. Traditionally, O/W emulsions are produced by homogenizing oil and aqueous phases together in the presence of one or more emulsifiers (Guzey & McClements, 2006). Proteins and polysaccharides are typical emulsifiers used in food industry for their safety, availability, low cost, and biocompatibility.

Protein-polysaccharide complexes as emulsifiers are well studied (Evans, Ratcliffe, & Williams, 2013; Xu, Wang, & Yao, 2017). Layer-by-layer (LBL) technique is also extensively studied as a strategy to improve emulsion stability, which allows the step-wise adsorption of various components (Lim & Roos, 2017; Shchukina & Shchukin, 2012; Xiang, Lyu, & Narsimhan, 2016). In these two methods, the binding between proteins and polysaccharides is a non-covalent interaction, mainly by electrostatic attractive interactions, followed by hydrophobic interactions, hydrogen bonding, and Van-der-Waals force. For the LBL technique, a primary emulsion is firstly prepared with the protein as emulsifier, because proteins can form a strongly adsorbed layer at the interface that prevents droplet coalescence. Then, the polysaccharide is added to form the secondary interfacial layer *via* electrostatic forces to improve the texture and the stability of the emulsion. A three-layered-emulsion can be prepared by adding another oppositely charged polyelectrolyte. For preparing complexes-stabilized emulsions, protein/polysaccharide complexes are prepared initially as emulsifiers, then oil is added to form emulsion by directly homogenizing. Due to the different process sequences, the resulting emulsion is also structurally different.

Each one of these two methods has its own advantages and drawbacks. According to many previous literatures, the emulsions prepared by LBL technique have improved stability to environmental stresses, such as temperature, pH, and ionic strength (Chang & McClements, 2015; Owens, Griffin, Khouryieh, & Williams, 2018; Shchukina & Shchukin, 2012; Zhao, Xiang, Wei, Yuan, & Gao, 2014). Regarding complexes-stabilized emulsions, they have shown good prospects. In fact, using protein-polysaccharide complexes as emulsifier has been shown to improve surface activity (Benichou, Aserin, Lutz, & Garti, 2007), absorption of the core material (Xu et al., 2017) and stability (Setiowati, Vermeir, Martins, De Meulenaer, & Van der Meeren, 2016; Ye, Gilliland, & Singh, 2011). These two methods have similar drawbacks: depended on the different properties of core materials, and the emulsifier is not necessarily applicable to all materials (Guzey & McClements, 2006). Because of the electrostatic interactions between proteins and polysaccharides in the interfacial membranes, the binding strength can be affected by environmental conditions (pH, ionic strength, among others), which can be a drawback, can also be used to control the release of the core material in different environments. When applied to actual production, compared to the process of preparing complexes-stabilized emulsions, LBL technique needs more steps to form the second layer or the third layer. It is therefore necessary to compare the consequences of these two methods on the stability of the emulsions and to evaluate whether the “benefits” generated justify the additional production steps.

In this study, complexes with different ratios of CAS/ LMP were formed at pH 3 to study the interactions between the two biopolymers in solution. Then, these complexes were used to prepare complexes-stabilized emulsions. LBL-stabilized emulsions were also prepared with the same biopolymers. Interfacial adsorption and consequences on the structure of these two kinds of emulsions were investigated to understand the interactions between caseinate and LMP at oil/water interface. The stability of emulsions was also investigated to compare these two strategies for emulsion preparation.

3.3. Materials and methods

3.3.1. Materials

LMP (Unipeptine™ OF 305 C SB; degree of esterification: 22-28%) was purchased from Cargill (Baupre, France). CAS was from Fisher Scientific (United Kingdom). Protein content in CAS determined by the Kjeldahl method was 93.20% (nitrogen conversion factor N=6.38 (Consoli et al., 2018)). Analytical grade imidazole ($C_3H_4N_2$), acetic acid, sodium hydroxide (NaOH), hydrochloric acid (HCl), and 8-Anilino-1-naphthalenesulfonic acid (ANS) were purchased from Sigma-Aldrich Chimie (St Quentin Fallavier, France). Sunflower seed oil was purchased from local supermarket in France. Distilled water was used for all the preparations.

3.3.2. Preparation of complexes suspensions

Imidazole-acetate buffer solutions (5.0 mM) were prepared by dispersing weighed amounts of imidazole and acetic acid into distilled water and then adjusting the pH to 3.0. The stock solutions were prepared by dispersing LMP and CAS powders to unadjusted imidazole-acetate buffer and stirring for at least 2 h at room temperature, and then adjusting the pH to 3.0. The pH was adjusted by using HCl (0.1 or 1.0 M) or NaOH (0.1 or 1.0 M). Complexes suspensions were prepared by mixing the biopolymer stock solutions and their dilution to the desired concentration by imidazole-acetate buffer (pH 3.0). CAS concentration was constant at 5.0 g/L while LMP concentration was variable from 0.0 to 8.0 g/L. After mixing, the suspensions of complexes were stirred for at least 2 h at room temperature.

3.3.3. Turbidity and UV-absorbance measurements

The turbidity of complexes suspensions at pH 3.0 was measured by using a UV/Vis spectrophotometer (Jenway 3705, Villepinte, France) at 600 nm in plastic cuvettes (1 cm path length). The solution with 0.0 g/L LMP and 5.0 g/L CAS was used as blank, and every suspension was measured at least three times. Absorbance was measured at 280 nm with a

UV/Vis spectrophotometer (Lightwave II 109233, Biochrom, Cambridge, UK) in a 1.0 cm quartz cell at room temperature (25 °C) against imidazole-acetate buffer (5.0 mM; pH 3). Samples were vortexed for 1 min before assays.

3.3.4. Protein surface hydrophobicity measurement

To study the effect of complexation on the surface hydrophobicity of CAS, 8-Anilino-1-naphthalenesulfonic acid (ANS) fluorescent probe ($\lambda_{\text{excitation}}$: 380 nm and $\lambda_{\text{emission}}$: 420 – 650 nm) was used due to its affinity for hydrophobic sites of protein molecules. Stock solution of ANS with a concentration of 20 mg/L was prepared by dissolving the probe in pH 3 imidazole-acetate buffer at 5.0 mM. In 10 mL complexes suspensions containing 5.0 g/L CAS and 0.0 to 8.0 g/L LMP, 10–50 μ L ANS solutions were added respectively. After preliminary experiments, the excitation and emission bandwidths were fixed at 7.5 nm and the scan rate was 500 nm/min.

The changes in fluorescence intensity associated with ANS binding to the protein surface hydrophobic regions were monitored with a LS 55 spectrofluorometer (Perkin Elmer, Courtaboeuf, France). The increase in fluorescence emission was recorded until no further increase was observed. The maximum fluorescence intensity was plotted as a function of ANS concentration. The initial slope of the fluorescence intensity (arbitrary unit, a.u.) *versus* ANS concentration (mg/L) plot was calculated and used as an index of CAS surface hydrophobicity (S_0). Each spectrum was obtained in triplicate. All measurements were made at room temperature (25 °C), using a quartz cuvette with 1 cm path length.

3.3.5. Emulsion preparation

3.3.5.1. Preparation of complexes-stabilized emulsions

Sunflower seed oil (10 g sunflower seed oil for 100 g emulsion) was added to CAS/ LMP complexes suspensions prepared as shown in section 2.2. Emulsions (5.0 g/L CAS; 0.0 – 8.0 g/L LMP) were obtained by using an Ultra Turrax PT 4000 homogenizer (IKA Lab. Technol. Co.) at 20 000 rpm for 5 min, and then further homogenized at 500 bar with five recirculations using a high pressure homogenizer (SPX Brand, APV Model 1000).

3.3.5.2. Preparation of emulsions by LBL technique

Primary emulsions containing 20% (w/w) sunflower seed oil, stabilized by 10% CAS solution were prepared firstly as detailed in the previous section, and LMP solutions with different concentrations were then added to dilute the concentration of sunflower seed oil to 10% (w/w) and that of CAS to 5.0 g/L. The final LMP concentrations ranged between 0.0 and 8.0

g/L.

3.3.6. Zeta potential measurement

The electric charge (ζ -potential) of CAS/ LMP complexes and oil droplets of the prepared emulsions were determined using a Zetasizer Nano ZS90 (Malvern Instruments, Malvern, UK). The samples were diluted 100 times with pH 3.0 imidazole-acetate buffer at 5.0 mM prior to the measurement in order to avoid significant multiple scattering. The mean ζ -potential (ZP) values (\pm SD (standard deviation)) were obtained from the instrument.

3.3.7. Particle size distribution

Particle size distributions of CAS/ LMP complexes and emulsions were assessed by a laser diffraction instrument (Mastersizer 3000, Malvern Instruments, Malvern, UK) using a refractive index of 1.46. The complexes or emulsions were injected into the measurement chamber where they were diluted with imidazole-acetate buffer (5.0 mM; pH 3.0) prior to the measurements. They were stirred continuously throughout the measurement to ensure the samples were homogeneous. The particle size distributions were obtained from three injections of three separate samples with five readings per sample.

3.3.8. Viscosity measurement

The viscosity of CAS/ LMP complexes and emulsions was measured with a coaxial cylinder viscometer (DV2T™ BROOKFIELD).

3.3.9. Emulsion stability measurement

In order to better visualize the limit that separates the aqueous phase (serum) from the creamed one, oil colored with Sudan red (50 mg/L) was used in the formulation of the emulsions. After emulsification, the emulsions were placed in test tubes and stored at 25 °C. During storage, all the unstable emulsions were separated into two phases: a pink phase (rich in oil) and a transparent phase at the bottom (serum). The Serum Index (SI) was calculated with the following formula:

$$SI (\%) = H_S/H_E \times 100 \quad (3.1)$$

H_E : the height of emulsion

H_S : the height of transparent phase (serum).

The serum index was measured and monitored daily.

3.3.10. Statistical analysis

All assays were measured at least in triplicate. Means and standard deviations were calculated and differences between means were determined with Fishers *Least Significant Difference* (LSD) test at $p < 0.05$ significance level (Statgraphics Centurion XV).

3.4. Results and discussion

3.4.1. Turbidity of complexes suspensions

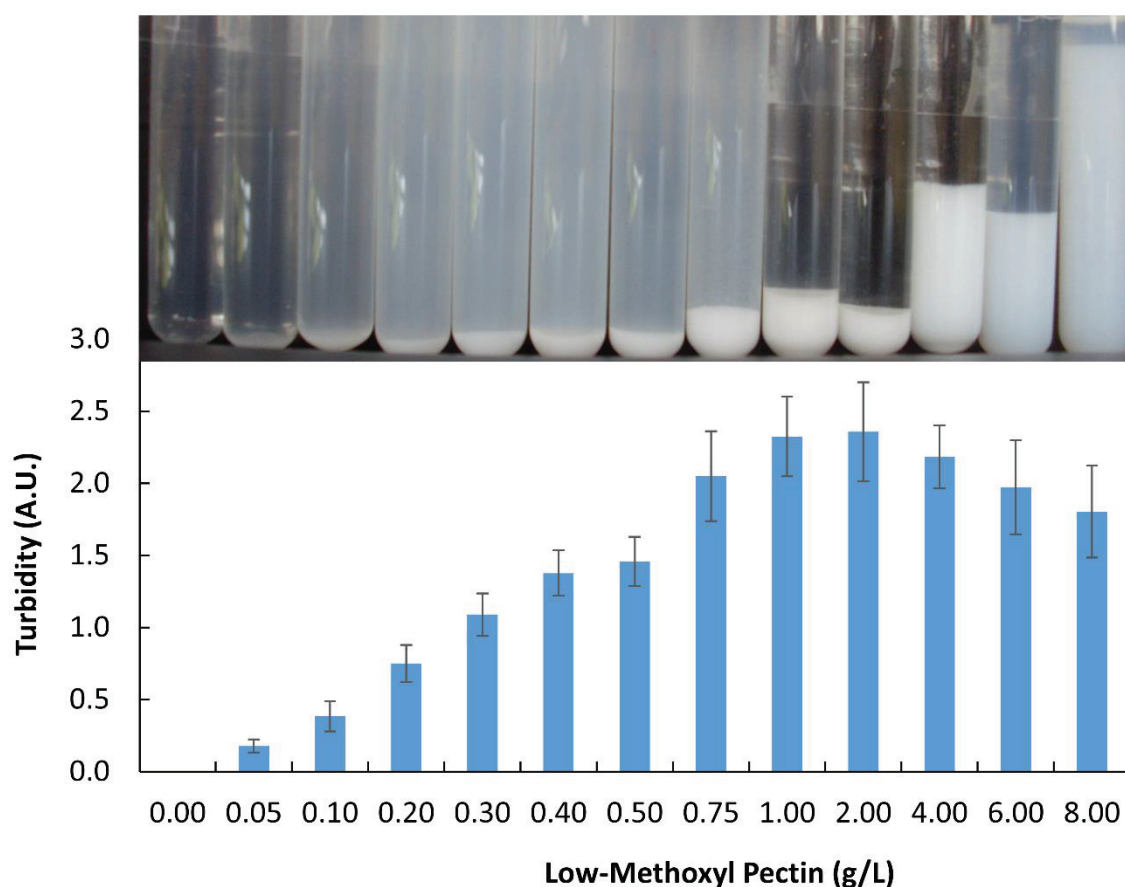


Figure 3.1. Turbidity (at 600 nm) of suspensions of complexes (5.0 g/L sodium caseinate) as a function of low methoxyl pectin concentration (0.0 – 8.0 g/L) and visual aspects after 2 h of tubes corresponding to each low methoxyl pectin concentration.

Fig. 3.1 shows that the turbidity increased as the LMP concentration increased until a maximum peak corresponding to a LMP concentration of 1.0 g/L, and decreased slightly when LMP concentration continued to increase. From the tubes corresponding to each concentration of LMP, the aggregation was first observed for low LMP concentrations. At these LMP concentrations, the complexes were slightly aggregated. Subsequently, increasing the concentration of LMP up to 1.0 g/L resulted in an increase of the number of individual complexes and/or an association of the individual complexes with each other and consequently an increase in the apparent average size followed by aggregation (Bayarri, Oulahal, Degraeve, & Gharsallaoui, 2014). For LMP concentrations higher than 2 g/L, turbidity slightly decreased, which could be explained by the formation of high size and less dense complexes allowing light to pass through the suspensions when measuring turbidity. From this LMP concentration, the

volume of the white phases increased significantly (tubes in Fig. 3.1 corresponding to 4, 6 and 8 g/L of LMP) confirming that insoluble complexes were less dense and having a loose structure. Thus, the formation of this loose structure could be due to the saturation of the cationic sites of CAS molecules allowing probably to partial dissociation of aggregates and segregation phase separation by electrostatic repulsions between the individual complexes. The increase of LMP concentration can also cause flocculation by depletion due to the presence of an excess of free LMP chains in the continuous phase.

3.4.2. Zeta potential and dynamic viscosity of complexes

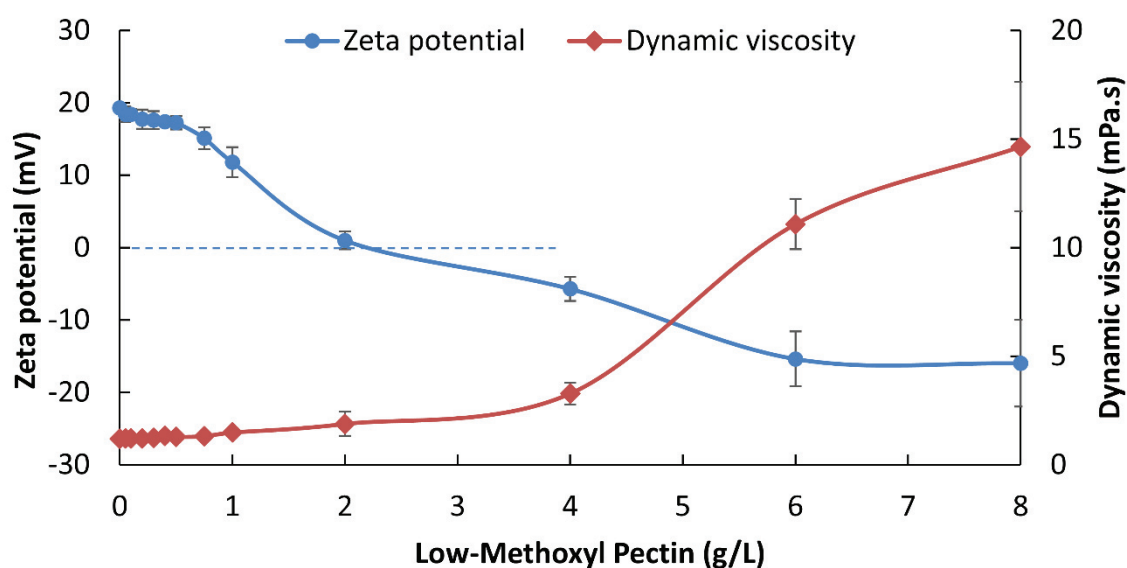


Figure 3.2. Zeta-potential and dynamic viscosity of suspensions of complexes (5.0 g/L sodium caseinate) as a function of low methoxyl pectin concentration (0.0 – 8.0 g/L).

As shown in Fig. 3.2, the Zeta potential of formed complexes changed from positive to negative when the LMP concentration increased, indicating that the polyanionic polysaccharide adsorbed gradually to the cationic surface of the protein molecules mainly *via* electrostatic interactions leading to complexation. The neutral charge of complexes was observed at a LMP concentration equal to 2 g/L. Then, the negative charge of the complexes reached a plateau when the LMP concentration reached 6 g/L, which confirmed that the cationic sites of CAS were saturated by the LMP chains at this concentration. The plateau was reached at a zeta potential value of approximately -15 mV (a mixture of complexes and free LMP chains). This result can be explained by the fact that several carboxyl groups of the LMP have been linked to the CAS. The dynamic viscosity of the complexes increased when LMP concentration increased (Fig. 3.2). At low concentrations of LMP, dynamic viscosity increased slightly until the LMP concentration reached 4 g/L. With LMP concentration increasing, cationic sites of CAS were

saturated and the strong hydration of the excess LMP chains (Einhorn-Stoll, 2018) could be responsible for the observed dynamic viscosity increase.

3.4.3. Effect of complexation on caseinate structure and surface hydrophobicity

The UV absorbance in the 280 nm region reflects the intrinsic absorbance of the phenyl moiety of aromatic amino acids (Tyrosine, Tryptophan and Phenylalanine). The intensity variation at 280 nm as a function of increasing concentrations of LMP was thus determined in order to study the effect of the complexation on the structure of CAS (Fig. 3.3). In the presence of increasing concentrations of LMP, a dramatical increase in absorbance intensity was observed until LMP concentration reached 0.5 g/L. Then, the increase rate slowed down, and reached a plateau. This increase could be attributed to the formation of CAS / LMP complexes and their aggregation. These results indicate the existence of molecular interactions between LMP and CAS at pH 3 which lead to an exposure of aromatic amino acids that occurs once small amounts of LMP were added. The addition of LMP above 0.5 g/L slightly affected the molecular structure of the protein. We can thus conclude that between 0.5 and 8.0 g/L of LMP, we have a phenomenon of macroscopic rearrangement linked to the aggregation of individual complexes and the molecular structure of CAS would be little modified.

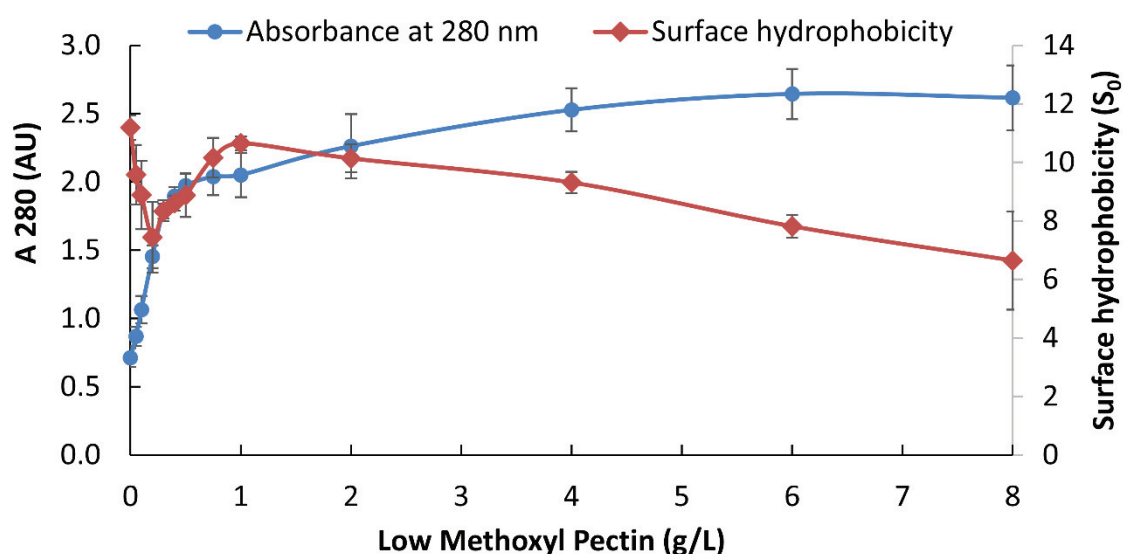


Figure 3.3. Absorbance (at 280 nm) and surface hydrophobicity of suspensions of complexes (5.0 g/L sodium caseinate) as a function of the concentration of low methoxyl pectin (0.0 – 8.0 g/L).

A decrease in surface hydrophobicity (S_0) was observed for low LMP concentrations up to 0.2 g/L (Fig. 3.3). This could indicate that the hydrophobic sites of the protein were gradually

masked by the adsorption of small amounts of LMP forming thus small individual complexes (Bayarri et al., 2014). A possible explanation for this initial decrease in S_0 would be the onset of aggregation where the non-native protein fraction aggregated primarily due to the segregative effect of the polysaccharide, and the native fraction will be probed thereafter. Nevertheless, increasing the concentration of LMP up to the turbidity peak at 1.0 g/L (Fig. 3.1) produced an increase in S_0 , which could be associated with the exposure of the hydrophobic sites of the protein (Bi, Tang, Gao, Jia, & Lv, 2016). The decrease in S_0 for high concentrations of LMP from 2.0 g/L can be correlated with the masking of the hydrophobic sites of the protein, which could be associated with the increase of the size of aggregates (Benichou, et al., 2007).

3.4.4. Zeta potential and dynamic viscosity of caseinate/low methoxyl pectin-stabilized emulsions

The zeta potential of oil droplets in complexes-stabilized emulsions and LBL-stabilized emulsions (Fig. 3.4A) varied as a function of the LMP concentration (0.0 to 8.0 g/L). As expected, in the absence of LMP, the oil droplet charge was positive (+35 mV) at pH 3 which is lower than the protein pHi (~ 4.6), and became negative with increasing the added LMP amount. The zeta potential of both emulsions became zero between 2.0 g/L and 4.0 g/L of LMP. From a LMP concentration of 6.0 g/L, the overall charge became constant (-15 mV for complexes-stabilized emulsion and -10 mV for LBL-stabilized emulsion). The decrease of the zeta potential values as a function of the increase in the LMP concentration proved the adsorption of LMP to CAS resulting in an overall electrical charge which decreased as a function of the LMP concentration. Then the zeta potential of both emulsions reached a plateau, indicating the existence of free LMP chains in excess giving this negative charge.

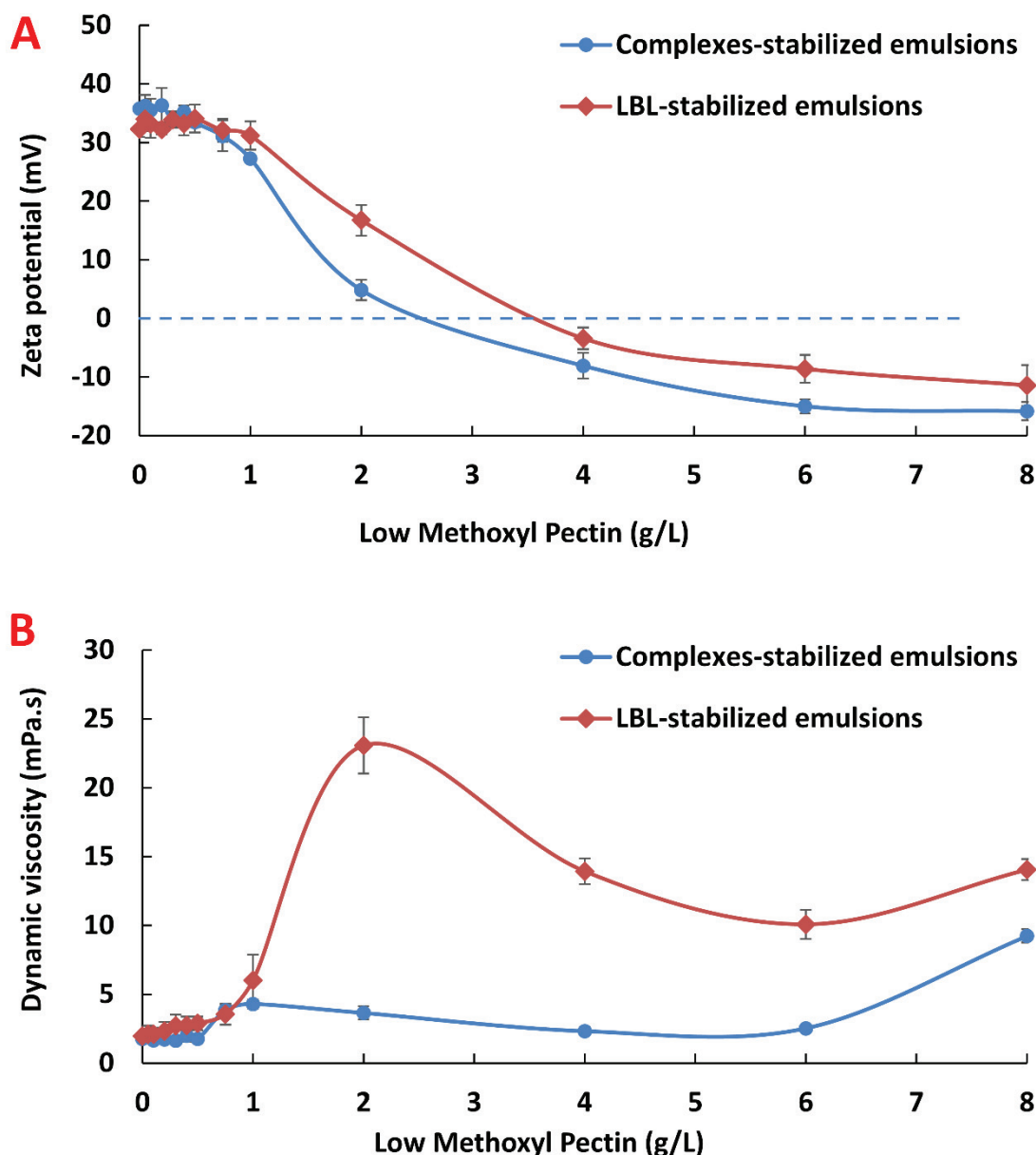


Figure 3.4. (A) Zeta-potential of complexes-stabilized emulsions and LBL-stabilized emulsions as a function of low methoxyl pectin concentration (0.0 – 8.0 g/L). (B) Dynamic viscosity of complexes-stabilized emulsions and LBL-stabilized emulsions as a function of low methoxyl pectin concentration (0.0 – 8.0 g/L). All emulsions contained 5.0 g/L sodium caseinate.

Fig. 3.4B showed that the dynamic viscosity varied as a function of the LMP concentration. By comparing the two types of emulsions, these results showed that at low concentrations of LMP from 0.0 to 1.0 g/L, the dynamic viscosities of these two emulsions were similar. With increasing LMP concentration, the dynamic viscosity of LBL-stabilized emulsions was much higher than that of complexes-stabilized emulsions. For complexes-stabilized emulsions, an increase in the dynamic viscosity was observed as a function of the increase in LMP

concentration until a maximum (5 mPas) reached at 1.0 g/L. For LBL-stabilized emulsions, the maximum viscosity was much higher (23 mPas) and was reached at 2.0 g/L. This can be explained by the interactions between CAS and LMP in complexes-stabilized emulsions that could cause exposition of LMP charged groups stronger than in LBL-stabilized emulsions. The maximum viscosity reached could mean that the presence of a sufficient amount of LMP which was already adsorbed on the surface of the protein during the formation of complexes would ensure strong repulsions between the droplets. Then, the viscosity decreased progressively at high LMP concentrations from 2.0 g/L to 6.0 g/L. This can be correlated with charge neutralization and the occurrence of two phases due to depletion flocculation which decreased the viscosity of the continuous phase (Surh, Decker, & McClements, 2006). The phenomenon of flocculation by depletion caused the enrichment of the aqueous phase in free LMP chains and "expulsion" of the droplets towards the surface. For 8.0 g/L of LMP, the large amount of LMP present in the aqueous phase could be the reason of the emulsion viscosity increase.

3.4.5. Stability and particle size distribution of emulsions

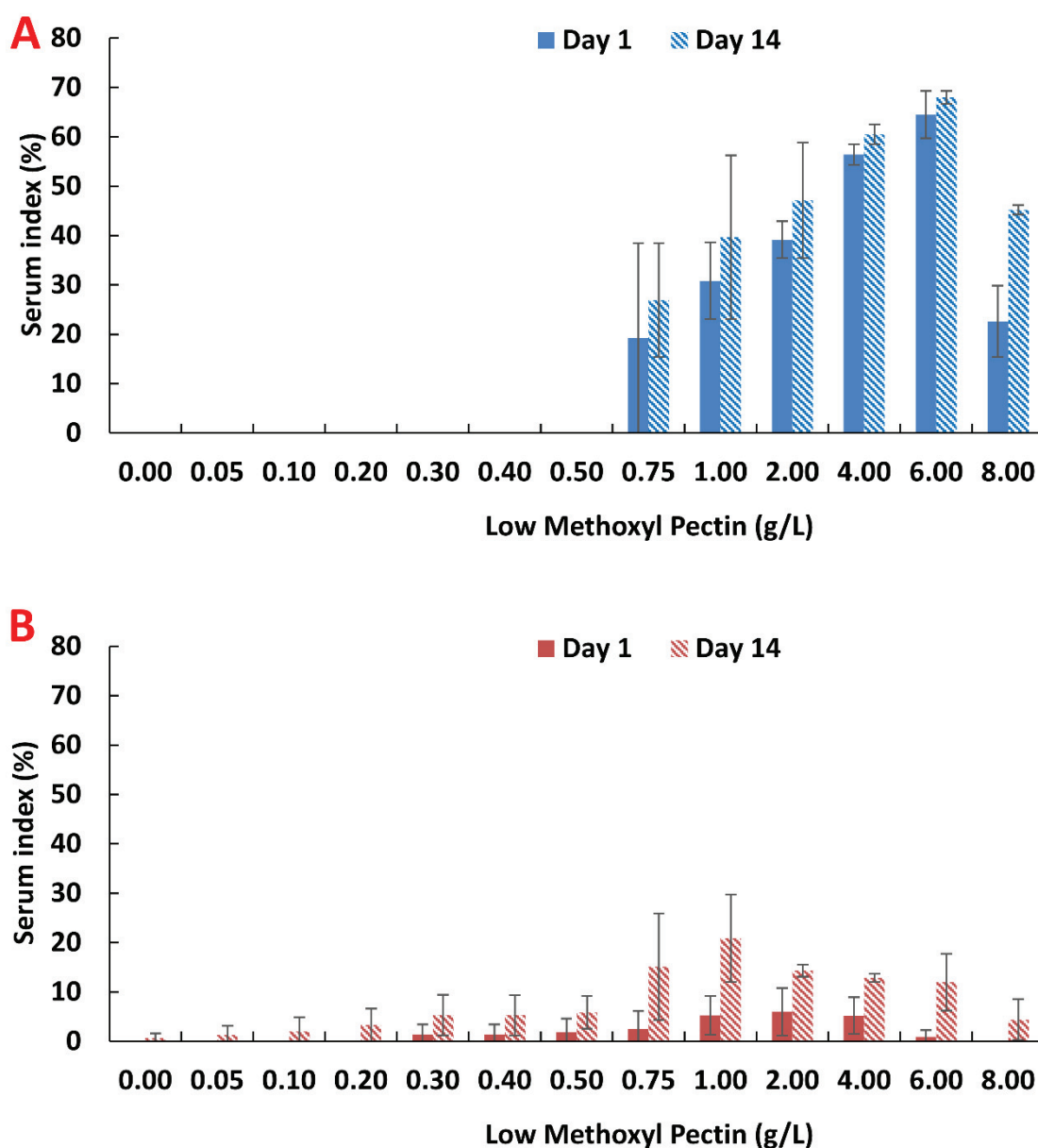


Figure 3.5. (A) Serum index of complexes-stabilized emulsions as a function of low methoxyl pectin concentration (0.0 – 8.0 g/L) after 1 and 14 days. (B) Serum index of LBL-stabilized emulsions as a function of low methoxyl pectin concentration (0.0 – 8.0 g/L). All emulsions contained 5.0 g/L sodium caseinate.

Creaming of emulsions stabilized by complexes or LBL method in day 1 and day 14 at different concentrations of LMP is shown in Fig. 3.5. For complexes-stabilized emulsions at low LMP concentrations (0.0 to 0.5 g/L), the emulsions were stable up to 14 days with a serum index of 0% (Fig. 3.5A). These emulsions have an average droplet size of about 0.7 μm (Fig 6). This stability could be partly due to relatively strong electrostatic repulsions between droplets that prevent them from getting closer and aggregating (Cho & McClements, 2009). At higher

LMP concentrations (0.75 to 6.0 g/L), the serum index of complexes-stabilized emulsions increased with increasing LMP concentration up to 6.0 g/L. The serum index changed between 1 and 14 days as well as the average size of the fat globules (Fig. 3.6). The low creaming stability observed at relatively high concentrations of LMP can be attributed to the increase in the apparent oil droplet size and/or depletion flocculation caused by the presence of unabsorbed LMP chains in the aqueous phase (Cho & McClements, 2009). For the concentration of 8.0 g/L of LMP, a moderately low serum index was observed compared to other high LMP concentrations which could be attributed to the relatively low viscosity of this emulsion (Fig. 3.4B).

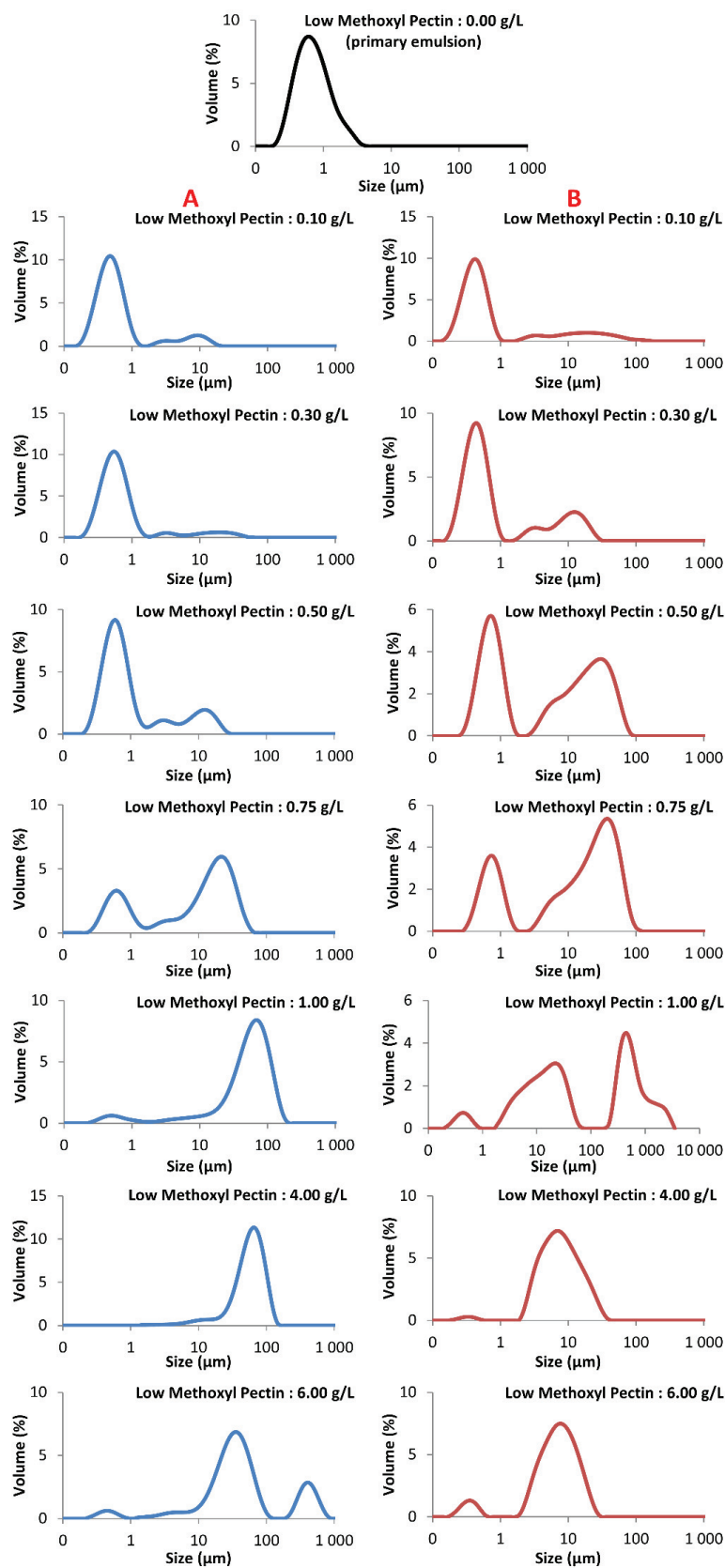


Figure 3.6. Particle size distribution of primary emulsions (stabilized by 5.0 g/L sodium caseinate), complexes-stabilized emulsions (A) and LBL-stabilized emulsions (B) as a function of low methoxyl pectin concentration (0.0 – 8.0 g/L).

As shown in Fig. 3.5B, the serum index of LBL-stabilized emulsions increased with LMP concentration up to 1.0 g/L and then decreased slightly for higher concentrations. For very low concentrations of LMP (≤ 0.5 g/L) there was an average size population of about 0.4 μm whereas for higher concentrations (> 0.5 g/L) there was a significant increase in the average size of the oil droplets (Fig. 3.6). For LMP concentrations from 0.1 to 1.0 g/L, two to three populations with different mean size appeared. For these intermediate concentrations of LMP, the emulsions were the most unstable and the serum index increased from the first day. This instability could be attributed to charge neutralization and bridging flocculation caused by sharing anionic LMP molecules between two or more cationic protein-coated droplets (Cho & McClements, 2009). For high concentrations of LMP (> 1.0 g/L), the sufficient amount of LMP allowed to cover the surface of the droplets by relatively increasing electrostatic and steric repulsions with a decrease in the average droplet size. These emulsions are poorly stable with a moderately high serum index, which is due to the phenomenon of flocculation by depletion. When LMP concentration exceeded 4.0 g/L, a more stable multilayered emulsions with a negative overall charge (Fig. 3.4A and 3.6B) have begun to appear.

3.5. Conclusion

In this work, the obtained results demonstrated that LMP is able to form insoluble complexes by coacervation with CAS. This association showed that for low concentrations of LMP, individual complexes were formed. For the intermediate concentrations up to the peak of turbidity, an aggregation of individual complexes was observed by bridging. For the high concentrations of LMP, a phase separation occurred by depletion flocculation with saturation of the protein cationic sites. It has been shown that the protein molecules have undergone structural changes in their spatial configuration in the presence of LMP. The stabilization of the emulsions by the formed complexes seems to be better than the LBL method in the case of low ratios of LMP/CAS, as demonstrated by the mean droplet size and the serum index measurements. Thus, it was shown that for the complexes-stabilized method, for low and intermediate LMP concentrations, the emulsions were stable up to 14 days whereas for the LBL method, instability appeared for all the emulsions at the different LMP concentrations on the 14th day but the stability of LBL emulsions was higher at high LMP concentrations. Concerning food applications of the developed emulsions, the organic phase which has been used will be replaced by hydrophobic molecules having antimicrobial activity (mainly essential oils). These molecules will subsequently be encapsulated by spray-drying and the interactions between CAS and LMP will be used to control their release kinetics. Indeed, these microcapsules could be incorporated into food matrices with different physicochemical conditions (pH and ionic strength, among others). The release of the encapsulated antimicrobials will thus be triggered by high concentrations of salts (salt ions are able to destabilize the attractive interactions between caseinate and pectin) or pH values higher than the isoelectric point of the protein (because of the repulsions between caseinate, which becomes negatively charged, and anionic pectin). Thus, the release kinetics could be predicted if one knows the physicochemical properties of the food product.

References

- Bayarri, M., Oulahal, N., Degraeve, P., & Gharsallaoui, A. (2014). Properties of lysozyme/low methoxyl (LM) pectin complexes for antimicrobial edible food packaging. *Journal of Food Engineering*, 131, 18-25.
- Benichou, A., Aserin, A., Lutz, R., & Garti, N. (2007). Formation and characterization of amphiphilic conjugates of whey protein isolate (WPI)/xanthan to improve surface activity. *Food Hydrocolloids*, 21(3), 379-391.
- Bi, H., Tang, L., Gao, X., Jia, J., & Lv, H. (2016). Spectroscopic analysis on the binding interaction between tetracycline hydrochloride and bovine proteins β -casein, α -lactalbumin. *Journal of Luminescence*, 178, 72-83.
- Chang, Y., & McClements, D. J. (2015). Interfacial deposition of an anionic polysaccharide (fucoidan) on protein-coated lipid droplets: Impact on the stability of fish oil-in-water emulsions. *Food Hydrocolloids*, 51, 252-260.
- Cho, Y. H., & McClements, D. J. (2009). Theoretical stability maps for guiding preparation of emulsions stabilized by protein-polysaccharide interfacial complexes. *Langmuir*, 25(12), 6649-6657.
- Consoli, L., Dias, R.A.O., Rabelo, R.S., Furtado, G. F., Sussulini, A., Cunha, R.L., & Hubinger, M.D. (2018). Sodium caseinate-corn starch hydrolysates conjugates obtained through the Maillard reaction as stabilizing agents in resveratrol-loaded emulsions. *Food Hydrocolloids*, 84, 458-472.
- Einhorn-Stoll, U. (2018). Pectin-water interactions in foods – From powder to gel. *Food Hydrocolloids*, 78, 109-119.
- Evans, M., Ratcliffe, I., & Williams, P. A. (2013). Emulsion stabilisation using polysaccharide-protein complexes. *Current Opinion in Colloid & Interface Science*, 18(4), 272-282.
- Guzey, D., & McClements, D. J. (2006). Formation, stability and properties of multilayer emulsions for application in the food industry. *Adv Colloid Interface Sci*, 128-130, 227-248.
- Lim, A. S. L., & Roos, Y. H. (2017). Carotenoids stability in spray dried high solids emulsions using layer-by-layer (LBL) interfacial structure and trehalose-high DE maltodextrin as glass former. *Journal of Functional Foods*, 33, 32-39.
- Owens, C., Griffin, K., Khouryieh, H., & Williams, K. (2018). Creaming and oxidative stability of fish oil-in-water emulsions stabilized by whey protein-xanthan-locust bean complexes: Impact of pH. *Food Chem*, 239, 314-322.
- Setiowati, A. D., Vermeir, L., Martins, J., De Meulenaer, B., & Van der Meeren, P. (2016). Improved heat stability of protein solutions and O/W emulsions upon dry heat treatment of whey protein isolate in the presence of low-methoxyl pectin. *Colloids and Surfaces A: Physicochemical and Engineering Aspects*, 510, 93-103.
- Shchukina, E. M., & Shchukin, D. G. (2012). Layer-by-layer coated emulsion microparticles as storage and delivery tool. *Current Opinion in Colloid & Interface Science*, 17(5), 281-289.
- Surh, J., Decker, E., & McClements, D. (2006). Influence of pH and pectin type on properties and stability of sodium-caseinate stabilized oil-in-water emulsions. *Food Hydrocolloids*, 20(5), 607-618.
- Xiang, N., Lyu, Y., & Narsimhan, G. (2016). Characterization of fish oil in water emulsion produced by layer-by-layer deposition of soy β -conglycinin and high methoxyl pectin. *Food Hydrocolloids*, 52, 678-689.

- Xu, G., Wang, C., & Yao, P. (2017). Stable emulsion produced from casein and soy polysaccharide compacted complex for protection and oral delivery of curcumin. *Food Hydrocolloids*, 71, 108-117.
- Ye, A., Gilliland, J., & Singh, H. (2011). Thermal treatment to form a complex surface layer of sodium caseinate and gum arabic on oil–water interfaces. *Food Hydrocolloids*, 25(7), 1677-1686.
- Zhao, J., Xiang, J., Wei, T., Yuan, F., & Gao, Y. (2014). Influence of environmental stresses on the physicochemical stability of orange oil bilayer emulsions coated by lactoferrin–soybean soluble polysaccharides and lactoferrin–beet pectin. *Food Research International*, 66, 216-227.

Summary of Chapter 4

After comparing the properties of emulsions stabilized by the two strategies at different CAS/LMP ratios, complexes-stabilized emulsions have shown better stability than LBL-stabilized emulsions at low and intermediate LMP concentrations. However, at high LMP concentrations, the stability was reversed showing that these two kinds of emulsions have their own advantages. Generally, to prolong the storage period, the prepared emulsions are transformed to solid state by spray-drying, spray-chilling or freeze-drying... Among these techniques, spray-drying is the most common one. This process can be dissociated in two steps: atomization and heat treatment. These two steps can have significant impacts on the properties of formed microcapsules, but the separate effects of these two steps were not studied previously. To study these impacts, CAS/LMP complexes were formed at pH 3, and three different CAS/LMP ratios were selected for this study. The dissociate effects of shearing and heating were studied through separating the nozzle from the spray-drier, and heating the atomized and un-atomized CAS/LMP complexes. This study is presented as a scientific article published in *“Food Chemistry”*.

CHAPTER 4

Spray-drying of protein/polysaccharide complexes: Dissociation of the effects of shearing and heating

Wang Jian, Faydi Maoulida, Chedia Ben Amara, Sami Ghnimi, Nour-Eddine Chihib, Emilie Dumas, and Adem Gharsallaoui

Food Chemistry, 2019. **297**: p. 124943

4.1. Abstract

The aim of this study was to dissociate the effect of atomization from that of heating during the spray-drying of Low Methoxyl (LM) pectin/sodium caseinate complexes. The properties of these complexes were studied by measuring turbidity, particle size distribution, zeta-potential, as well as surface hydrophobicity of caseinate within the formed complexes. The results showed that the spraying step had a significant effect on the charge and the size of the complexes. In fact, the application of atomization resulted in the dissociation of caseinate/pectin aggregates especially for high pectin concentrations. Besides, the analysis of the surface hydrophobicity of caseinate indicated that complexation with high concentrations of pectin is able to protect the structure of the protein against heat denaturation. This study allowed a better understanding of the influence of atomization and heat treatment (during the dehydration step) on the molecular interactions within caseinate/pectin complexes.

4.2. Introduction

In the past few decades, spray-drying technique has been widely used for encapsulation of food ingredients, which focus on protecting and controlling the release of active compounds. During this drying process, the solvent, that is most often water, will be rapidly evaporated, and the active compounds will be entrapped with encapsulating material ([Gharsallaoui, Roudaut, Chambin, Voilley, & Saurel, 2007](#)). There are four stages involved in spray drying, namely (i) atomization of the feed solution, (ii) contact of spray with the hot gas, (iii) evaporation of moisture and (iv) particle separation. The loss of free water results in a reduction of water activity and thus extend the shelf life of food products. However, the spray-drying process is accompanied with thermo-mechanical stresses on the active compounds through exposure to

high temperatures, distribution of air-water interfaces, shearing, and dehydration ([Ben Amara, Eghbal, Degraeve, & Gharsallaoui, 2016](#)). During the spray-drying process, the pressure is mainly from two stages, the stage of atomization (distribution of air-water interfaces, shearing) and the stage of heating (high temperature, dehydration). Atomization is a very important and complex step ([Foerster, Gengenbach, Woo, & Selomulya, 2016](#); [Wittner, Karbstein, & Gaukel, 2018](#)), which is same for other microencapsulation technologies like spray-cooling or spray-chilling. Heat treatment can easily change the structure of thermal sensitive material, especially for protein. This process may cause reversible or irreversible denaturation of proteins, which involves the disruption and possible destruction of both the secondary and tertiary structures. When proteins denatured, they can lose solubility to aggregation due to the exposure of hydrophobic groups and some bio-functional proteins (enzymes) can lose their biological function due to the loss of the active site.

The research concerning the formation of complexes between proteins and polysaccharides has received more and more attention ([Devi, Sarmah, Khatun, & Maji, 2017](#); [Li & de Vries, 2018](#)). In fact, adding polysaccharides to form protein-polysaccharide complexes can somehow protect protein against denaturation during spray-drying process as shown in our previous works ([Ben Amara, Eghbal, Degraeve, & Gharsallaoui, 2016](#); [Ormus, Oulahal, Noël, Degraeve, & Gharsallaoui, 2015](#)).

Sodium caseinate is a kind of milk proteins containing α_{s1} -, α_{s2} -, β -, and κ -caseins. These four proteins have a strong tendency to associate with each other to form supra-molecular aggregates ([Surh, Decker, & McClements, 2006](#)). Pectin is a natural polysaccharide found as a component of cell walls in fruits and some roots, which is widely used in the food industry for its thickening and gelling properties. It is composed by a chain of α -(1-4)-linked D-galacturonic acid. According to the degree of methyl esterification, pectin can be classified as high-methoxyl (HM) and low-methoxyl (LM) pectin. Compared to HM pectin, LM pectin requires less sugar to form gels, and can form gels in a wider range of pH (from 2.6 to 7.0). The system of pectin and caseinate is extensively investigated since over twenty years ([Cheng & McClements, 2016](#); [Matia-Merino, Lau, & Dickinson, 2004](#); [Turgeon, Schmitt, & Sanchez, 2007](#)) and it was recently explored in our previous studies ([Eghbal, Degraeve, Oulahal, Yarmand, Mousavi, & Gharsallaoui, 2017](#); [Eghbal, Yarmand, Mousavi, Degraeve, Oulahal, & Gharsallaoui, 2016](#)). According to these studies, complex coacervation of caseinate and LM pectin could happen at pH 3. At this pH, positively-charged caseinate and negatively-charged pectin can form insoluble complexes due to electrostatic interactions. A greater understanding of how caseinate interact with pectin is essential to control structure, functionality and applicability of this system.

In this study, we separated the atomization process and heating process in spray-drying by dissociating the atomizer from spray-drier and replacing heating process with water bath heat treatment. To the best of our knowledge, the separate effects of atomization and heating steps during spray-drying on the properties of protein/polysaccharide complexes were not reported in literature. Through testing the physicochemical properties of caseinate/pectin complexes before and after atomization and heat treatment, we hoped to investigate the effect of atomization and heat treatment on the formation of protein/polysaccharide complexes.

4.3. Materials and methods

4.3.1. Materials

LM pectin (Unipectine™ OF 305 C SB) was purchased from Cargill (Baupre, France). The degree of esterification was from 22% to 28% and the degree of acetylation was from 20% to 23%. Sodium caseinate was purchased from Fisher Scientific (United Kingdom). Protein content in sodium caseinate determined by the Kjeldahl method was 93.20% (nitrogen conversion factor N=6.38). Analytical grade imidazole ($C_3H_4N_2$), acetic acid, sodium hydroxide (NaOH), hydrochloric acid (HCl), 8-Anilino-1-naphthalenesulfonic acid (ANS) were purchased from Sigma-Aldrich Chimie (St Quentin Fallavier, France).

4.3.2. Solution preparation

Imidazole-acetate buffer solutions (5 mM) were prepared by dispersing imidazole and acetic acid into distilled water and then adjusting the pH to 3.0. The stock solutions were prepared by dispersing LM pectin and sodium caseinate powders to unadjusted imidazole-acetate buffer and stirring for at least 2 h at room temperature, and then adjusting the pH to 3.0. The pH was adjusted by using HCl (0.1 or 1.0 M) or NaOH (0.1 or 1.0 M). Complexes solutions were prepared by mixing the stock solutions and then diluted to the desired concentration by imidazole-acetate buffer (pH 3.0). The final sodium caseinate concentration was constant at 5.0 g/L, and the LM pectin concentration was 0.5, 2.0 and 6.0 g/L. After mixing, the complexes solutions were stirred for at least 2 h at room temperature and the pH was checked again.

4.3.3. The atomization process

The atomizer (Mini spray-dryer B-290) was manufactured by BUCHI (Switzerland). The atomizer nozzle was disassembled to prepare the complex solutions after atomization. The nozzle consists of three inputs: an air inlet and two inputs for the liquid as well as an outlet. An atomizer pump that set at a flowrate of 0.5 L/h was used to feed the nozzle with the previously

prepared complex solutions. In order to study the effect of the shearing applied during the spray-drying process, the sodium caseinate/LM pectin complex mixtures were subsequently sprayed at a rate of 0.5 L/h through the nozzle of the atomizer (complex after spraying) and recovered in containers until the tests are carried out. All the atomization experiments were carried at room temperature, the suspensions of complexes before and after spraying were also maintained at room temperature.

4.3.4. Heat treatment

During spray-drying, the suspensions of complexes are exposed to high temperatures during a very short time, which makes it possible to dry the sprayed micro-droplets rapidly. For separately studying the effect of the heat treatment, the various mixtures obtained (in 10 mL tubes) were heated in a water bath at 80 °C for time intervals set at 1 min (T1), 2 min (T2), 3 min (T3) and 4 min (T4). Complexes that underwent heat treatment were compared with unheated complexes (T0).

4.3.5. Turbidity measurement

The turbidity of all complexes suspensions at pH 3 were measured by using a UV/Vis spectrophotometer (Jenway 3705, Villepinte, France) at 600 nm in plastic cuvettes (1 cm path length). Each suspension was diluted 3 to 6 times with imidazole-acetate buffer at pH 3 until the optical density value of each diluted suspension was less than 1.5. The solution of (5.0 g/L) sodium caseinate was used as a control during the measurements, and every suspension was analyzed at least three times.

4.3.6. Particle size distribution

Particle size distributions of sodium caseinate/LM pectin complexes were assessed by a laser diffraction instrument (Mastersizer 3000, Malvern Instruments, Malvern, UK). To avoid multiple scattering effects, the complexes were injected into the measurement chamber where it was diluted with imidazole-acetate buffer (5 mM; pH 3) prior to the measurements. The complexes were continuously stirred throughout the measurement to ensure the samples were homogeneous. The volume mean particle diameter (D_{43}) was calculated by the software from the three injections of three separate samples with five readings per sample.

4.3.7. Zeta potential measurement

The electric charges (ζ -potential) of sodium caseinate/LM pectin complexes were determined using a Zetasizer Nano ZS90 (Malvern Instruments, Malvern, UK). If necessary,

the samples were diluted with pH 3 imidazole-acetate buffer. The mean ζ -potential (ZP) values (\pm SD (standard deviation)) were obtained from the instrument, standard deviation of measurements that are repeated three times for each suspension.

4.3.8. Measurement of surface hydrophobicity

For the surface hydrophobicity study, the 8-anilino-1-naphthalenesulfonic acid (ANS) fluorescent probe was used (Bi, Tang, Gao, Jia, & Lv, 2016). For each suspension studied, increasing volumes of the probe (20 mg/L) ranging from 10 to 30 μ L were added to 4.0 ml of the suspension. The maximum fluorescence intensity due to the binding of the ANS molecules to the hydrophobic sites of the protein was measured by carrying out a scanning of the wavelength between 420 nm and 650 nm for an excitation wavelength of 380 nm. The excitation and emission bandwidths were set at 5.0 nm. The scan rate was 500 nm/min. Fluorescence intensity measurements were performed with a LS 55 spectrofluorometer (PerkinElmer, Courtaboeuf, France). All measurements were performed at room temperature using a quartz cuvette (4 faces, 1 cm path length). The addition of the probe was achieved until no increase of the fluorescence intensity was observed. The maximum fluorescence intensity was plotted against the concentration of ANS. The initial slope of the curve of maximum fluorescence intensity (arbitrary unit, U.A) versus ANS concentration (mg/L) was calculated and used as an index of surface hydrophobicity (S_0). For each suspension, the test was repeated three times.

4.3.9. Statistical analysis

All assays were measured at least in triplicate. Means and standard deviations were calculated and differences between means were determined with the Least Significant Difference (LSD) test at $p < 0.05$ significance level (Statgraphics Centurion XV).

4.4. Results and discussion

4.4.1. Effect of atomization on the properties of caseinate/pectin complexes

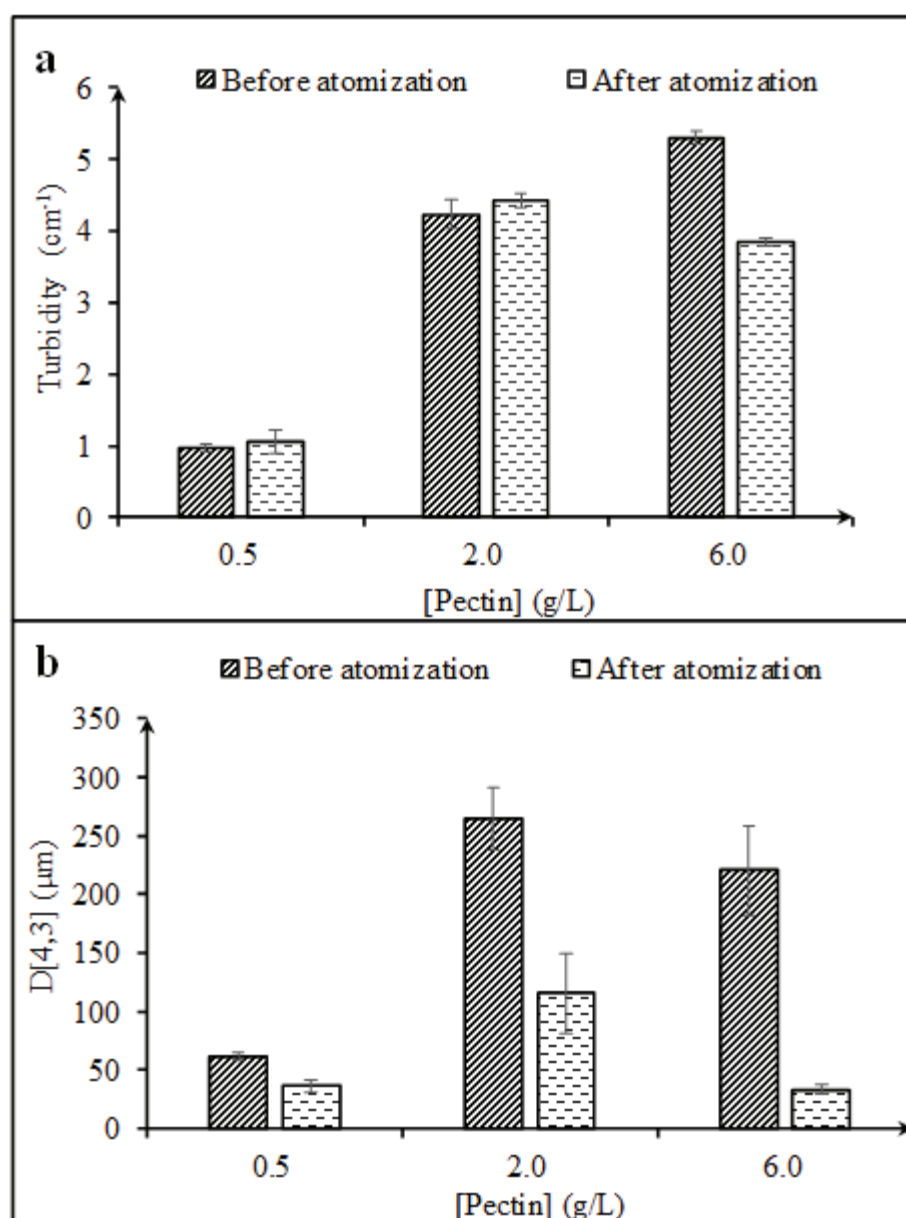


Figure 4.1. Effect of atomization on turbidity (a) and particle size (b) of caseinate/pectin complexes at three different concentrations of pectin (the concentration of caseinate was kept constant at 5.0 g/L; pectin concentrations was varied from 0.5 to 6.0 g/L; pH 3).

The effect of atomization (shearing) on the properties of caseinate/pectin complexes was studied at three different ratios (sodium caseinate concentration kept constant: 5.0 g/L; LM pectin concentration changed: 0.5, 2.0 or 6.0 g/L). Before atomization, the turbidity of complexes increased (Fig. 4.1a) with increasing pectin concentration while the average size reached a peak (Fig. 4.1b). This indicated that, with addition of pectin, caseinate could combine more and more pectin to form complexes leading to a growing size until a pectin concentration

of 2 g/L and turbidity increase. When pectin amount continued to increase, the particle size decreased leading to the formation of numerous small complexes resulting in the still increase of turbidity.

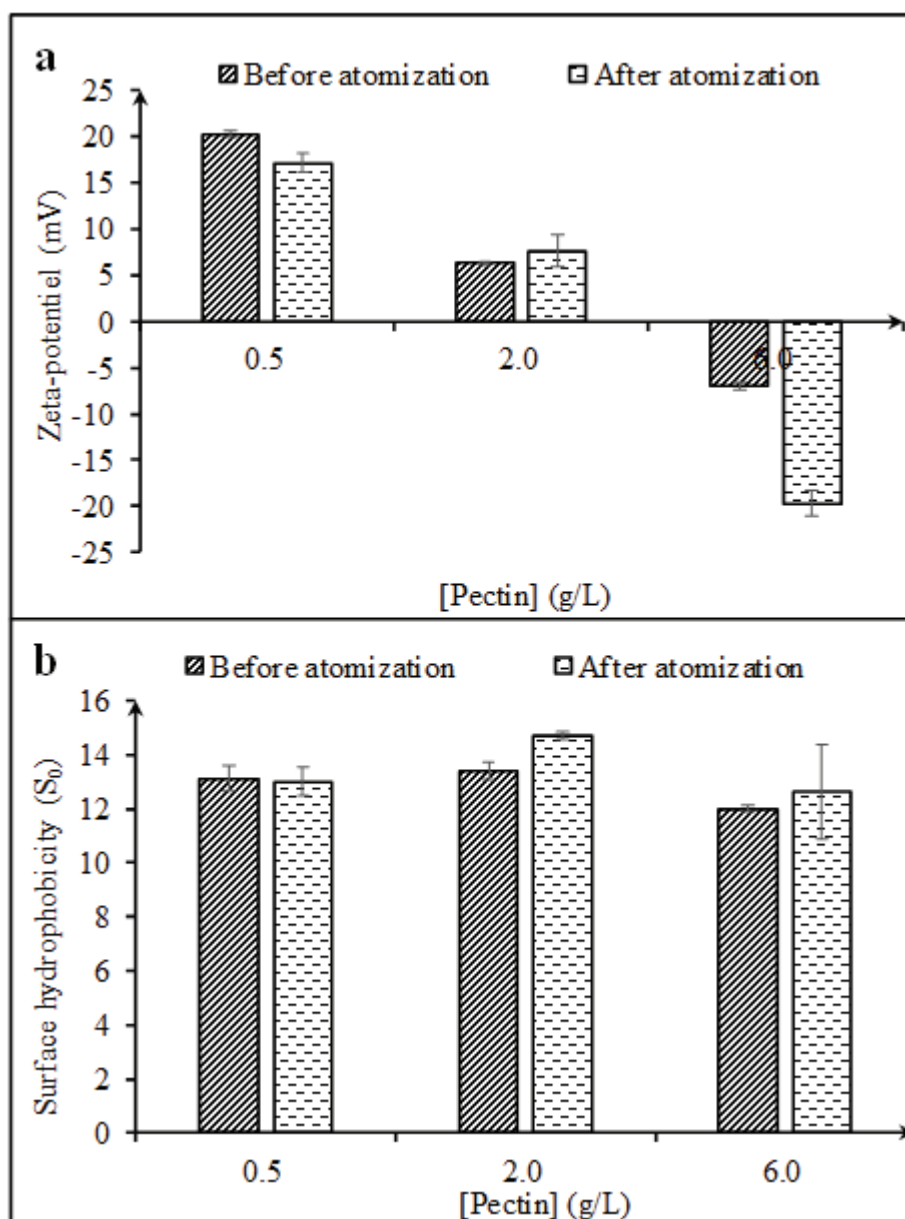


Figure 4.2. Effect of atomization on ζ -potential (a) and surface hydrophobicity (b) profiles of caseinate/pectin complexes at three different concentrations of pectin (the concentration of caseinate was kept constant at 5.0 g/L; pectin concentrations was varied from 0.5 to 6.0 g/L; pH 3).

As shown in Fig. 4.2a, the ζ -potential values of complexes changed from positive to negative with increasing pectin concentration, due to the constant amount of positively charged caseinate molecules neutralized by the increase amount of negatively-charged pectin. At the low (0.5 g/L) and high (6.0 g/L) concentrations of pectin, the caseinate/pectin complexes were

highly charged, and at intermediate (2.0 g/L) concentration of pectin, the complexes were more neutrally charged. These results also confirmed that the size decrease at high (6.0 g/L) concentration of pectin was due to electrostatic repulsions. There was a slight decrease of the protein hydrophobicity only at high pectin concentration (6.0 g/L) (Fig. 4.2b), which means that hydrophobic sites of caseinate would be masked by the pectin chains.

After atomization, the turbidity of complexes was almost constant at low (0.5 g/L) and intermediate (2.0 g/L) concentrations of pectin. At high concentration (6.0 g/L) of pectin, the turbidity of complexes significantly decreased ($p < 0.05$) after atomization (Fig. 4.1a). The average size of complexes significantly decreased ($p < 0.05$) at all the 3 tested ratios (Fig. 4.1b), which is in agreement with other published studies (Serfert, Schröder, Mescher, Laackmann, Rätzke, Shaikh, et al., 2013). The partial dissociation of complexes was due to shear forces during their passage in the nozzle and an increase in their overall charge favoring electrostatic repulsions, especially at high concentration (6.0 g/L) of pectin (Fig. 4.2a). In addition, there was a significant increase of the hydrophobicity S_0 (particularly at 2.0 g/L and 6.0 g/L of pectin), which could indicate molecular rearrangements and unfolding of the structure of the protein caused by exposure of hydrophobic sites (Fig. 4.2b).

4.4.2. Effect of heat treatment on the properties of caseinate/pectin complexes

Heat treatment had a significant effect on the turbidity and the size of the complexes (Fig. 4.3). With the increase of the heat treatment time, the turbidity value of complexes increased ($p < 0.05$) from 0.98 ± 0.05 to $2.87 \pm 0.28 \text{ cm}^{-1}$ at the lower concentration of pectin. It was almost constant ($\sim 4.22 \text{ cm}^{-1}$) at the intermediate concentration of pectin. However, at the higher concentration of pectin, the turbidity value of complexes increased ($p < 0.05$) from $5.29 \pm 0.09 \text{ cm}^{-1}$ to $6.78 \pm 0.04 \text{ cm}^{-1}$ until the 4th min where we had a decrease up to $6.05 \pm 0.17 \text{ cm}^{-1}$ (Fig. 4.3a).

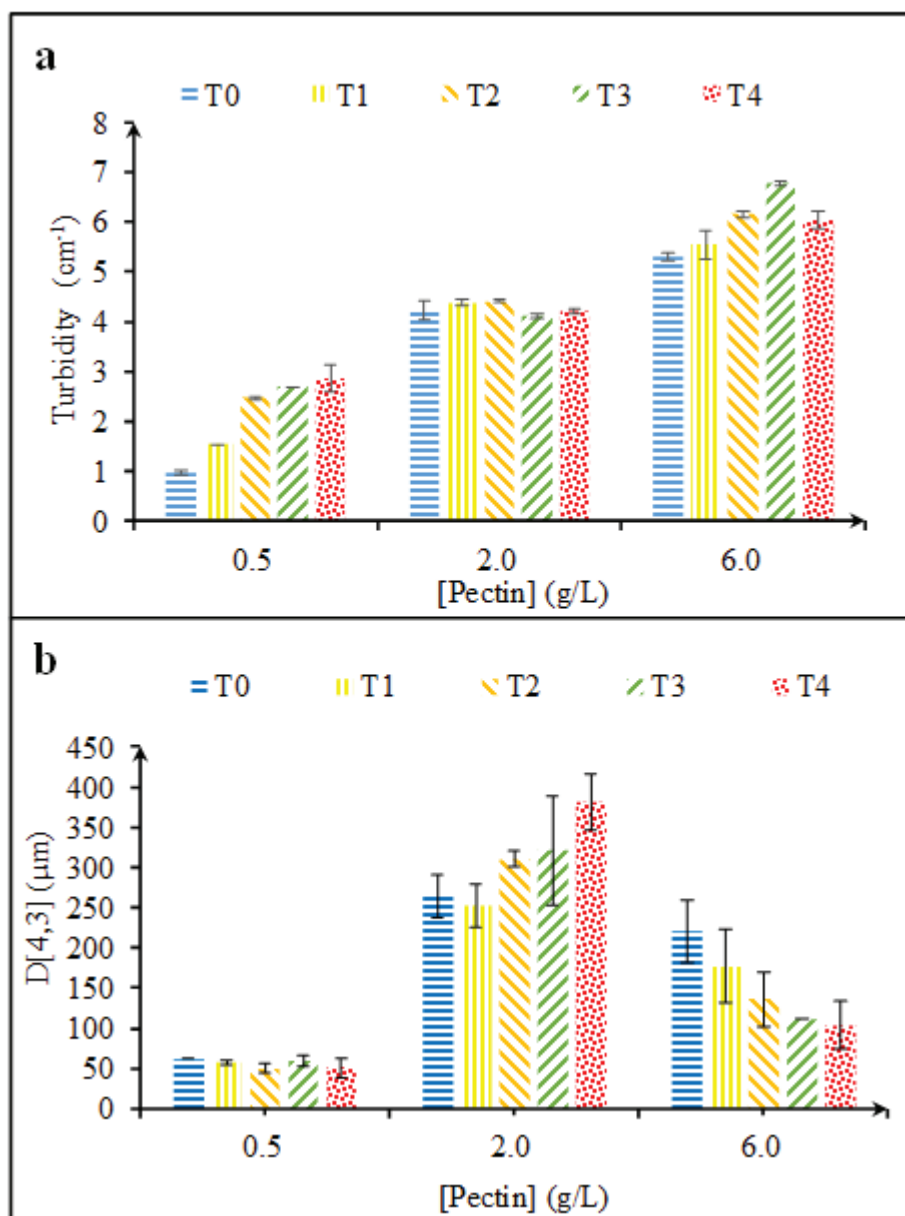


Figure 4.3. Turbidity (a) and particle size (b) of caseinate/pectin complexes at three different concentrations of pectin as function of heat treatment duration from 0 to 4 min at 80 °C (T0: unheated control, T1: 1 min, T2: 2 min, T3: 3 min, T4: 4 min; the concentration of caseinate was kept constant at 5.0 g/L; pectin concentrations was varied from 0.5 to 6.0 g/L; pH 3).

As shown in Fig. 4.3b, the size of complexes formed at low concentration of pectin (0.5 g/L) was constant as a function of heating time ($55.77 \pm 4.53 \mu\text{m}$). Combined with the increased turbidity (Fig. 4.3a), it can be concluded that heat treatment caused the formation of more numerous particles which had the same size as the caseinate/pectin complexes at low pectin concentration. At intermediate concentration of pectin (2.0 g/L), the size increased from 264.17 ± 26.36 to $380.80 \pm 35.05 \mu\text{m}$ ($p < 0.05$) with increase of heat treatment time. Combined with the stable turbidity (Fig. 4.3a), it clarified that heat treatment caused the aggregation of complexes at this pectin concentration. The most interest part was the significant decrease ($p <$

0.05) of particle size from 220.46 ± 38.08 to 104.16 ± 29.62 μm at high concentration of pectin (6.0 g/L), with increase of heating time. This result indicated that heat treatment caused dissociation of aggregates. This also explained the decrease of turbidity after 4 min of heating time (Fig. 4.3a). High concentration of LM pectin may have induced bridging flocculation of protein aggregates (Jones, Lesmes, Dubin, & McClements, 2010). It can be assumed that, after heating treatment, bridging flocculation was suppressed.

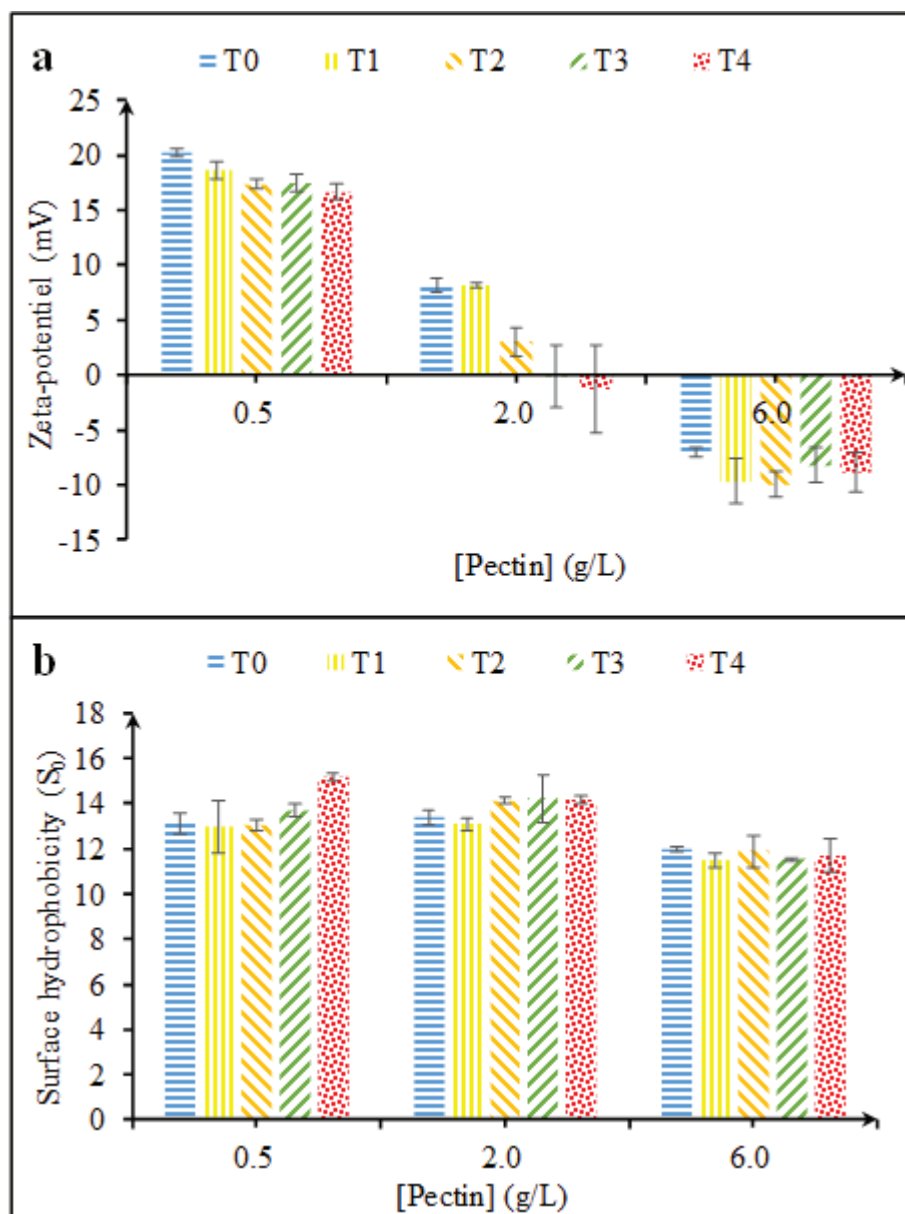
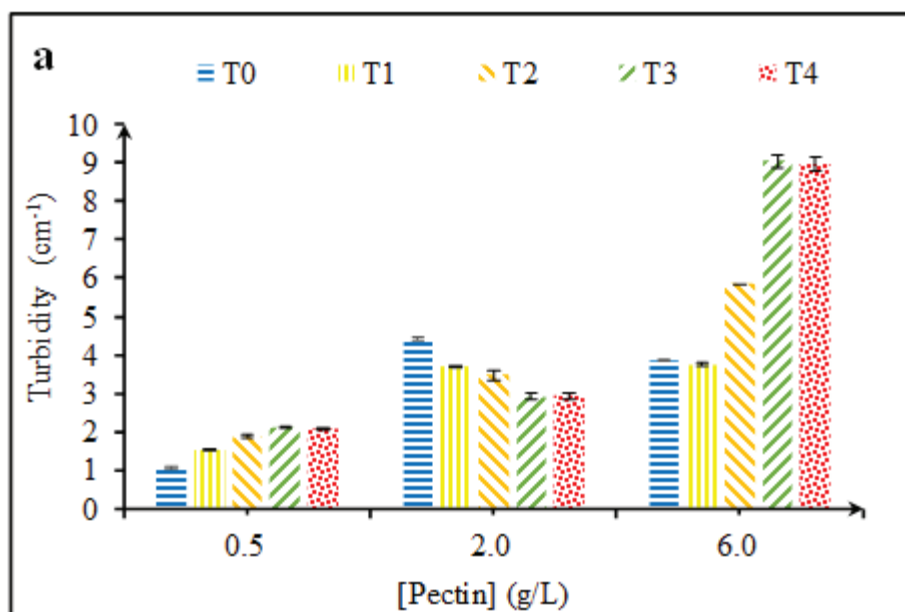


Figure 4.4. ζ -potential (a) and surface hydrophobicity (b) of caseinate/pectin complexes at three different concentrations of pectin as function of heat treatment duration from 0 to 4 min at 80 °C (T0: unheated control, T1: 1 min, T2: 2 min, T3: 3 min, T4: 4 min; the concentration of caseinate was kept constant at 5.0 g/L; pectin concentrations was varied from 0.5 to 6.0 g/L; pH 3).

At low concentration of pectin, slight decrease ($p < 0.05$) in ζ -potential (Fig. 4.4a) and increase in surface hydrophobicity (Fig. 4.4b) indicated that the structure of complexes changed. Anionic groups of pectin and hydrophobic sites in caseinate molecules could be exposed following heat treatment. The change of the electrostatic charge from positive to negative and a slight increase in the hydrophobicity at intermediate concentrations of pectin indicated that the molecular rearrangement allowed to “protect” the protein from heat denaturation. At high concentration of pectin, surface hydrophobicity was almost constant as the increasing time, which confirmed the protective effect of pectin against heat treatment. According to Jones, Decker and McClements (2010), the ability of LM pectin to increase the thermal denaturation temperature may be due to differences in the electrostatic interactions between carboxyl groups on the pectin molecules and charged groups on the folded and unfolded protein surfaces.

4.4.3. Combined effect of atomization and heat treatment on the properties of complexes

To simulate the whole spray-drying process, the caseinate/pectin complexes were atomized and subsequently heated. Combined effect of atomization and heat treatment was evaluated by measuring the properties of atomized complexes treated by heating at 80 °C water bath for 0 to 4 min.



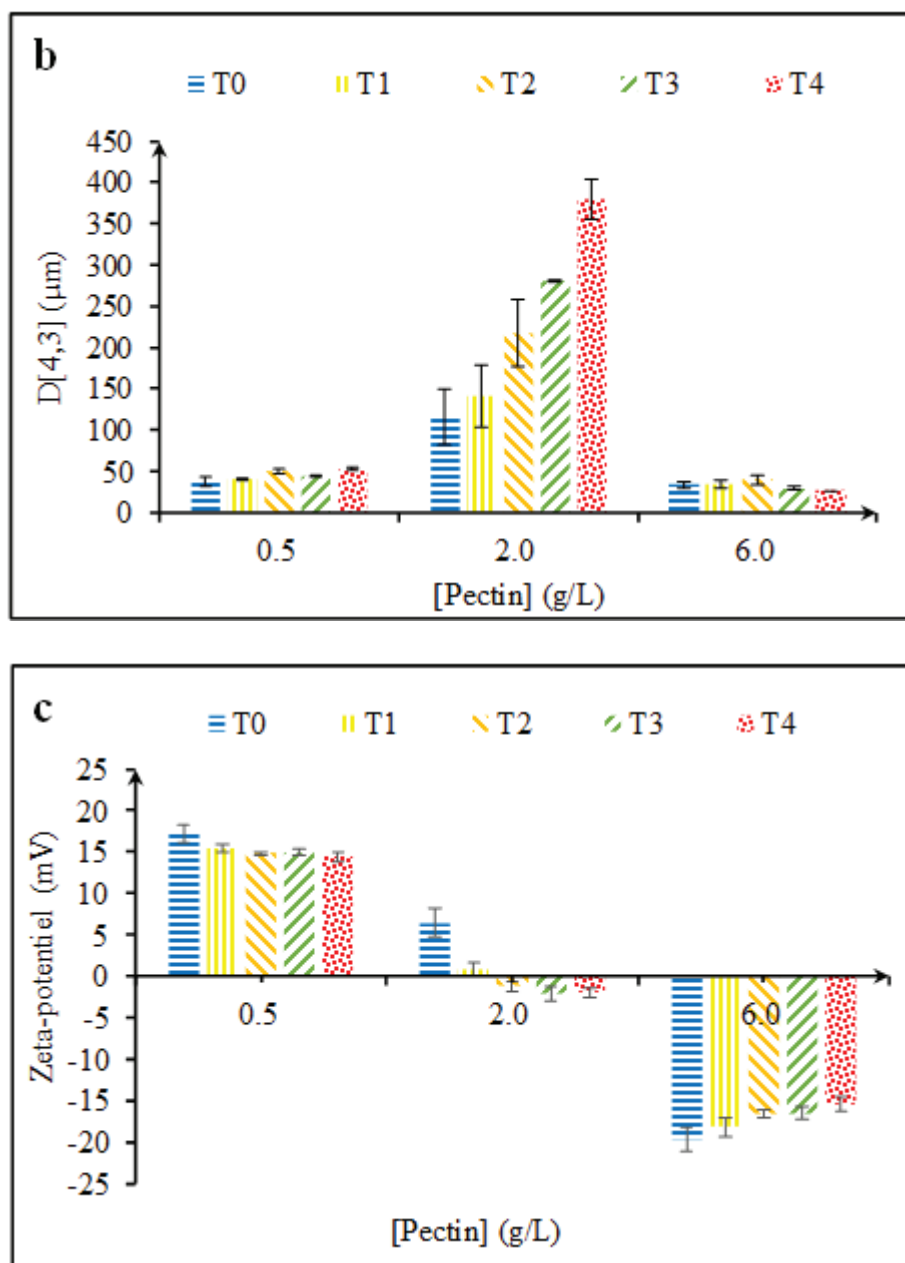


Figure 4.5. Combined effect of atomization and heat treatment (80 °C) on turbidity (a), particle size (b) and ζ -potential (c) of caseinate/pectin complexes at three different concentrations of pectin (T0: unheated control, T1: 1 min, T2: 2 min, T3: 3 min, T4: 4 min; the concentration of caseinate was kept constant at 5.0 g/L; pectin concentrations was varied from 0.5 to 6.0 g/L; pH 3).

As shown in Fig. 4.5, with increasing heat treatment duration, at low concentration of pectin (0.5 g/L), the turbidity of atomized complexes slightly increased ($p < 0.05$) from $1.05 \pm 0.17 \text{ cm}^{-1}$ to $2.08 \pm 0.03 \text{ cm}^{-1}$ and the particle size was constant ($44.52 \pm 5.73 \text{ μm}$). The increase in number of particles could be due to the aggregation of free or partially complexed caseinate molecules. Compared to the properties of caseinate/pectin complexes directly treated by heating without atomization at low pectin concentration (Fig. 4.3), the atomized complexes had a

smaller size and the turbidity of atomized complexes as function of heat treatment duration increased more slightly.

At intermediate pectin concentration (2.0 g/L), with the increase of heating duration, compared to the stable turbidity of caseinate/pectin complexes without atomization (Fig. 4.3a), heat treatment caused the slight decrease ($p < 0.05$) in turbidity of atomized complexes from $4.42 \pm 1.00 \text{ cm}^{-1}$ to $2.93 \pm 0.12 \text{ cm}^{-1}$ (Fig. 4.5a), and significant increase ($p < 0.05$) in particle size from 115.70 ± 34.17 to $379.22 \pm 24.72 \text{ }\mu\text{m}$ (Fig. 4.5b). Thus, we can assume that the association between small complexes could be accentuated by electrostatic charge neutralization (Fig. 4.5c). Compared to the caseinate/pectin complexes directly treated by heating without atomization, atomized complexes formed at intermediate pectin concentration were more sensitive to heat treatment.

Atomized complexes formed at high pectin concentration (6.0 g/L) showed a constant particle size ($32.61 \pm 4.62 \text{ }\mu\text{m}$) and an increased turbidity from $3.85 \pm 0.06 \text{ cm}^{-1}$ to $8.97 \pm 0.97 \text{ cm}^{-1}$ with the increase of heat treatment duration (Fig. 4.5). Similar results were also found in our previous research (Amara, Eghbal, Degraeve, & Gharsallaoui, 2016). The increase of turbidity could be due to thermal dissociation of aggregates, which was already deconstructed by shearing, and formation of new complexes with free pectin chains. Highly negatively charged complexes could be protected from aggregation by electrostatic repulsions (Fig. 4.5c).

4.5. Conclusion

In this study, caseinate/pectin complexes were prepared at pH 3 at three different caseinate/pectin ratios. To evaluate the separate effect of mechanical and thermal steps on the complexes during the spray-drying process, atomization and heat treatment were dissociated and applied to the caseinate/pectin complexes. The properties like turbidity, ζ -potential, particle size and surface hydrophobicity of complexes were measured.

The results indicated that atomization caused dissociation of aggregates into smaller size complexes at all pectin concentrations. At low concentration of pectin, heat treatment caused the aggregation of excess caseinate. At intermediate concentration of pectin, heat treatment intensified aggregation of complexes. At high concentration of pectin, heat treatment favored the dissociation of the aggregates. Complexes after atomization were more sensitive to heat treatment, but a high concentration of pectin could protect the complexes against heat aggregation. These results could help to develop new delivery systems based on spray-dried protein/polysaccharide complexes.

References

- Ben Amara, C. B., Eghbal, N., Degraeve, P., & Gharsallaoui, A. (2016). Using complex coacervation for lysozyme encapsulation by spray-drying. *Journal of Food Engineering*, 183, 50-57.
- Bi, H., Tang, L., Gao, X., Jia, J., & Lv, H. (2016). Spectroscopic analysis on the binding interaction between tetracycline hydrochloride and bovine proteins β -casein, α -lactalbumin. *Journal of Luminescence*, 178, 72-83.
- Cheng, W., & McClements, D. J. (2016). Biopolymer-stabilized conjugated linoleic acid (CLA) oil-in-water emulsions: Impact of electrostatic interactions on formation and stability of pectin-caseinate-coated lipid droplets. *Colloids and Surfaces A: Physicochemical and Engineering Aspects*, 511, 172-179.
- Devi, N., Sarmah, M., Khatun, B., & Maji, T. K. (2017). Encapsulation of active ingredients in polysaccharide-protein complex coacervates. *Advances in Colloid and Interface Science*, 239, 136-145.
- Eghbal, N., Degraeve, P., Oulahal, N., Yarmand, M. S., Mousavi, M. E., & Gharsallaoui, A. (2017). Low methoxyl pectin/sodium caseinate interactions and composite film formation at neutral pH. *Food Hydrocolloids*, 69, 132-140.
- Eghbal, N., Yarmand, M. S., Mousavi, M., Degraeve, P., Oulahal, N., & Gharsallaoui, A. (2016). Complex coacervation for the development of composite edible films based on LM pectin and sodium caseinate. *Carbohydrate Polymers*, 151, 947-956.
- Foerster, M., Gengenbach, T., Woo, M. W., & Selomulya, C. (2016). The impact of atomization on the surface composition of spray-dried milk droplets. *Colloids Surf B Biointerfaces*, 140, 460-471.
- Gharsallaoui, A., Roudaut, G., Chambin, O., Voilley, A., & Saurel, R. (2007). Applications of spray-drying in microencapsulation of food ingredients: An overview. *Food Research International*, 40(9), 1107-1121.
- Li, X., & de Vries, R. (2018). Interfacial stabilization using complexes of plant proteins and polysaccharides. *Current Opinion in Food Science*, 21, 51-56.
- Jones, O., Decker, E. A., & McClements, D. J. (2010). Thermal analysis of β -lactoglobulin complexes with pectins or carrageenan for production of stable biopolymer particles. *Food Hydrocolloids*, 24(2-3), 239-248.

- Jones, O. G., Lesmes, U., Dubin, P., & McClements, D. J. (2010). Effect of polysaccharide charge on formation and properties of biopolymer nanoparticles created by heat treatment of β -lactoglobulin–pectin complexes. *Food Hydrocolloids*, 24(4), 374-383.
- Matia-Merino, L., Lau, K., & Dickinson, E. (2004). Effects of low-methoxyl amidated pectin and ionic calcium on rheology and microstructure of acid-induced sodium caseinate gels. *Food Hydrocolloids*, 18(2), 271-281.
- Ormus, S., Oulahal, N., Noël, C., Degraeve, P., & Gharsallaoui, A. (2015). Effect of low methoxyl (LM) pectin complexation on the thermal and proteolytic inactivation of lysozyme: A kinetic study. *Food Hydrocolloids*, 43, 812-818.
- Serfert, Y., Schröder, J., Mescher, A., Laackmann, J., Rätzke, K., Shaikh, M. Q., Gaukel, V., Moritz, H. U., Schuchmann, H. P., Walzel, P., Drusch, S., & Schwarz, K. (2013). Spray drying behaviour and functionality of emulsions with β -lactoglobulin/pectin interfacial complexes. *Food Hydrocolloids*, 31(2), 438-445.
- Surh, J., Decker, E., & McClements, D. (2006). Influence of pH and pectin type on properties and stability of sodium-caseinate stabilized oil-in-water emulsions. *Food Hydrocolloids*, 20(5), 607-618.
- Turgeon, S. L., Schmitt, C., & Sanchez, C. (2007). Protein–polysaccharide complexes and coacervates. *Current Opinion in Colloid & Interface Science*, 12(4-5), 166-178.
- Wittner, M. O., Karbstein, H. P., & Gaukel, V. (2018). Spray performance and steadiness of an effervescent atomizer and an air-core-liquid-ring atomizer for application in spray drying processes of highly concentrated feeds. *Chemical Engineering and Processing - Process Intensification*, 128, 96-102.

Summary of Chapter 5

According to the results concerning the effect of spray-drying process on the properties of CAS/LMP complexes, atomization caused dissociation of aggregates into smaller size complexes at all pectin concentrations, which make complexes more sensitive to heat treatment. However, compared to low and intermediate concentration of LMP, high concentration of LMP can protect CAS/LMP complexes against heat aggregation. Considering the above conclusions, citral, an essential oil molecule which has an interesting antimicrobial activity, was encapsulated by CAS/LMP system. Indeed, encapsulation of this hydrophobic molecule can improve its dispersion in aqueous based products, preserve it from lost due to its volatility or to its degradation. After studying the effects of emulsion preparing strategies and spray-drying process, LBL (CAS with high concentration of LMP) stabilized emulsions were used to encapsulate citral, and compared to ML (monolayer) emulsions, prepared without LMP addition. All the emulsions were prepared at pH 3 and then spray-dried to obtain microcapsules containing citral. The antimicrobial activity of the formed microcapsules on Gram⁺ and Gram⁻ bacteria was compared to free citral to study the impact of drying and interfacial membrane composition. The results were published in *Food chemistry*.

CHAPTER 5

Effect of drying and interfacial membrane composition on the antimicrobial activity of emulsified citral

Wang Jian, Simon Oussama Khelissa, Nour-Eddine Chihib, Emilie Dumas, and Adem Gharsallaoui

Food Chemistry, 2019. **298**: p. 125079

5.1. Abstract

Citral-in-water emulsions were prepared with two different essential oil concentrations of 2.5 and 5.0% (w/w), then spray-dried in the presence of the same amount of maltodextrins (20%). The microcapsules were prepared with two different emulsifier compositions: monolayer microcapsules (ML) stabilized by sodium caseinate alone and layer-by-layer microcapsules (LBL) stabilized by sodium caseinate and pectin. The encapsulation efficiency was higher for LBL microcapsules (*e.g.* 99.6 ± 0.4 % for 2.5% citral) than that for ML ones (*e.g.* 78.6 ± 0.6 % for 2.5% citral) which confirm that the additional pectin layer was able to protect citral during the spray-drying process whatever citral concentration. Furthermore, our results showed that the antibacterial activity of the obtained microcapsules significantly depends on both citral concentration and interfacial membrane composition. The presence of two layers surrounding the citral droplets may result in a progressive and controlled release of the encapsulated citral.

5.2. Introduction

Essential oils, as secondary metabolites of plants, have many applications in cosmetics, food flavoring and preservation as well as in pharmaceutical industries. To satisfy the growing demand for new and natural antimicrobials for preventing microbial food spoilage and bacterial infections, many research work are carried out on essential oils ([Kayode et al., 2018](#); [Khorshidian, Yousefi, Khanniri, & Mortazavian, 2018](#); [Prakash, Baskaran, Paramasivam, & Vadivel, 2018](#)).

Due to the common features of most essential oils as their hydrophobic, volatile and chemically unstable nature, many studies focused on improving their dispersion in aqueous-based product. The challenge is also to maintain their flavor and their potential bioactivity by

developing delivery systems containing essential oils (Prakash, Baskaran, Paramasivam, & Vadivel, 2018). The delivery system which encapsulate essential oils can be prepared by emulsification, spray-drying, coaxial electrospray system, freeze-drying, coacervation, *in situ* polymerization, melt-extrusion, supercritical fluid technology, and fluidized-bed-coating (Bakry, Abbas, Ali, Majeed, Abouelwafa, Mousa, et al., 2016).

Citral (3,7-dimethyl-2,6-octadienal) is one of the most important compounds of citrus flavors, and is widely used as flavoring agent in food, beverage and cosmetics industries. As a monoterpene aldehyde, citral consists of two geometrical isomers (geranial and neral). Geranial has a strong lemon odor, and neral's odor is less intense, but sweeter. Besides the appetite stimulating property of citral as flavoring agent, citral has good antifungal and antibacterial activities (Espina, Berdejo, Alfonso, García-Gonzalo, & Pagán, 2017; Li, Wu, Yin, Long, & Li, 2015; Saddiq & Khayyat, 2010), and can be used as insecticide and deodorant (Tak & Isman, 2016). In the pharmaceutical industry, citral is used as antispasmodic, analgesic, anti-inflammatory, antipyretic, diuretic and sedative, due to its spasmolytic, anti-inflammatory, expectorant and weak diuretic effects (Maswal & Dar, 2014; Nishijima, et al., 2014). However, citral is highly vulnerable to acid and oxygen. In fact, acid-catalyzed cyclization and oxidative degradation of citral can reduce the intensity of the fresh lemon flavor and antimicrobial activity that limit the shelf-life of acidic citrus flavored foods, beverages, deodorant and insecticide (Maswal & Dar, 2014). For solving these problems, there are continuous research reports focused on encapsulation of citral in the last ten years. Choi et al. (2009) prepared oil-in-water emulsions and encapsulated citral with medium-chain triacylglycerols and triacetin to improve its chemical stability (Choi, Decker, Henson, Popplewell, & McClements, 2009). The authors used cationic, non-ionic and anionic surfactants to prepare emulsions and investigated the influence of droplet charge on the chemical stability of citral in oil-in-water emulsions. They showed that emulsions prepared by using non-ionic or cationic surfactants were more stable than those prepared by using anionic surfactants (Choi, Decker, Henson, Popplewell, & McClements, 2010). Citral retention after spray-drying in sucrose or trehalose matrices was similar for both matrices; however, physical stability of trehalose formulations was better as compared to sucrose (Sosa, Zamora, Chirife, & Schebor, 2011). Therefore, the authors put focus on the emulsions properties and stability before and after spray-drying. The properties of both emulsions and spray-dried powders were similar for the formulations containing sucrose or trehalose which confirmed that trehalose could be used as a replacer for sucrose (Sosa, Schebor, & Pérez, 2014). Yang et al. (2015) stabilized citral with a soy protein-polysaccharides Maillard reaction product to enhance the physical stability of oil-in-water emulsions. Lu et al. (2018)

encapsulated citral in nanoemulsions and evaluated the antimicrobial activity. Tian, Lu, Li, & Hu (2018) prepared solid lipid nanoparticles loaded with citral by a high-pressure homogenization method. Afzal, Maswal, & Dar (2018) utilized hydrogels prepared by chitosan and alginate to encapsulate citral.

In the present study, Layer-by-Layer (LBL) emulsions and Monolayer (ML) emulsions were prepared to encapsulate two different amounts of citral (2.5% and 5%), then the emulsions were spray-dried to obtain citral microcapsules. The antimicrobial activity of citral microcapsules against both Gram-negative and Gram-positive bacteria were evaluated. Sodium caseinate and pectin were chosen as emulsifiers for emulsification and maltodextrins as carrier material for spray-drying because they are natural ingredients already widely used in food industry. In a previous work, the system of sodium caseinate and pectin was already studied for its ability to form composite films (Eghbal *et al.*, 2016). The aim of this work was to investigate the effect of drying and interfacial membrane composition on the antimicrobial activity of emulsified citral.

5.3. Materials and methods

5.3.1. Materials: chemicals and bacteria

Sodium caseinate was purchased from Fisher Scientific (United Kingdom). Protein content in CAS determined by the Kjeldahl method was 93.20% (nitrogen conversion factor N=6.38). Pectin was from Cargill (Baupre, France). The degree of esterification was from 22% to 28% and degree of acetylation was from 20% to 23%. Maltodextrins DE 19 (dextrose equivalent value of 19) was obtained from Roquette-freres SA, (Lestrem, France). Citral (mixture of *cis* and *trans* isomers, 95% pure) was purchased from Sigma Aldrich Chimie. Analytical grade imidazole (C₃H₄N₂), acetic acid, sodium hydroxide (NaOH), hydrochloric acid (HCl), n-hexane (98% of purity), and ethanol were purchased from Sigma-Aldrich Chimie (St Quentin Fallavier, France). Distilled water was used for the preparation of all solutions.

The target strains used in this study were: *Listeria innocua* (ATCC 33090), *Kocuria rhizophila* (ATCC 9341), *Salmonella enterica* (CIP 8297) and *Staphylococcus aureus* (CIP 4.83). All stains were maintained at -80 °C in Tryptone Soy Broth (TSB, Biokar Diagnostics, France) supplemented with 20% (v/v) glycerol.

5.3.2. Solution preparation

Imidazole-acetate buffer solutions (5 mM) were prepared by dispersing weighed amounts

of imidazole and acetic acid into distilled water and then adjusting the pH to 3.0. The stock solutions were prepared by dispersing sodium caseinate, pectin and maltodextrins powders to unadjusted imidazole-acetate buffer and stirring at room temperature until total hydration, and then the pH was adjusted to 3.0. The pH was adjusted by using HCl (0.1 or 1.0 M) or NaOH (0.1 or 1.0 M). The concentration of each stock solution (w/w) was: sodium caseinate 1.667%, pectin 4%, and maltodextrins 50%. The pH of each solution was adjusted again to 3.0.

5.3.3. Emulsion preparation

Coarse emulsions were prepared by adding weighted amount of citral to sodium caseinate solution followed by homogenization using an Ultra Turrax PT 4000 homogenizer (Polytron, Kinematica, Switzerland) at 20 000 rpm for 5 min. The obtained emulsions (primary emulsions) were further homogenized at 500 bar and five recirculations using a high pressure homogenizer (SPX Brand, APV Model 1000). Monolayer emulsions (ML) were obtained by diluting primary emulsions with pH 3.0 buffer. Layer by layer (LBL) emulsions were obtained by slowly adding pectin solution to the primary emulsions and stirring for at least 2 h. All the emulsions were readjusted to pH 3.0 before measurements.

5.3.4. Spray-drying process

Stock maltodextrins solutions were added to the prepared emulsions, in order to have a final composition (w/w) of 20% maltodextrins DE 19, 0.5% sodium caseinate, 0.8% pectin (only for LBL emulsions) and 2.5% or 5.0% citral. The mixtures were stirred for 30 min and then spray-dried using a laboratory scale device equipped with a 0.5 mm nozzle atomizer (Mini Spray-Dryer Büchi B-290, Switzerland). The operational conditions of the drying process were: feed flow rate 0.5 L/h, inlet air temperature 180 ± 2 °C, outlet air temperature 80 ± 5 °C, and air pressure 3.2 bar. After spray-drying, the powders were collected in sealed containers and stored at 4 °C until analysis. Reconstituted emulsions were prepared by dispersing weighted amounts (the same dry matter as before spray-drying) of spray-dried powders in imidazole-acetate buffer solutions (5 mM, pH 3.0) and stirring for 1 h.

5.3.5. ζ -potential measurement

The electric charge (ζ -potential) of emulsions were determined using a Zetasizer Nano ZS90 (Malvern Instruments, Malvern, UK). If necessary, the samples were diluted with pH 3.0 imidazole-acetate buffer. Each test was repeated at least three times. The mean ζ -potential (ZP) values (\pm SD (standard deviation)) were obtained from the instrument.

5.3.6. Particle size distribution

Particle size distribution of emulsions and spray-dried powders were assessed by a laser diffraction instrument (Mastersizer 3000, Malvern Instruments, Malvern, UK) with a value of 1.5 for relative refractive index (droplet to solvent), 0.1 absorption, and an index of refraction of 1.33 for water phase, 1.36 for ethanol. For measuring the droplet size distribution of emulsions, the emulsions were injected into the measurement chamber containing imidazole-acetate buffer (5 mM; pH 3.0). For measuring the particle size distribution of spray-dried powders, the powder was slowly added into the measurement chamber containing ethanol. The emulsions and spray-dried powders were continuously stirred throughout the measurement to ensure that the samples were homogeneous. The volume mean particle diameter (D_{43}) was calculated by the software from the three injections of three separate samples with five readings per sample.

5.3.7. Encapsulation Efficiency (EE)

A weighted amount (the same dry matter as in 1 mL of emulsion) of each spray-dried powder was dissolved in 1 mL distilled water in a centrifuge tube and 10 mL hexane were then added. After vortexing the tube for 10 minutes, centrifugation at 5 000 g at 4 °C for 30 min was applied to separate the organic phase. After dilution (1:10 or 1:100) of the organic phase in hexane, the amount of citral was quantified by measuring the absorbance by spectrophotometry (Jenway 3705, Villepinte, France) at 252 nm using a prepared standard calibration curve of citral in hexane. The encapsulation efficiency was calculated as follows (Lu *et al.*, 2018):

$$\text{Encapsulation Efficiency (\%)} = \frac{\text{Amount of encapsulated citral}}{\text{Total amount of added citral}} \times 100$$

5.3.8. Minimum inhibitory concentration (MIC)

Listeria innocua (ATCC 33090), *Kocuria rhizophila* (ATCC 9341), *Salmonella enterica* (CIP 8297) and *Staphylococcus aureus* (CIP 4.83) were pre-cultured in TSB at 10% (v/v) for 24 h and then cultured by inoculating 10^4 CFU/L (from the pre-culture) in 50 mL of TSB and incubation for 16 h at 37 °C under shaking (160 rpm). Cells were harvested by centrifugation (5 000 g for 5 min at 25 °C) then washed twice with Potassium Phosphate Buffer (PPB; 100 mM, pH 7) before being diluted in Tryptone Salt (TS) broth to 1×10^6 CFU/mL. The minimum inhibitory concentration (MIC) of citral microcapsules was determined by measuring kinetically, the development of turbidity by vertical photometry using a Bioscreen C (Labsystems, Helsinki, Finland). 100 μ L of bacterial suspension (10^6 CFU/mL) were added

to the plate wells containing serial 2-fold dilutions from citral microcapsules stock solution in TSB. Each test plate, included a growth control (bacteria with microcapsule-free TSB), and a sterility control with only microcapsule-free TSB. The plates were incubated at 37 °C under continuous shaking in the Bioscreen C which measured the OD_{600 nm} every 2 h during 24 h. The MIC was defined as the lowest citral microcapsules concentration preventing the bacterial growth, as measured by optical density. The experiment was repeated three times and mean OD_{600 nm} values were plotted versus time.

5.3.9. Growth rate and lag time

The lag time, of each growth curve, was estimated by extrapolating the linear portion of OD_{600 nm} versus time plot back to the initial OD_{600 nm}. The growth rate (μ) was calculated during the exponential growth according to [Hall, Acar, Nandipati, & Barlow \(2014\)](#).

5.3.10. Measurement of inhibition zone

Kocuria rhizophila (ATCC 9341) was pre-cultured in TSB at 10% (v/v) for 8 h and then pre-cultured in TSB at 10% (v/v) for 16 h at 37 °C. One milliliter of this pre-culture was transferred into 9 mL of TSB and incubated for 5 h at 37 °C. The cells were then diluted in Tryptone Salt (TS) broth to final concentrations of 1×10^6 CFU/mL, incorporated at 5% (v/v) in melted (~50 °C) Tryptone Soy Agar (TSA), and cooled in Petri dishes. A sterilized filter paper with a hole (15 mm in diameter) was placed on the TSA Petri plates inoculated with *K. rhizophila*, and weighted amounts of citral microcapsules were added in the hole. After spreading the powder, the paper was gently removed. The plates were then incubated for 2 h at 4 °C and then incubated at 37 °C. Inhibition zones were measured after 24 h and each experiment was repeated three times.

5.3.11. Statistical analysis

All experiments were performed using at least three freshly prepared samples. The results presented are the averages and standard deviations that were calculated from these replicate measurements. Statistical differences between samples were calculated using Student's t test for independent samples (Microsoft Excel, Microsoft Corporation, Redmond, WA).

5.4. Results and discussion

5.4.1. Physicochemical properties of emulsions

5.4.1.1. Droplet size distribution of emulsions

The average droplet size of ML and LBL emulsions containing 2.5% or 5.0% citral before and after spray-drying is shown in [Fig. 5.1A](#). Through comparing the droplet size of LBL emulsions with ML emulsions, the effect of interfacial membrane composition was evaluated. Before spray-drying, the mean droplet size of LBL emulsions containing 2.5% or 5.0% citral was around 15 μm , which was significantly ($p < 0.05$) bigger than the mean droplet size of ML emulsions ($\sim 4 \mu\text{m}$).

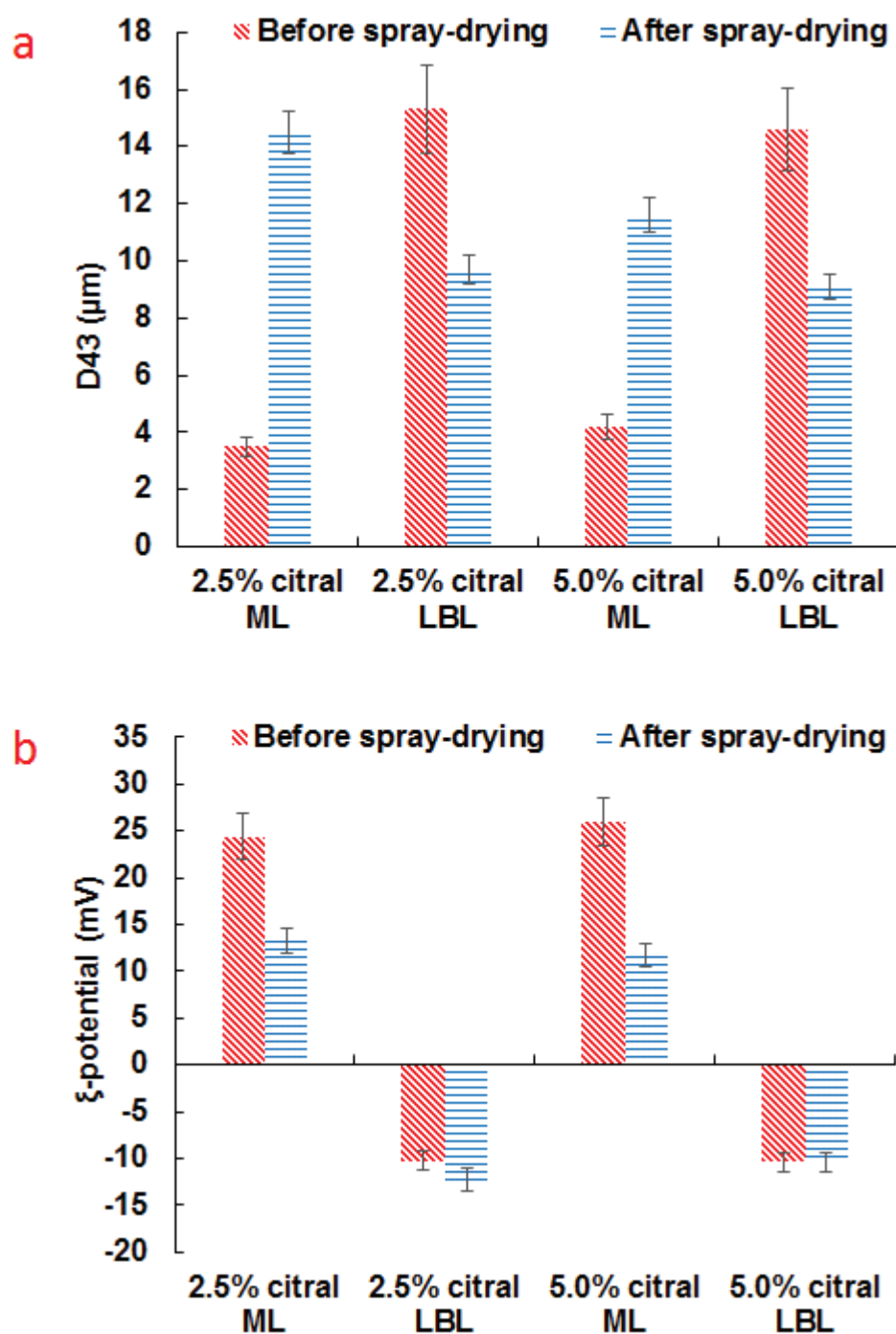


Figure 5.1. Physicochemical properties of emulsions: (a) Droplet size distribution of emulsions before and after spray-drying; (b) Zeta-potential of emulsions before and after spray-drying.

The effect of spray-drying on the properties of emulsions was evaluated by comparing the droplet size of fresh emulsions before spray-drying and reconstituted emulsions after spray-drying. After spray-drying, the droplet size of ML emulsions increased, whatever the citral concentration. Indeed, ML emulsions containing 2.5% citral increased from $3.5 \pm 1.2 \mu\text{m}$ to $14.5 \pm 2.6 \mu\text{m}$ and for ML emulsions containing 5.0% citral, the droplet size increased from 4.2

$\pm 0.6 \mu\text{m}$ to $11.6 \pm 1.4 \mu\text{m}$. This could be mainly caused by flocculation and/or coalescence. On the other hand, the droplet size of LBL emulsions slightly decreased after spray-drying. For LBL emulsions containing 2.5% citral, the droplet size decreased from $15.3 \pm 2.3 \mu\text{m}$ to $9.7 \pm 1.8 \mu\text{m}$. For LBL emulsions containing 5.0% citral, the droplet size decreased from $14.6 \pm 1.4 \mu\text{m}$ to $9.1 \pm 0.5 \mu\text{m}$. The size decrease of LBL emulsions could be due to the dissociation of flocculated droplets during the shearing inside the atomization nozzle, the collapse of surface hairy layers and the shrinkage of overall structures (Liu *et al.*, 2019). The final droplet size of reconstituted LBL emulsions ($\sim 9 \mu\text{m}$) was significantly ($p < 0.05$) smaller than reconstituted ML emulsions ($\sim 13 \mu\text{m}$).

Compared to ML emulsions, the addition of the second layer (pectin) made the droplet size of LBL emulsions increase and improved the stability of LBL emulsions against the shearing and thermal stresses during the spray-drying process. Increasing the amount of citral from 2.5% to 5.0% did not significantly changed the droplet size of each emulsion.

5.4.1.2. ζ -potential of emulsions

The ζ -potential of ML and LBL emulsions containing 2.5% or 5.0% citral before and after spray-drying was also measured as shown in Fig. 5.1B. For ML emulsions, the ζ -potential was positive (about 25 mV) because of the positively-charged caseinate layer which covered droplets. A decrease of ζ -potential value (from ~ 25 mV to ~ 12 mV) occurred after spray-drying. In fact, the spray-drying process would cause some structure changes of caseinate on the droplet surface followed by flocculation and/or coalescence. Compared to positively-charged ML emulsions, the ζ -potential value of LBL emulsions was negative (about -10 mV), this transition was due to the addition of negatively-charged pectin which formed the second layer to cover citral droplets (Sejersen *et al.*, 2007). Indeed, the absolute values of zeta potential in LBL systems were lower than in ML systems, which indicated that the electrostatic repulsions in LBL systems were weaker than that in ML systems. However, the stability of emulsions can be attributed to many factors like viscosity, density, size... The change of ζ -potential indicated also that the structure of droplets in the emulsion was changed (Kovacevic *et al.*, 2011). No significant change of ζ -potential value was measured before and after spray-drying for LBL emulsions, which confirmed the stability of LBL emulsions. The ζ -potential of each emulsion was also independent of the amount of citral (2.5% or 5.0%).

5.4.2. Properties of citral microcapsules

In this section, the physicochemical properties of spray-dried powder were characterized

by measuring particle size and encapsulation efficiency, as shown in Fig. 5.2. The particle size of citral microcapsules obtained by spray-drying ML emulsions containing 2.5% or 5.0% citral were both around 8.0 μm . However, the powder obtained by spray-drying LBL emulsions had a slight larger size ($\sim 12 \mu\text{m}$). It is important to note also that the increase of citral amount did not influence the particle size in both ML and LBL cases.

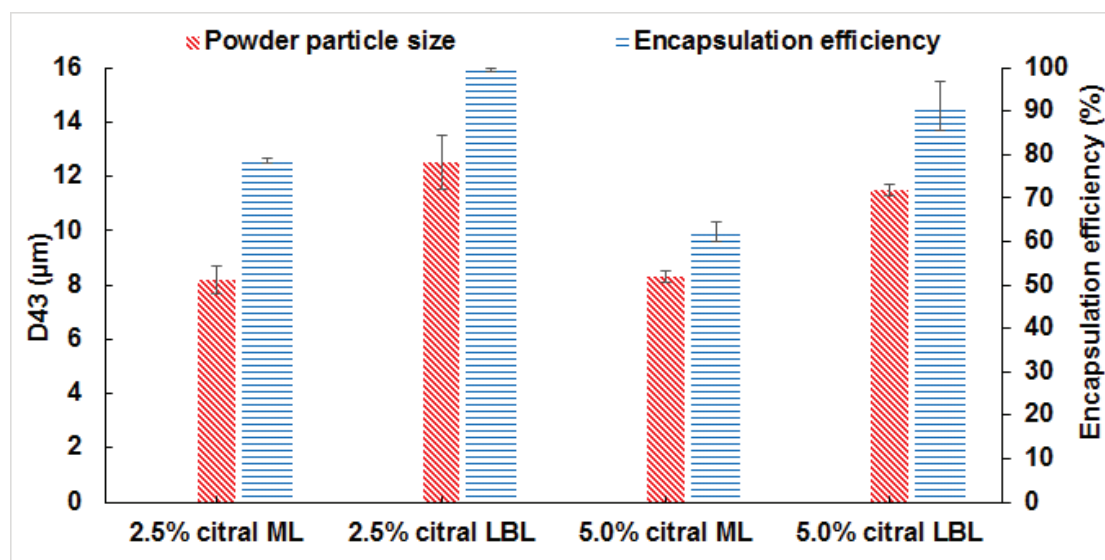


Figure 5.2. Particle size distribution and encapsulation efficiency of spray-dried powders.

Encapsulation efficiency is an important parameter in the evaluation of a microencapsulation technique (Jelvehgari, Valizadeh, Rezapour, & Nokhodchi, 2010). Among the four kinds of citral microcapsules, the spray-dried 2.5% citral LBL emulsion showed the highest encapsulation efficiency ($99.6 \pm 0.4 \%$), which was closed to 100%, followed by 5.0% citral LBL ($91.2 \pm 5.6 \%$), 2.5% citral ML ($78.6 \pm 0.6 \%$) and 5.0% citral ML ($62.3 \pm 2.4 \%$). According to these results, with increase of citral amount, the encapsulation efficiency decreased, which is expected because of the limit of loading capacity in microencapsulation system. Compared to the citral microcapsules based on ML emulsions, the spray-dried powder based on LBL emulsions had a higher encapsulation efficiency in both concentrations of citral, which further confirmed the protection of added pectin against the stress sustained during the spray-drying process.

5.4.3. Antimicrobial activity assessments

5.4.3.1. Minimum Inhibitory Concentration (MIC) in liquid media

Table 5.1. Minimum inhibitory concentration (mg/mL) of encapsulated citral

	2.5% citral ML	2.5% citral LBL	5.0% citral ML	5.0% citral LBL
<i>Salmonella enterica</i> CIP 8297	4	4	4	2
<i>Staphylococcus aureus</i> CIP 4.83	2	2	2	1
<i>Listeria innocua</i> ATCC 3309	2	2	2	1
<i>Kocuria rhizophila</i> ATCC 9341	2	2	2	1

The minimum inhibitory concentration of the four kinds of citral microcapsules was measured against four target strains as shown in Table 5.1. The results showed that *Salmonella enterica* CIP 8297 (Gram-negative) was more resistant to encapsulated citral, compared to the other 3 Gram-positive bacteria, which could be due to the diffusion restriction of hydrophobic compounds by means of the lipopolysaccharide outer membrane barrier (Belda-Galbis, Pina-Pérez, Leufvén, Martínez, & Rodrigo, 2013). This result was consistent with the properties of most essential oils and their components (Tajkarimi, Ibrahim, & Cliver, 2010). In these 4 tested citral microcapsules, 5.0 % citral LBL microcapsules showed the lowest MIC (2 mg/mL for *Salmonella enterica*, 1 mg/mL for *Staphylococcus aureus*, *Listeria innocua* and *Kocuria rhizophila*), which was two times less than the MICs measured for the other 3 citral microcapsules. This could be due to their good encapsulation efficiency combined with the proper concentration of entrapped citral that resulted in controlled release of encapsulated citral.

5.4.3.2. Growth rate and lag time

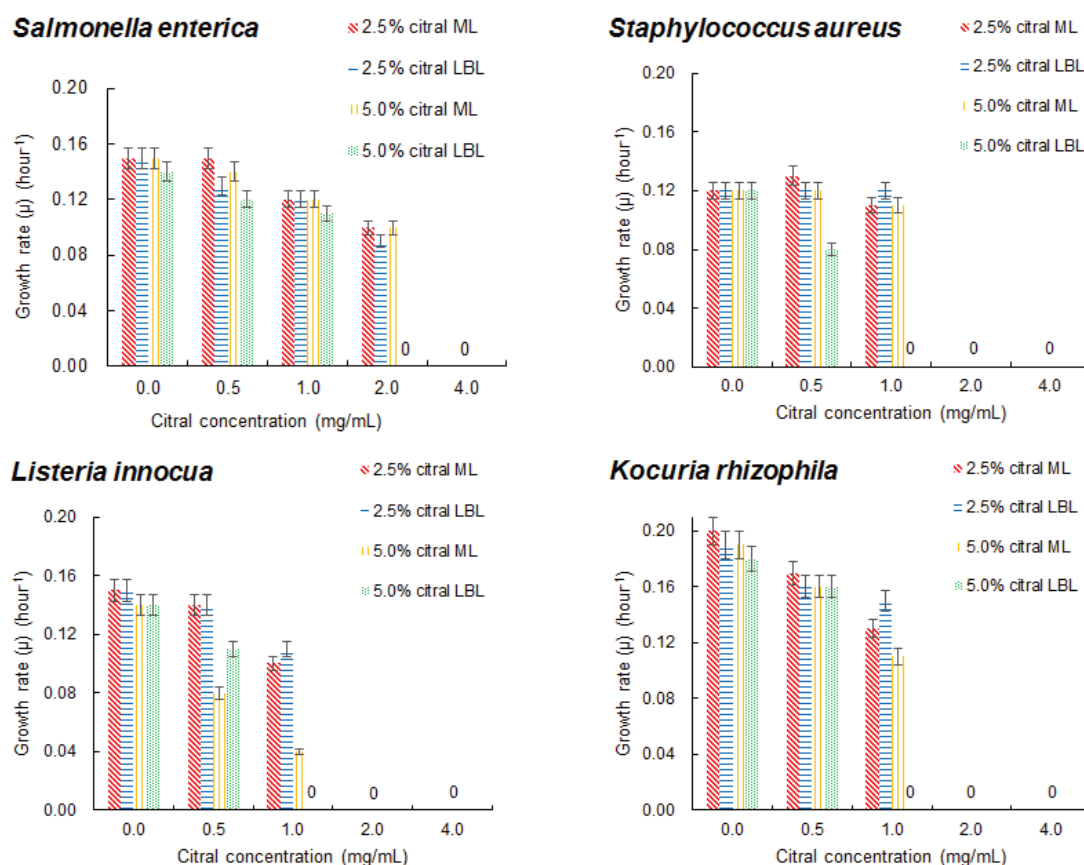
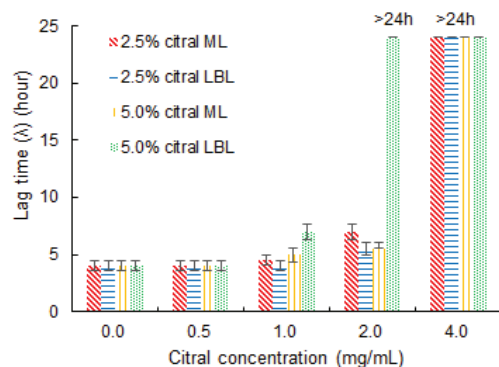


Figure 5.3. Growth rate of 4 tested bacteria (*Salmonella enterica*; *Staphylococcus aureus*; *Listeria innocua*; *Kocuria rhizophila*) treated with 4 kinds of spray-dried powders.

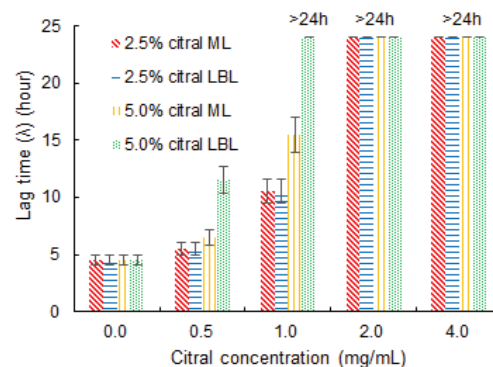
For all tested bacteria, the increase of citral capsule concentration reduced the growth rates (Fig. 5.3) while increasing the lag time (Fig. 5.4). This behavior was also described in other studies (Shi *et al.*, 2016; Silva-Angulo *et al.*, 2015). Compared to the other strains, *Salmonella enterica*, was 2-fold more resistant to citral microcapsules and presented higher growth rates at 37 °C whatever the sub-MIC. In fact, it has been reported that fast-growing cells have been recognized to be more sensitive to the stresses than slow-growing cells (Berney, Weilenmann, Ihssen, Bassin, & Egli, 2006). Moreover, when grown under sub-MIC, *Salmonella enterica* showed longer lag times before starting a fast and exponential growth phase (Fig. 5.4). The increase of the lag time is synonym of the time needed by bacteria to adapt to the non-inhibitory doses of citral (Silva-Angulo *et al.*, 2015). Thus, the presence of *Salmonella enterica* in food products represents a real threat for the consumer because of its great proliferation and adaptation ability to unfavorable conditions. Nevertheless, the formulated citral microcapsules seem to be good food preservatives even when used at non-inhibitory doses since they slowdown the bacterial growth. The application of such citral microcapsule-based delivery

systems can be combined with cold storage to prolong the shelf life of several food products. The obtained citral microcapsules were able to allow a reduction in the concentration of citral and maximize the effectiveness of a given dose, which could reduce the alteration of the organoleptic properties of foods.

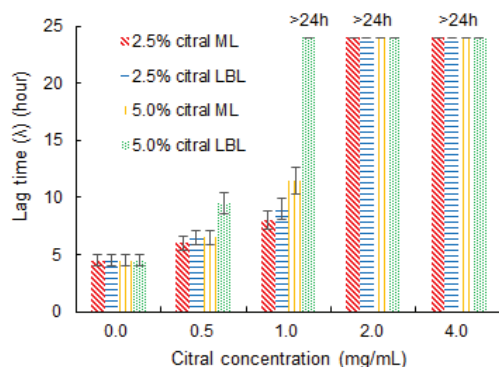
Salmonella enterica



Staphylococcus aureus



Listeria innocua



Kocuria rhizophila

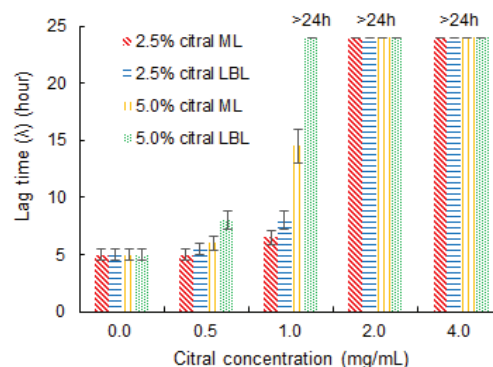


Figure 5.4. Lag time of four tested bacteria (*Salmonella enterica*; *Staphylococcus aureus*; *Listeria innocua*; *Kocuria rhizophila*) treated with 4 kinds of spray-dried powders.

5.4.4. Inhibition zone measurements

Citral microcapsules were added on the surface of a medium containing bacteria. A photograph of inhibition zones of citral microcapsules on medium containing bacteria are shown in Fig. 5.5. After using the same amount of powder (30 mg) for each type of microcapsules inhibition zones with of different sizes were observed: 19.2 ± 0.2 mm for 2.5% citral ML microcapsules; 21.8 ± 0.8 mm for 2.5% citral LBL microcapsules; 25.7 ± 1.9 mm for 5.0% citral ML microcapsules; and 32.5 ± 3.1 mm for 5.0% citral LBL microcapsules (these results were significantly different ($p < 0.05$, $n = 3$)). For the same initial concentration of citral (2.5% or 5.0%), LBL microcapsules had a larger inhibition zone than ML microcapsules. 5% citral microcapsules showed a larger inhibition zone than 2.5% citral microcapsules for both LBL and ML cases. The largest inhibition zone observed for 5.0% citral LBL microcapsules,

was due to the high initial citral loaded concentration and high encapsulation efficiency (91.2%). As a result, 5.0% citral LBL microcapsules contained more citral than the other three types of microcapsules.

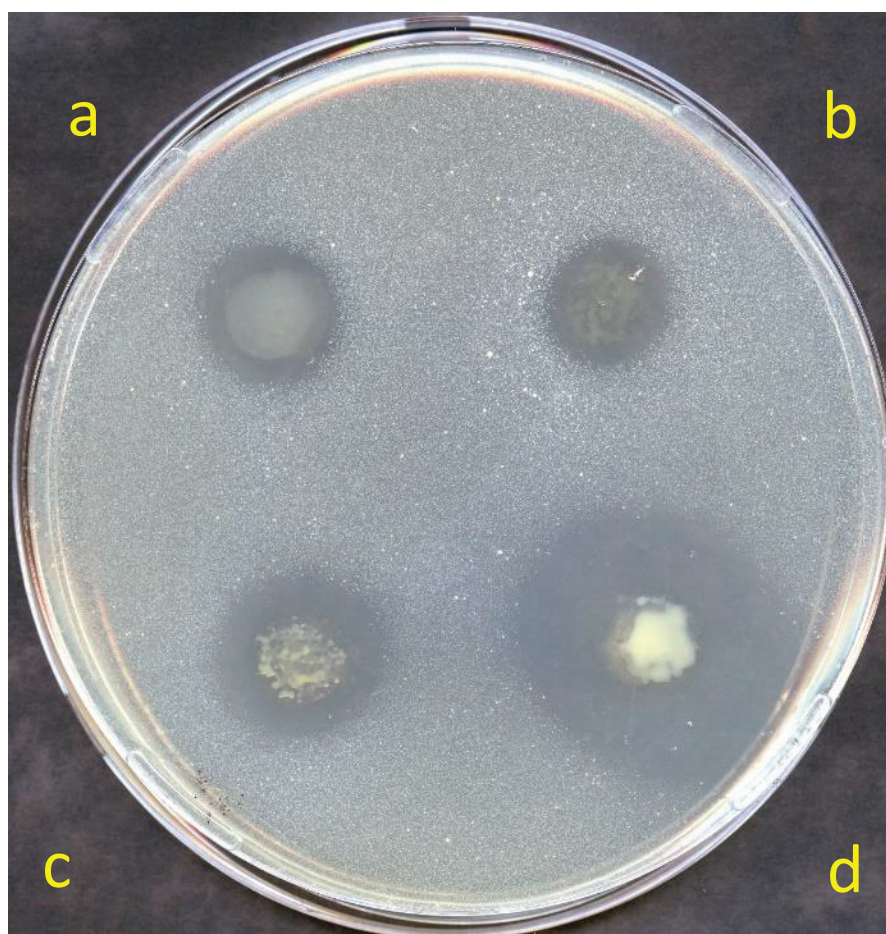


Figure 5.5. Inhibition zones on TSA containing *Kocuria rhizophila* (1×10^6 CFU/mL) with four kinds of spray-dried powders: (a) 2.5% citral ML microcapsules; (b) 2.5% citral LBL microcapsules; (c) 5.0% citral ML microcapsules; (d) 5.0% citral LBL microcapsules.

The size of inhibition zone can be affected by several parameters, like the amount of citral microcapsules, the spread area of citral microcapsules, the amount of citral contained in citral microcapsules, the mechanism of citral's release, the number of bacteria in the medium, the time of measuring inhibition zone.... To evaluate the effect of the release rate of encapsulated citral in these four kinds of citral microcapsules, the amount of citral in each citral microcapsule was calculated according to the encapsulation efficiency (Lu *et al.*, 2018). Then, different amount of the four types of microcapsules containing the same quantity of citral were tested. The inhibition zones of the 4 kinds of citral microcapsules were 24.5 ± 0.5^a mm for 2.5% citral ML microcapsules; 25.4 ± 0.6^a mm for 2.5% citral LBL microcapsules; 30.8 ± 1.0^b mm for 5.0% citral ML microcapsules; and 34.5 ± 1.5^c mm for 5.0% citral LBL microcapsules (different

letters followed by the data are significantly different ($p < 0.05$, $n = 3$)). For this test with the same amount of citral, 5.0% citral LBL microcapsules still had the largest inhibition zone.

5.5. Conclusion

Through preparing and spray-drying ML and LBL emulsions containing 2.5% or 5.0% citral, we studied the effect of interfacial membrane composition and spray-drying on the properties of emulsions. The results illustrated that the addition of the second layer (pectin) could improve the stability of emulsions against the stress sustained during the spray-drying process. With increase of the citral amount, the encapsulation efficiency slightly decreased and particle size had no change in both ML and LBL cases. Microbiological tests demonstrated that 5.0% citral LBL microcapsules had the highest antimicrobial activity, which was further confirmed by the application of the dried powders on a medium surface (inhibition zone measurement). Therefore, our formulated microcapsules seem to be a good food preservative even when used at non-inhibitory doses since they slowdown the bacterial growth. The application of such essential oils microcapsule-based delivery systems combined with storage at low temperatures is a promising technique to prolong the shelf life of perishable food products.

References

- Afzal, S., Maswal, M., & Dar, A. A. (2018). Rheological behavior of pH responsive composite hydrogels of chitosan and alginate: Characterization and its use in encapsulation of citral. *Colloids Surf B Biointerfaces*, 169, 99-106.
- Bakry, A. M., Abbas, S., Ali, B., Majeed, H., Abouelwafa, M. Y., Mousa, A., & Liang, L. (2016). Microencapsulation of Oils: A Comprehensive Review of Benefits, Techniques, and Applications. *Comprehensive Reviews in Food Science and Food Safety*, 15(1), 143-182.
- Belda-Galbis, C. M., Pina-Pérez, M. C., Leufvén, A., Martínez, A., & Rodrigo, D. (2013). Impact assessment of carvacrol and citral effect on *Escherichia coli* K12 and *Listeria innocua* growth. *Food Control*, 33(2), 536-544.
- Berney, M., Weilenmann, H.-U., Ihssen, J., Bassin, C., & Egli, T., (2006). Specific growth rate determines the sensitivity of *Escherichia coli* to thermal, UVA, and solar disinfection. *Applied and Environmental Microbiology*, 72, 2586-2593.
- Choi, S. J., Decker, E. A., Henson, L., Popplewell, L. M., & McClements, D. J. (2009). Stability of citral in oil-in-water emulsions prepared with medium-chain triacylglycerols and triacetin. *J Agric Food Chem*, 57(23), 11349-11353.
- Choi, S. J., Decker, E. A., Henson, L., Popplewell, L. M., & McClements, D. J. (2010). Influence of droplet charge on the chemical stability of citral in oil-in-water emulsions. *J Food Sci*, 75(6), C536-540.
- Eghbal, N., Yarmand, M. S., Mousavi, M., Degraeve, P., Oulahal, N., & Gharsallaoui, A. (2016). Complex coacervation for the development of composite edible films based on LM pectin and sodium caseinate. *Carbohydr Polym*, 151, 947-956.
- Espina, L., Berdejo, D., Alfonso, P., García-Gonzalo, D., & Pagán, R. (2017). Potential use of carvacrol and citral to inactivate biofilm cells and eliminate biofouling. *Food Control*, 82, 256-265.
- Hall, B.G., Acar, H., Nandipati, A., & Barlow, M. (2014). Growth Rates Made Easy. *Molecular Biology and Evolution* 31, 232–238.
- Jelvehgari, M., Valizadeh, H., Rezapour, M., & Nokhodchi, A. (2010). Control of encapsulation efficiency in polymeric microparticle system of tolmetin. *Pharmaceutical Development and Technology*, 15(1), 71-79.

- Kayode, R. M., Azubuike, C. U., Laba, S. A., Dauda, A. O., Balogun, M. A., & Ajala, S. A. (2018). Chemical composition and anti-microbial activities of the essential oil of *A. dansonii* digitata stem-bark and leaf on post-harvest control of tomato spoilage. *Lwt*, 93, 58-63.
- Khorshidian, N., Yousefi, M., Khanniri, E., & Mortazavian, A. M. (2018). Potential application of essential oils as antimicrobial preservatives in cheese. *Innovative Food Science & Emerging Technologies*, 45, 62-72.
- Kovacevic, A., Savic, S., Vuleta, G., Müller, R.H., & Keck, C.M. (2011). Polyhydroxy surfactants for the formulation of lipid nanoparticles (SLN and NLC): effects on size, physical stability and particle matrix structure. *International Journal of Pharmaceutics*, 406(1-2), 163-172.
- Li, R. Y., Wu, X. M., Yin, X. H., Long, Y. H., & Li, M. (2015). Naturally produced citral can significantly inhibit normal physiology and induce cytotoxicity on *Magnaporthe oryzae*. *Pestic Biochem Physiol*, 118, 19-25.
- Liu, D., Zhang, J., Yang, T., Liu, X., Hemar, Y., Regenstein, J. M., & Zhou, P. (2019). Effects of skim milk pre-acidification and retentate pH-restoration on spray-drying performance, physico-chemical and functional properties of milk protein concentrates. *Food Chem*, 272, 539-548.
- Lu, W.-C., Huang, D.-W., Wang, C.-C. R., Yeh, C.-H., Tsai, J.-C., Huang, Y.-T., & Li, P.-H. (2018). Preparation, characterization, and antimicrobial activity of nanoemulsions incorporating citral essential oil. *Journal of Food and Drug Analysis*, 26(1), 82-89.
- Maswal, M., & Dar, A. A. (2014). Formulation challenges in encapsulation and delivery of citral for improved food quality. *Food Hydrocolloids*, 37, 182-195.
- Nishijima, C. M., Ganev, E. G., Mazzardo-Martins, L., Martins, D. F., Rocha, L. R., Santos, A. R., & Hiruma-Lima, C. A. (2014). Citral: a monoterpene with prophylactic and therapeutic anti-nociceptive effects in experimental models of acute and chronic pain. *Eur J Pharmacol*, 736, 16-25.
- Prakash, A., Baskaran, R., Paramasivam, N., & Vadivel, V. (2018). Essential oil based nanoemulsions to improve the microbial quality of minimally processed fruits and vegetables: A review. *Food Res Int*, 111, 509-523.
- Saddiq, A. A., & Khayyat, S. A. (2010). Chemical and antimicrobial studies of monoterpene: Citral. *Pesticide Biochemistry and Physiology*, 98(1), 89-93.

- Sejersen, M. T., Salomonsen, T., Ipsen, R., Clark, R., Rolin, C., & Engelsen, S. B. (2007) Zeta potential of pectin-stabilised casein aggregates in acidified milk drinks. *International Dairy Journal*, 17(4), 302-307.
- Shi, C., Song, K., Zhang, X., Sun, Y., Sui, Y., Chen, Y., et al. (2016). Antimicrobial activity and possible mechanism of action of citral against *Cronobacter sakazakii*. *PLoS ONE* 11(7), e0159006.
- Silva-Angulo, A.B., Zanini, S.F., Rosenthal, A., Rodrigo, D., Klein, G., & Martínez A. (2015). Comparative study of the effects of citral on the growth and injury of *Listeria innocua* and *Listeria monocytogenes* cells. *PLoS ONE* 10(2), e0114026.
- Sosa, N., Schebor, C., & Pérez, O. E. (2014). Encapsulation of citral in formulations containing sucrose or trehalose: Emulsions properties and stability. *Food and Bioprocess Technology*, 92(3), 266-274.
- Sosa, N., Zamora, M. C., Chirife, J., & Schebor, C. (2011). Spray-drying encapsulation of citral in sucrose or trehalose matrices: physicochemical and sensory characteristics. *International Journal of Food Science & Technology*, 46(10), 2096-2102.
- Tajkarimi, M. M., Ibrahim, S. A., & Cliver, D. O. (2010). Antimicrobial herb and spice compounds in food. *Food Control*, 21(9), 1199-1218.
- Tak, J. H., & Isman, M. B. (2016). Metabolism of citral, the major constituent of lemongrass oil, in the cabbage looper, *Trichoplusia ni*, and effects of enzyme inhibitors on toxicity and metabolism. *Pestic Biochem Physiol*, 133, 20-25.
- Tian, H., Lu, Z., Li, D., & Hu, J. (2018). Preparation and characterization of citral-loaded solid lipid nanoparticles. *Food Chem*, 248, 78-85.
- Yang, Y., Cui, S. W., Gong, J., Guo, Q., Wang, Q., & Hua, Y. (2015). A soy protein-polysaccharides Maillard reaction product enhanced the physical stability of oil-in-water emulsions containing citral. *Food Hydrocolloids*, 48, 155-164.

Summary of Chapter 6

After the encapsulation of the bioactive hydrophobic molecule citral, lysozyme (LYS) was chosen as the model of bioactive hydrophilic molecules to be encapsulated. Therefore, heteroprotein complex coacervation between LYS and CAS was investigated at pH 7. At this pH, LYS has the maximum hydrolytic activity, besides, LYS and CAS carried opposite charges allowing these two proteins to be combined by electrostatic forces. The complexation behaviors between the two proteins were investigated by turbidity, zeta-potential, particle size and ITC analysis. Furthermore, LYS activity in heteroprotein complexes with different LYS/CAS ratios was evaluated. The heteroprotein complexes with optimized conditions were spray-dried with a carrier of maltodextrins. The release of LYS from the spray-dried microcapsules can be triggered by adding calcium ions, the LYS activity was recovered over 80% of its initial activity.

CHAPTER 6

Formation and properties of lysozyme-caseinate heteroprotein complexes

To be submitted

6.1. Abstract

The formation of heteroprotein complexes obtained by mixing sodium caseinate (CAS) and lysozyme (LYS) at pH 7 was investigated by using turbidimetric analysis, particle size distribution and zeta potential at different CAS/LYS ratios. Moreover, isothermal titration calorimetry (ITC) was used to determine the type and magnitude of the energies involved in the CAS/LYS complexation process and to evaluate the thermodynamic behavior of their complexation. Results revealed that the structure of CAS/LYS complexes drastically changed when CAS/LYS ratio reached 1.0 and the structuring stages were characterized by exothermic signals and were controlled by favorable enthalpy changes due to electrostatic interactions between both proteins. In addition, the interactions between the two proteins were shown to be temperature-dependent and mainly entropy-driven. Furthermore, CAS/LYS complexes showed minimum LYS enzymatic activity at CAS/LYS ratio 1.0. Though spray-drying of CAS/LYS complexes with ratio 1.0, the LYS activity in reconstituted suspension recovered more than 80% of its initial activity after calcium chloride addition. The present study provided useful information about CAS/LYS complexation and binding processes, which could facilitate the application of lysozyme in antimicrobial edible food packaging.

6.2. Introduction

Heteroprotein complex coacervation, which can be simply defined as the complex coacervation between two proteins, has drawn more and more attention recently. Compared to complex coacervation between proteins and polysaccharides, heteroprotein complex coacervation is less studied. Heteroprotein complex coacervation is driven by the attractive forces of two oppositely charged proteins, rather than oppositely charged proteins and polysaccharides. This also indicates that heteroprotein complex coacervation only happens in a pH range between the isoelectric points of the two proteins. Similar to protein-polysaccharide complexes, heteroprotein complexes are also formed by mixing two proteins in order to add a nutritional or a functional value to one of them, as well as to exert a technological function

when used, for example, as a microencapsulation agent.

Some pairs of proteins have already been reported as heteroprotein complex coacervates and showed good properties in different applications. Lysozyme and β -lactoglobulin microspheres were used to encapsulate vitamin D3 ([Diarrassouba, et al., 2015](#)), however, lactoferrin and β -lactoglobulin complexes were used to encapsulate vitamin B9 ([Chapeau, et al., 2017](#); [Chapeau, et al., 2016](#)). In the heteroprotein systems, lactoferrin and lysozyme are mostly selected as positively-charged proteins, due to their high isoelectric points; and other proteins like β -lactoglobulin, caseins, α -lactalbumin, ovalbumin and pea protein are selected as negatively-charged ones, which have isoelectric points close to pH 5. The coacervation between lysozyme and α -lactalbumin is the most described system in the literature compared to the other systems involving lysozyme ([Croguennec, et al., 2017](#)). Some other studies described the coacervation between lysozyme and other proteins such as β -lactoglobulin ([Diarrassouba, et al., 2015](#)), caseins ([Antonov, et al., 2017](#)), bovine serum albumin ([Santos, Carvalho, et al., 2018](#)), ovalbumin ([Santos, Costa, et al., 2018](#)), ovotransferrin ([Wei, et al., 2019](#)) and soy protein isolate ([Zheng, et al., 2020](#)).

Sodium caseinate (CAS) is a kind of milk proteins, which is made by adding sodium hydroxide to acid caseins and contains α_{s1} -, α_{s2} -, β -, and κ -caseins. These four proteins have a strong tendency to associate with each other to form supra-molecular aggregates ([Surh, et al., 2006](#)). The flexible random coil structure of caseinate gives it good emulsifying properties and thermal stability.

Lysozyme (LYS) is a well-studied globular glycoprotein with an enzymatic activity. It has a molar mass of 14.3 kDa and an isoelectric point (pI) of 10.7. LYS presents a denaturation temperature of around 74 °C and its activity significantly decreased by spray-drying as well as by pasteurization ([Bouhallab & Croguennec, 2014](#); [Santos, Carvalho, et al., 2018](#)). The sequence of lysozyme contains 129 amino acid residues, five α -helices, three-stranded antiparallel β -sheet, and a large amount of random coil and β -turns. In addition, its structure is stabilized by four disulfide bonds with most of the cysteins situated in the α -helices. Antimicrobial activity of LYS against wide range of food spoilage organisms is due to its ability to hydrolyze β -1-4 glycosidic bonds between N-acetylmuramic acid and N-acetylglucosamin of bacterial cell wall peptidoglycan. Hen egg white lysozyme (E1105) is a widely used enzyme in food preservation and is present at high concentrations in egg white (3.4%). It has been authorized for food preservation in the European Union under 2008/1333/EC Regulation on food additives. High natural abundance is also one of the significant reasons for selecting hen egg white lysozyme as a model protein.

Sodium caseinate based films containing LYS were prepared by extrusion processes

([Yilin., et al., 2015](#)), which confirmed the possibility to prepare CAS/LYS films at industrial scale. In a similar work, sodium caseinate films were prepared for releasing LYS at the pH around pI of CAS ([Mendes de Souza, et al., 2010](#)). The authors highlighted that pH and glyoxal efficiently retarded the release of LYS, but other crosslinkers, as calcium chloride or transglutaminase, generated stronger interactions between CAS and LYS that almost blocked the LYS activity. The complexation behavior of LYS with CAS and micellar casein at pH 7 was also studied ([Antonov, et al., 2017](#)), and the authors highlighted that the structure of the complexes formed in LYS-CAS system were changed as a function of concentration, pH, and charge ratio. However, LYS activity in CAS/LYS complexes at different CAS/LYS ratios was not well studied, and the thermal behavior of CAS/LYS complexes is still not clear.

The purpose of this work was to define conditions limiting thermal inactivation of LYS and to optimize the mass ratio of CAS/LYS to improve thermal stability of lysozyme during spray-drying. Considering that heteroprotein coacervation only happened in the pH range between two isoelectric points of the two proteins (pI of CAS: ~ 4.5 ; pI of LYS: ~ 10.7) and LYS had good activity at neutral pH, pH 7.0 was chosen as the studied condition in this research. The information resulting from this study will be relevant to estimate the potential applications of lysozyme-caseinate complexes for thermo-mechanical processing and design of antimicrobial edible food packaging films and microcapsules.

6.3. Materials and methods

6.3.1. Materials

Lysozyme (LYS) sourced from hen egg white (lyophilized powder) with an isoelectric point of ~ 10.7 was purchased from Sigma-Aldrich Chimie (St Quentin Fallavier, France). Sodium caseinate (CAS) powder was purchased from Fisher Scientific (United Kingdom). Through Kjeldahl method, the protein content in CAS was 93.20% (nitrogen conversion factor $N=6.38$). Maltodextrins DE 19 were given by Roquette-frères SA (Lestrem, France). The *Micrococcus lysodeikticus* ATCC 4698 cell wall membranes, analytical grade calcium chloride (CaCl_2), imidazole ($\text{C}_3\text{H}_4\text{N}_2$), acetic acid, sodium hydroxide (NaOH), and hydrochloric acid (HCl) were purchased from Sigma-Aldrich Chimie (St Quentin Fallavier, France). Distilled water was used for all aqueous solution preparations.

6.3.2. Preparation of stock solutions and heteroprotein complexes

Imidazole-acetate buffer solutions (5 mM, pH 7.0) were prepared by solubilizing imidazole and acetic acid in distilled water and then adjusting the solution pH to 7.0. Stock

solutions of LYS (7.142 g/L) and CAS (7.142 g/L) were separately prepared by solubilizing each powder in imidazole-acetate buffer (5 mM, pH 7.0) and mildly stirred for 1 h until it was completely solubilized. HCl (0.1 M) or NaOH (0.1 M) was added to adjust the solution pH to 7.0. To obtain the designed CAS/LYS ratio, the two stock solutions were combined at appropriated volumes and imidazole-acetate buffer (5 mM, pH 7.0) was added to obtain solution with 0.714 g/L LYS and 0–2.856 g/L CAS (CAS/LYS ratio: 0 – 4). These solutions were then agitated for 1 h and their pH was checked, and readjusted to pH 7.0 if necessary.

6.3.3. Turbidity measurement

Heteroprotein suspensions turbidity of pH 7.0 complexes was measured at 600 nm in plastic cuvettes (1 cm path length) with an UV/Vis spectrophotometer (Jenway 3705, Villepinte, France). If the value was higher than 1.0, the suspensions were diluted with buffer to have correct optical density. Before the turbidity measurement, all solutions were homogenized during 10 min and the pH was verified again.

6.3.4. Zeta potential measurement

The zeta potential (ζ -potential) of LYS-CAS complexes were measured with a Zetasizer NanoZS90 (Malvern Instruments, Malvern, UK). The samples were diluted with imidazole-acetate buffer (5 mM, pH 7.0). The mean ζ -potential (ZP) values and the corresponding standard deviation (SD) were reported from the Zetasizer.

6.3.5. Particle size measurement

Particle size of CAS/LYS complexes were measured by a laser diffraction instrument (Mastersizer 3000, Malvern Instruments, Worcestershire, UK). Before the measurements, the complexes were added into the measurement chamber filled with imidazole-acetate buffer (5 mM, pH 7.0) to avoid multiple scattering effects. In order to have homogeneous samples, the complexes were continually stirred at 2000 rpm during the measure. The volume weighted mean particle diameter ($D_{[4,3]}$) was determined by the software from three injections of three separate samples with five readings per sample.

6.3.6. Isothermal titration calorimetry (ITC)

The heat change during the interaction between CAS and LYS was detected by using an isothermal titration calorimeter (VP-ITC, MicroCal, Northampton, USA). LYS and CAS solutions were prepared by using 5 mM imidazole-acetate buffer (pH 7.0) and degassed while stirring for 10 min before the test. The LYS solution (0.714 g/L) was added into the calorimetric

cell (cell volume as 1.4214 mL), and equilibrated at 25, 35, 45 or 55 °C. The CAS solution (5.0 g/L) was loaded into injecting syringe. The titration process was set as a 2 µL initial injection. Twenty-eight successive 10 µL injections of CAS (5.0 g/L), with continuously stirring at 307 rpm, were realized. Every injection went on 20 s, and there was an interval of 200 s between each injection. Control titrations were carried out to exclude the impact of the heat from dilution and injection by injecting the CAS solution into imidazole-acetate buffer. Hence, corrected raw data was obtained through the software in the instrument by subtracting the heat of dilution and injection data from the raw data. Data analysis was carried out with Origin 7.0 software (MicroCal LLC). The enthalpy change and entropy change were obtained by fitting the titration curve with “one set of sites” model in the software. The Gibbs free energy was calculated from the equation (6.1)

$$\Delta G = \Delta H - T\Delta S \quad (6.1)$$

Measurements were performed 3 times, and the results were expressed as the mean with standard deviation.

6.3.7. Spray-drying and reconstitution of lysozyme/caseinate complexes

A laboratory scale spray-drier equipped with a 0.5 mm nozzle atomizer (Mini spray-dryer B-290, BUCHI, Switzerland) was used to dry the LYS/CAS complexes prepared in imidazole-acetate buffer (5 mM, pH 7.0) containing 10 wt.% maltodextrins DE 19. LYS/CAS complexes were pumped to the spray-drier at a feed rate of 0.5 L/h at room temperature and dried at an inlet temperature of 180 °C and an outlet temperature of 80 ± 5 °C. After Spray-drying, the dried powders were collected and stored in airtight containers at 4 °C. Reconstituted suspensions of complexes were prepared by dispersing weighted Spray-dried powders (the same dry matter as before drying) in imidazole-acetate buffer (5 mM, pH 7.0). After 1 h of stirring at around 200 rpm, the reconstituted suspensions were examined. To dissociate CAS/LYS coacervates, calcium chloride (40 g/L) were added in reconstituted suspensions at appropriate volume.

6.3.8. Lysozyme activity evaluation

The lysozyme activity of the heteroprotein complexes before and after spray-drying was determined at 25 °C by tracking the decrease of optical density at 450 nm (OD_{450}) due to the lysis of *M. lysodeikticus* cells. In a 1 cm plastic cuvette, 2.9 mL of *M. lysodeikticus* suspension solution ($OD_{450} = 1$) prepared in imidazole-acetate buffer (5 mM, pH 7.0) were homogenized with 0.1 mL of the sample solution. The OD_{450} decrease was registered each 10 s with an UV/Vis spectrophotometer (photoLab® 7600 UV-VIS series, WTW, Weilheim, Germany).

When a plateau was obtained, the measures were stopped. Lysozyme activity was calculated from the slope of the initial linear portion of OD₄₅₀ versus time curve. Equation (6.2) was used to determine the hydrolytic activity of the sample:

$$Activity (U/mL) = \frac{S}{0.001 \times V} \quad (6.2)$$

where S is the slope of the initial linear portion of optical density versus time (min) curve and V is the volume of added sample suspension (0.1 mL).

6.3.9. Statistical analysis

At least triplicate was realized for all assays. Means and standard deviations were computed and Fishers Least Significant Difference (LSD) test at $p < 0.05$ significance level (Statgraphics Centurion XV) was used to determine differences between means.

6.4. Results and discussion

6.4.1. Properties of heteroprotein complexes in solution

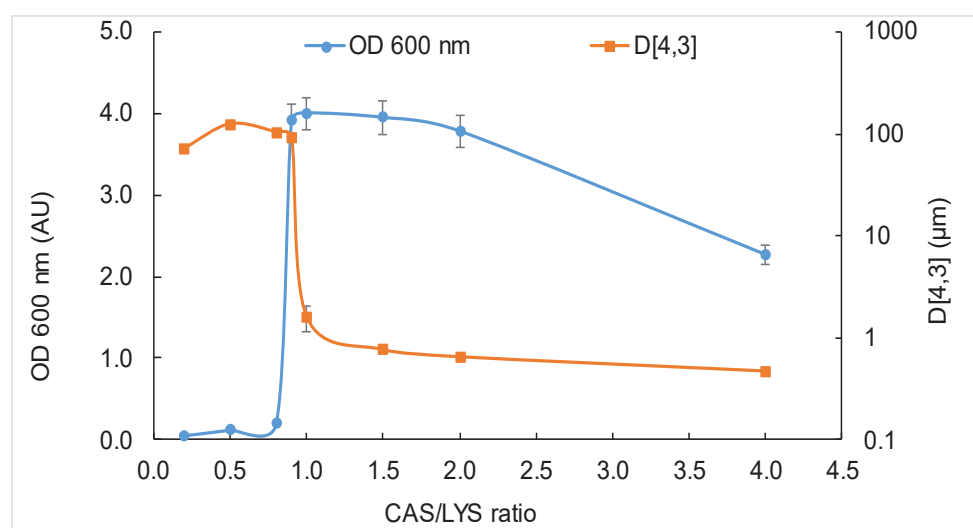


Figure 6.1. Particle size and optical density at 600 nm (OD 600) of CAS/LYS suspensions as a function of CAS/LYS ratio at pH 7 (the concentration of lysozyme is constant: 0.714 g/L).

The change of turbidity can reflect the phase transition between soluble complexes and insoluble ones. As shown in Fig. 6.1, the optical density (OD) of CAS/LYS complexes at pH 7.0 was evaluated as a function of CAS/LYS ratio. At low CAS/LYS ratio range, from 0.0 to 0.8, the turbidity was relatively low but increased slightly from 0.0 to 0.2, which could be due to the formation of insoluble complexes. With CAS/LYS ratio increase from 0.8 to 1.0, the turbidity was drastically increased from 0.2 to 4.0, which could indicate a transition from insoluble complexes to more soluble complexes. After reaching a maximum value at CAS/LYS

ratio 1.0, the turbidity then decreased as the CAS/LYS ratio continues to increase. Due to the opposite charges carried by lysozyme and caseinate at pH 7.0, complexation could occur *via* electrostatic forces immediately after adding small amounts of caseinate to lysozyme. When the CAS/LYS ratio was below 1.0, lysozyme was sufficient to combine with added caseinate. Due to the flexible chain structure of caseinate, limited amount of caseinate molecules possess several negatively charged sites to combine with sufficient lysozyme molecules in the medium. As a result, one molecule of caseinate chain would be combined with several molecules of lysozyme to form large and loose structure complexes allowing light to pass through which gives a low absorbance value. When CAS/LYS ratio was close to 1.0, the continued added caseinate would dissociate the large CAS/LYS complexes to form numerous and more soluble particles, which result in a sharp increase of turbidity from ratio 0.8 to ratio 0.9, the turbidity then reached the maximum at CAS/LYS ratio 1.0. After that, excessively added caseinate induced the increase of electrostatic repulsive forces and the dissociation of the small particles, which resulted in the decrease of turbidity. These results were in accordance with other published studies ([Antonov, et al., 2017](#)).

The turbidity results were further analyzed in relation to the results of particle size measurements, as shown in [Fig. 6.1](#). When the CAS/LYS ratio was below 0.9, the mean particle size of CAS/LYS complexes was close to 100 μm . This confirmed that limited added caseinate molecules were complexed with lysozyme to form large size particles. These large size complexes can be assumed to be composed of a caseinate main chain combined with several lysozyme molecules. The resulted insoluble complexes had no significant effect on the turbidity until the CAS/LYS ratio was closed to 1.0. When the CAS/LYS ratio reached 1.0, particle size of complexes dramatically decreased which was accompanied by a sharp increase of turbidity. This result further confirmed that the structure of CAS/LYS complexes was changed from insoluble complexes to soluble complexes. This could indicate that, at CAS/LYS ratio 1.0, the introduced caseinate molecules were sufficient in number to combine with lysozyme molecules in the system, which inhibited the aggregation of CAS/LYS complexes. When the CAS/LYS ratio further increased over 1.0, significant decrease in both OD and particle size of CAS/LYS complexes was observed. It could be assumed that caseinate was in excess in this situation which formed ionic screen to strengthen electrostatic repulsive force and dissociation of large complexes.

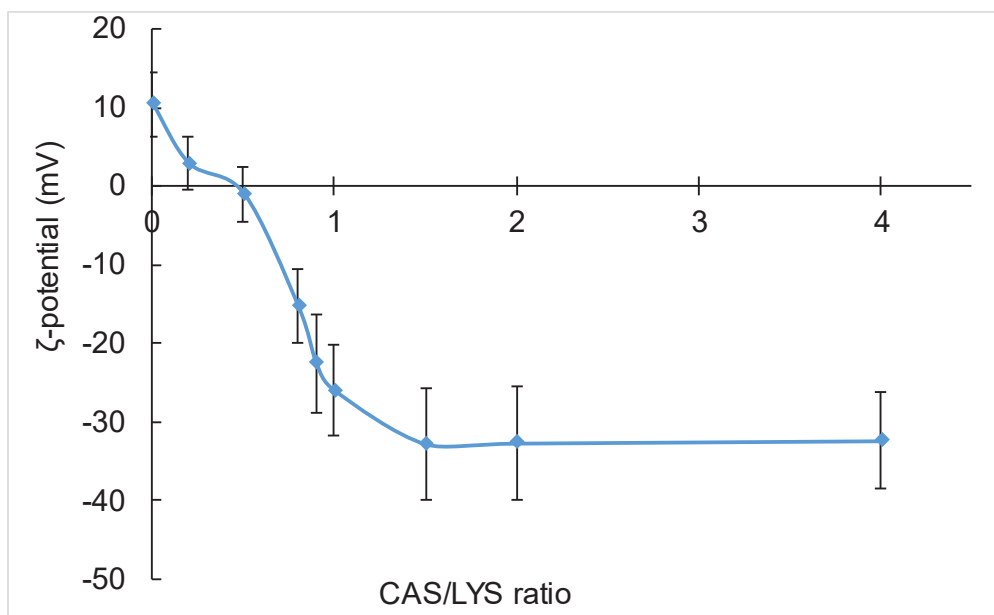


Figure 6.2. Zeta-potential of CAS/LYS complexes as a function of CAS/LYS ratio.

Because CAS/LYS complexation is assumed to be mainly driven by electrostatic forces, surface charge change of CAS/LYS complexes as a function of CAS/LYS ratio was necessary to study for a better understanding of the formation of complexes. As shown in Fig. 6.2, the zeta-potential of CAS/LYS complexes decreased from +10 mV to −32 mV with addition of caseinate until the CAS/LYS ratio reached 1.5 ratio, after that the zeta-potential was constant at around −32 mV. At pH 7.0, lysozyme was positively charged which was due to positively charged arginine and lysine residues on the surface of lysozyme ([Steudle & Pleiss, 2011](#)), while caseinate carried negative charges from the phosphoserine residues and carboxyl groups ([Nagy, et al., 2010](#)). With increase of CAS/LYS ratio, more and more positively-charged lysozyme molecules were neutralized by negatively-charged caseinate molecules, which results in a decrease in surface charges of CAS/LYS complexes. After CAS/LYS ratio reached ratio 1.5, the positive charges from lysozyme were screened by negative charges from added caseinate, resulting in a stable zeta-potential with continued increase of CAS/LYS ratio over 1.5.

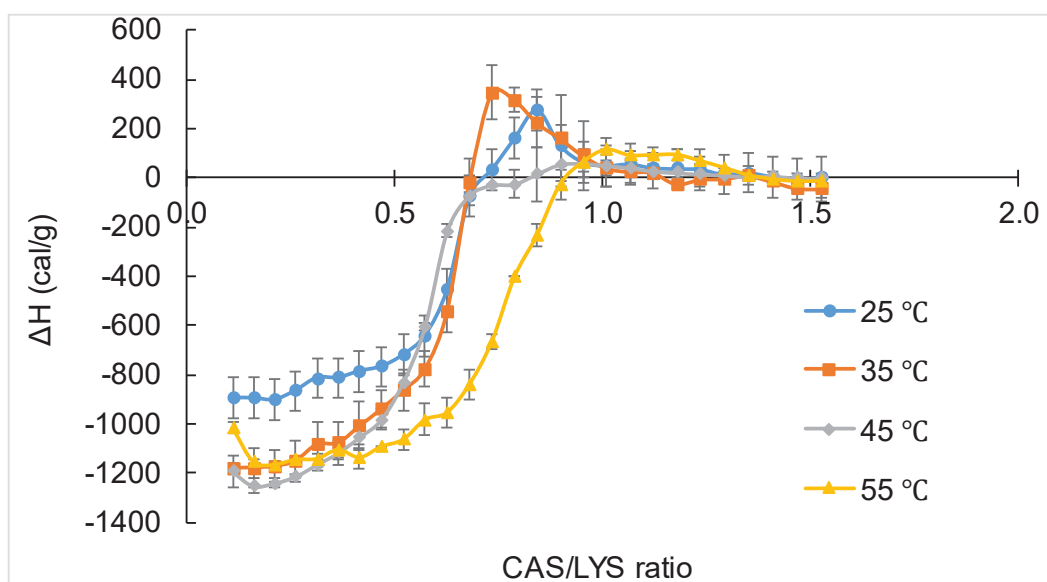
6.4.2. Thermodynamics of CAS/LYS interactions

There are many researches about the thermal stability of CAS ([Sauer & Moraru, 2012](#)) and improving stability of thermal sensitive proteins by combination with CAS ([Li & Zhao, 2017](#); [Wu, et al., 2018](#)). Therefore, it seems useful to study the effect of temperature on the binding interactions between CAS and LYS by ITC tests performed at different temperatures (25 °C, 35 °C, 45 °C and 55 °C).

Table 6.1. Thermodynamic binding parameters for CAS-LYS interactions at 25 - 55 °C.

T (°C)	ΔH (kcal/g)	ΔS (kcal/g/degree)	ΔG (kcal/g)
25	-814.5 ± 24.5	25.4	-8387.5
35	-1090.7 ± 60.6	24.83	-8742.1
45	-1156.7 ± 24.0	22.93	-8451.9
55	-1090.0 ± 62.5	21.7	-8210.9

The thermodynamic binding parameters of ITC tests at different temperatures are shown in Table 6.1, which are obtained by modeling raw ITC data with “one set of sites”. The enthalpy changes (ΔH) per gram of CAS versus CAS/LYS mass ratio were obtained by software. In this study, mass unit was used rather than molecular unit, because CAS had no certain molecular weight because it mainly consists of α_{s1} -, α_{s2} -, β -, and κ -caseins and its molecular weight would change depending on its composition proportion.

**Figure 6.3.** Isothermal titration calorimetry graphics of the interactions between CAS and LYS at different temperatures (25, 35, 45 and 55 °C) at pH 7.

As shown in Fig. 6.3, the interactions between CAS and LYS were similar at the temperature range from 25 to 55 °C. At low CAS/LYS ratio, the interactions between CAS and LYS were exothermic at tested temperatures, which indicate that enthalpy driven interactions are predominant due to electrostatic interactions caused between oppositely charged biopolymers. The enthalpy change increased with increasing the temperature from 25 to 45 °C, and decreased from 45 to 55 °C. This result indicates that temperature modified the protein structure, which affected the interactions between the two proteins. These two proteins could

expose more oppositely-charged moieties at around 45 °C than other temperatures. Another assumption could be that temperature increase could induce structural changes that increased hydrophobic interactions between the two proteins. In fact, hydrophobic interactions are endothermic reactions that can occur at the same time as electrostatic interactions that can increase by exposition of more charged groups in both proteins. The integrated impacts of increased hydrophobic and electrostatic interactions could explain the maximum enthalpy change shown at around 45 °C (Table 6.1). At high temperatures (> 45 °C), hydrophobic interactions between two proteins could be enhanced due to the exposure of hydrophobic sites in the surface of protein molecules, this endothermic reaction could absorb the heat released by electrostatic interactions that resulted in an enthalpy decrease.

At CAS/LYS ratio 1.0, some endothermic interactions could be observed at 25 and 35 °C (Fig. 6.3), which means that some entropy driven interactions happened. Combined with the results from particle size and turbidity measurements, this corroborated with a hypothesis of a structural change of CAS/LYS complexes from insoluble complexes to soluble complexes. When CAS/LYS ratio was over 1.0, no interaction was observed at all tested temperatures, which was also consistent with previous results indicating a saturation of interaction sites of lysozyme molecules.

6.4.3. Lysozyme activity of CAS/LYS complexes

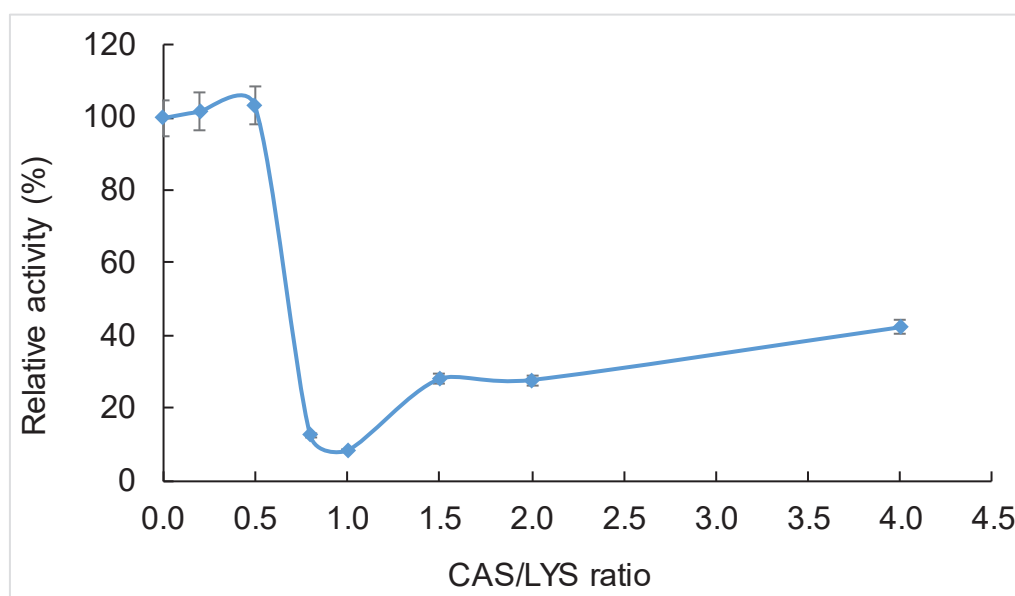


Figure 6.4. Relative activity of CAS/LYS complexes against *Micrococcus lysodeikticus* cell membrane as a function of CAS/LYS ratio.

To evaluate the feasibility of LYS encapsulation with CAS by spray-drying, the LYS activity in heteroprotein complexes with different CAS/LYS ratios was measured firstly. It can

be seen from Fig. 6.4, that the activity of CAS/LYS complexes to *Micrococcus lysodeikticus* was basically stable from CAS/LYS ratios 0.0 to 0.5. A sharp decrease in LYS activity, from 10 266 U/mL to 851 U/mL (8.29%), was noticed when CAS/LYS ratio reached around 1.0. From this ratio, the LYS activity increased again until reaching a plateau around 2 877 U/mL (28.03%) at ratio 1.5 to 2.0. After ratio 2.0, the LYS activity increased slightly with further increase of CAS/LYS ratio, the LYS activity was around 4 345 U/mL (42.33%) at ratio 4.0.

At low CAS/LYS ratio, there were sufficient free lysozyme molecules to react with *Micrococcus lysodeikticus* and few caseinate molecules that surround lysozyme in the system. These positively-charged lysozyme molecules and CAS/LYS complexes could be easily adsorbed to negatively-charged bacterial membranes. When CAS/LYS ratio was above 0.5, surface charge of CAS/LYS complexes became negative, which indicated that LYS molecules in the system were complexed by CAS, and the active hydrolytic sites of LYS were probably masked by caseinate. At ratio 1.0, LYS activity became minimum, which indicates that the active sites of LYS could be fully covered by CAS. With CAS/LYS ratio increase over 1.0, the CAS/LYS complexes were dissociated (Fig. 6.1) which resulted in exposure of the active sites of LYS, the activity of CAS/LYS complexes to *Micrococcus lysodeikticus* was consequently partially recovered.

To keep the LYS activity during the spray-drying process, the active sites in LYS should be fully covered by CAS. Meanwhile, the size of complexes should be small enough to minimize the effect of shear forces during the atomization step of the spray-drying process. Therefore, the CAS/LYS complexes formed at ratio 1.0 were chosen for LYS encapsulation by spray-drying. After spray-drying, LYS activity in reconstituted CAS/LYS complexes was recovered by addition of calcium ions to release lysozyme molecules from CAS/LYS complexes.

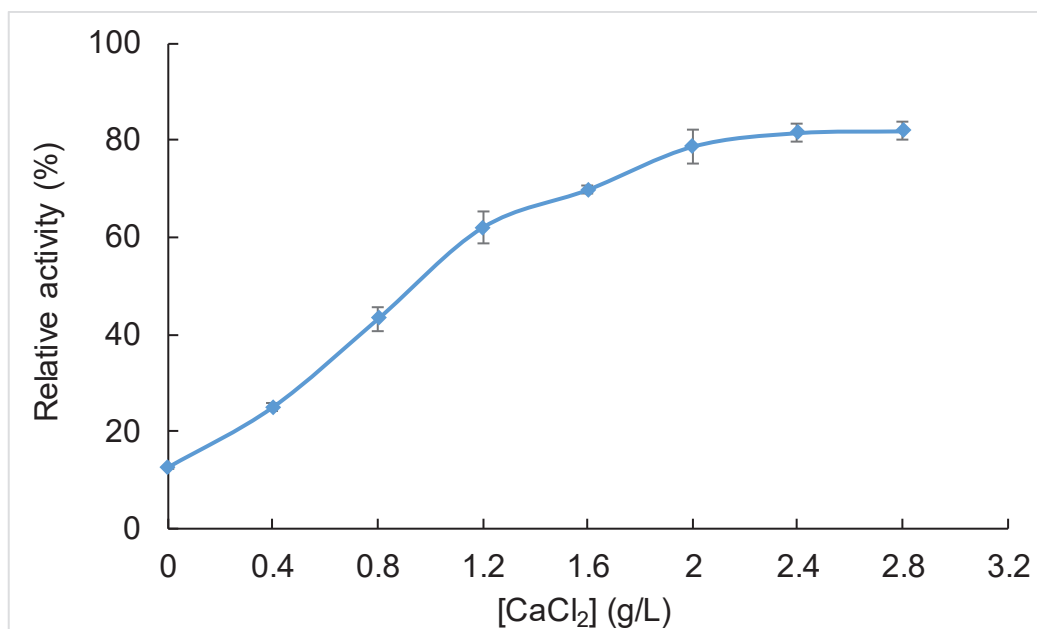


Figure 6.5. Relative activity of reconstituted CAS/LYS complexes against *Micrococcus lysodeikticus* cell membrane as a function of calcium chloride concentration.

According to [Fig. 6.5](#), the relative activity of reconstituted CAS/LYS complexes to *Micrococcus lysodeikticus* was around 12.78% without addition of CaCl₂, which was slightly higher than the relative activity of CAS/LYS complexes before spray-drying. This activity increase could be due to a slight dissociation of large complexes during the pulverization step inside the nozzle (shearing forces). With the addition of calcium chloride, the relative activity of reconstituted CAS/LYS complexes significantly increased from 10% to 80% until the concentration of calcium chloride reached 2.0 g/L, after that, the relative activity was constant at 80%. It can be concluded that the formed CAS/LYS complexes were dissociated with the presence of divalent calcium ions. As expected, lysozyme in the CAS/LYS complexes could be replaced by calcium ions, which resulted in the increase of the enzymatic activity against *Micrococcus lysodeikticus* cell membranes. In one of our previous studies ([Ben Amara, et al., 2016](#)), we showed that free lysozyme (uncomplexed) showed a decrease of its activity (residual activity: 63.5%) when this protein was spray-dried in the same conditions. The results obtained in the present work showed clearly that lysozyme complexation by caseinate can protect lysozyme against thermomechanical inactivation particularly during the spray-drying process. Moreover, to trigger the release of LYS from CAS/LYS complexes, the release mechanism by introducing calcium ions could be replaced by decreasing environmental pH below the isoelectric point of CAS (pH ~ 4.5). However, LYS can loss a part of its activity at acidic pH ([Bayarri, et al., 2014](#)) and further researches could be done to improve the release mechanism of complexed lysozyme from spray-dried microcapsules.

6.5. Conclusion

The present study investigated the formation of heteroprotein coacervates between CAS and LYS at pH 7. By measuring turbidity, particle size distribution and zeta-potential, we found that, when CAS/LYS ratio was below 1.0, limited caseinate chains could combine with abundant lysozyme molecules to form complexes with a big size ($\sim 100\ \mu\text{m}$). However, when CAS/LYS ratio reached 1.0, the lysozyme molecules were saturated with caseinate chains, which induced structural changes of CAS/LYS complexes, allowing to a dramatical increase of turbidity and a decrease of particle size and lysozyme activity. These results were further confirmed with data from ITC tests. The CAS/LYS coacervates at ratio 1.0 were thermally stable during the spray-drying operation. After adding calcium ions to release lysozyme, lysozyme recovered more than 80% of its initial activity. The present study provided useful information about CAS/LYS complexation and binding mechanism, which could facilitate the encapsulation of lysozyme, its incorporation in active packaging films and its controlled release.

References

- Antonov, Y. A., Moldenaers, P., & Cardinaels, R. (2017). Complexation of lysozyme with sodium caseinate and micellar casein in aqueous buffered solutions. *Food Hydrocolloids*, 62, 102-118.
- Bayarri, M., Oulahal, N., Degraeve, P., & Gharsallaoui, A. (2014). Properties of lysozyme/low methoxyl (LM) pectin complexes for antimicrobial edible food packaging. *Journal of Food Engineering*, 131, 18-25.
- Ben Amara, C., Eghbal, N., Degraeve, P., & Gharsallaoui, A. (2016). Using complex coacervation for lysozyme encapsulation by spray-drying. *Journal of Food Engineering*, 183, 50-57.
- Bouhallab, S., & Croguennec, T. (2014). Spontaneous Assembly and Induced Aggregation of Food Proteins. In M. Müller (Ed.), *Polyelectrolyte Complexes in the Dispersed and Solid State II: Application Aspects*, (pp. 67-101). Berlin, Heidelberg: Springer Berlin Heidelberg.
- Chapeau, A.-L., Hamon, P., Rousseau, F., Croguennec, T., Poncelet, D., & Bouhallab, S. (2017). Scale-up production of vitamin loaded heteroprotein coacervates and their protective property. *Journal of Food Engineering*, 206, 67-76.
- Chapeau, A.-L., Tavares, G. M., Hamon, P., Croguennec, T., Poncelet, D., & Bouhallab, S. (2016). Spontaneous co-assembly of lactoferrin and β -lactoglobulin as a promising biocarrier for vitamin B9. *Food Hydrocolloids*, 57, 280-290.
- Croguennec, T., Tavares, G. M., & Bouhallab, S. (2017). Heteroprotein complex coacervation: A generic process. *Advances in Colloid and Interface Science*, 239, 115-126.
- Diarrassouba, F., Remondetto, G., Garrait, G., Alvarez, P., Beyssac, E., & Subirade, M. (2015). Self-assembly of beta-lactoglobulin and egg white lysozyme as a potential carrier for nutraceuticals. *Food Chemistry*, 173, 203-209.
- Li, Q., & Zhao, Z. (2017). Formation of lactoferrin/sodium caseinate complexes and their adsorption behaviour at the air/water interface. *Food Chemistry*, 232, 697-703.
- Mendes de Souza, P., Fernández, A., López-Carballo, G., Gavara, R., & Hernández-Muñoz, P. (2010). Modified sodium caseinate films as releasing carriers of lysozyme. *Food Hydrocolloids*, 24(4), 300-306.
- Nagy, K., Pilbat, A. M., Groma, G., Szalontai, B., & Cuisinier, F. J. (2010). Casein aggregates built step-by-step on charged polyelectrolyte film surfaces are calcium phosphate-cemented. *Journal of Biological Chemistry*, 285(50), 38811-38817.
- Santos, M. B., Carvalho, C. W. P., & Garcia-Rojas, E. E. (2018). Heteroprotein complex formation of bovine serum albumin and lysozyme: Structure and thermal stability. *Food Hydrocolloids*, 74, 267-274.
- Santos, M. B., Costa, A. R. D., & Garcia-Rojas, E. E. (2018). Heteroprotein complex coacervates of ovalbumin and lysozyme: Formation and thermodynamic characterization. *International Journal of Biological Macromolecules*, 106, 1323-1329.
- Sauer, A., & Moraru, C. I. (2012). Heat stability of micellar casein concentrates as affected by temperature and pH. *Journal of Dairy Science*, 95(11), 6339-6350.
- Steudle, A., & Pleiss, J. (2011). Modelling of lysozyme binding to a cation exchange surface at atomic detail: the role of flexibility. *Biophysical Journal*, 100(12), 3016-3024.
- Surh, J., Decker, E., & McClements, D. (2006). Influence of pH and pectin type on properties and stability of sodium-caseinate stabilized oil-in-water emulsions. *Food Hydrocolloids*, 20(5), 607-618.
- Wei, Z., Cheng, Y., & Huang, Q. (2019). Heteroprotein complex formation of ovotransferrin and lysozyme: Fabrication of food-grade particles to stabilize Pickering emulsions. *Food Hydrocolloids*, 96, 190-200.
- Wu, X., Liu, A., Wang, W., & Ye, R. (2018). Improved mechanical properties and thermal-stability of collagen fiber based film by crosslinking with casein, keratin or SPI: Effect

- of crosslinking process and concentrations of proteins. *International Journal of Biological Macromolecules*, 109, 1319-1328.
- Yilin., C. B., Pierre., P., Sophie., G., Nadia., O., Gilles., A., Frédéric., P., & Pascal., D. (2015). Active biodegradable sodium caseinate films manufactured by blown-film extrusion: Effect of thermo-mechanical processing parameters and formulation on lysozyme stability. *Industrial Crops and Products*, 72, 142-151.
- Zheng, J., Tang, C.-h., Ge, G., Zhao, M., & Sun, W. (2020). Heteroprotein complex of soy protein isolate and lysozyme: Formation mechanism and thermodynamic characterization. *Food Hydrocolloids*, 101, 105571.

Summary of Chapter 7

Based on our previous works, there were no interactions between CAS and LMP at pH 7, and at the same pH, LYS could interact with CAS and LMP, separately. We designed ternary complexes consisting of LYS, CAS and LMP. Different formulations would result in different properties of ternary complexes. The complexation behaviors between the three biopolymers were studied through the techniques we used before.

CHAPTER 7

Formation and characterization of lysozyme-caseinate-pectin ternary complexes

To be submitted

7.1. Abstract

The ternary complexes were formed by adding three different ratios of sodium caseinate (CAS) and low methoxyl pectin (LMP) mixture to lysozyme (LYS) at pH 7. The formation was investigated by using turbidimetric analysis, particle size distribution and zeta-potential at different CAS-LMP/LYS ratios. With the CAS/LMP ratio increasing from 1:2 to 2:1 in CAS-LMP mixture, the interactions between LYS and CAS-LMP mixture were delayed, because CAS has fewer negative charges than LMP to combine with positively-charged LYS at pH 7. Moreover, isothermal titration calorimetry (ITC) was used to determine the type and magnitude of the energies involved in the CAS-LMP/LYS complexation process and to evaluate the thermodynamic behavior of their complexation. ITC results revealed that the interactions were an exothermic process with a favorable entropic and entropic contribution. The titration curve in ITC tests corroborated the turbidity change of ternary complexes at different ratios, the CAS-LMP/LYS ratio marked the end of interactions between CAS-LMP mixture and LYS detected by ITC. In addition, the LYS activity in different forms of ternary complexes was measured. The present study provided useful information about the interactions between LYS and CAS-LMP, which could facilitate the application of LYS for dairy food preservation.

7.2. Introduction

During many decades, complex coacervation between proteins and polysaccharides has been widely studied ([de Kruif et al., 2004](#); [Eghbal & Choudhary, 2018](#)). These studies showed this complexation is mainly driven by the attractive electrostatic force between oppositely charged proteins and polysaccharides. Recently, there are some researches about heteroprotein complex coacervation, or the complex coacervation between two proteins ([Croguennec et al., 2017](#)). Basically, the formation of heteroprotein complex coacervates is the consequence of the binding between two oppositely charged proteins, which is similar to the complex coacervation between the oppositely charged proteins and polysaccharides. The formation of these different kinds of binary complexes can add a nutritional or a functional value to one of them, especially

when these complexes are used for the encapsulation and controlled release of bioactive compounds ([Eghbal & Choudhary, 2018](#)). In addition, the purification of some proteins can be achieved by the formation and dissociation of coacervates.

Besides binary complexes, ternary complexes were also studied for last years. Ternary polysaccharide complexes were formed through complexation among chitosan, hyaluronan and dextran sulphate or heparin ([Wu et al., 2017](#)). Zein, propylene glycol alginate and surfactant (rhamnolipid or lecithin) ternary complexes were fabricated by antisolvent co-precipitation method ([Dai et al., 2018](#)). Meanwhile, a kind of ternary complexes formed by proteins, polysaccharides and polyphenols has also drawn some attention. A covalent ternary complex composed of lactoferrin, dextran and chlorogenic acid was found to show better emulsifying property and physicochemical stability than pure protein or binary conjugates ([Liu et al., 2016](#)). However, the utilization of covalent reactions is limited in real food systems due to the usage of toxic organic reagents, surfactants or chemical cross-linkers. Proteins, polysaccharides and polyphenols are hoped to be interacted through non-covalent interactions (electrostatic force, hydrophobic force, hydrogen bonding and Van der Waals force). The formation of ternary complexes through adding pectin or chitosan on β -lactoglobulin and (+)-catechin was also showed ([Oliveira et al., 2016](#)). Ternary complexes composed of lactoferrin, pectin and (-)-epigallocatechin gallate were fabricated and applied for the encapsulation of β -carotene ([Yang et al., 2018](#); [Yang et al., 2015](#)), similarly as pea protein-pectin-curcumin ternary complex ([Yi et al., 2020](#)), and zein-carboxymethyl chitosan-tea polyphenols ternary ones ([Ba et al., 2020](#); [Wang et al., 2018](#)).

Lysozyme (LYS) is a strongly basic globular protein, which has an isoelectric point (pI) of 10.7. LYS is famous for its broad-spectrum antibacterial activity, especially for Gram-positive bacteria. The composition of bacterial cell walls as peptidoglycan can be hydrolyzed by LYS through breakdown of β -(1,4)-glycosidic bonds between N-acetylmuramic acid and N-acetylglucosamine. LYS can be extracted from hen egg white, and is classified as GRAS (Generally Recognized As Safe). Therefore, LYS could be widely used for food preservation as a food additive. However, in practical applications, LYS can be affected by high temperatures in the application processes and combined with other ingredients in the application environment, resulting in a reduction in its antibacterial activity. Therefore, in order to overcome these problems, there are continuous researches to improve the thermal stability of LYS and study the effects of other components (like proteins, polysaccharides, liposomes...) which could combine with LYS ([Ormus et al., 2015](#); [Wang et al., 2020](#)).

Sodium caseinate (CAS) is commercial form of caseins, which is made by adding sodium hydroxide to acid caseins in dairy industry. As the main content of milk proteins, casein is

composed of four strongly-associated proteins: α_{s1} -, α_{s2} -, β -, and κ -casein. These four proteins result in the flexible structure giving sodium caseinate with excellent emulsifying and foaming abilities. Pectin is an anionic polysaccharide, which is normally extracted from plant raw materials (such as apple pomace, sugar beet chips, and citrus peels). As a safe food additive, pectin is widely used due to its thickening, gelling, and stabilizing properties. Chemically, pectin is mainly composed of α -(1,4)-glycosidic bonded D-galacturonic acid. According to the degree of esterification (DE), high methoxyl pectin (HMP) or low methoxyl pectin (LMP) is corresponding to those higher or lower than 50% methylation, respectively.

In our previous work, we have studied the complexation between lysozyme (LYS) and low methoxyl pectin (LMP) ([Bayarri et al., 2014](#)), and found that the formation of LYS/LMP complexes could improve the physicochemical stability of LYS ([Ormus et al., 2015](#)). In addition, heteroprotein coacervation between sodium caseinate (CAS) and lysozyme (LYS) was also investigated, similar results were found that, like LMP, CAS could combine with LYS through electrostatic force at pH 7. The coverage of active site in LYS by CAS could enhance the thermal stability of LYS. In addition, there is no interaction between CAS and LMP at pH 7.0 ([Wang et al., 2019](#)), allowing to a co-solubility of two biopolymers in solution and LMP are co-soluble in the solution. The purpose of this work was to form a kind of ternary complexes with CAS, LMP and LYS and to study the effect of the different compositions on the physicochemical properties of the formed ternary complexes. According to our previous results, LYS is positively-charged at pH 7 and exhibits good activity at neutral pH. At this pH, CAS and LMP are negatively-charged. Hence, negatively-charged CAS-LMP mixtures could combine with positively-charged LYS. The properties of resulted complexes could be evaluated to know better about the mechanism of the complexation behavior in the ternary complexes. The information resulting from this study could be relevant to estimate the potential applications of LYS in dairy industry for food preservation and the ternary complexes for the encapsulation of bioactive compounds.

7.3. Materials and methods

7.3.1. Materials

Lysozyme (LYS) sourced from hen egg white in lyophilized form with an isoelectric point of 10.7 was purchased from Sigma-Aldrich Chimie (St Quentin Fallavier, France). Sodium caseinate (CAS) in white powder was purchased from Fisher Scientific (United Kingdom). Protein content in CAS determined by the Kjeldahl method was 93.20% (nitrogen conversion factor N=6.38). Low methoxyl pectin (LMP) (Unipektine™ OF 305 C SB) was from Cargill

(Baupte, France). Its degree of esterification was from 22% to 28% and degree of acetylation was from 20% to 23%. The *Micrococcus lysodeikticus* cell walls, imidazole ($C_3H_4N_2$), acetic acid, sodium hydroxide (NaOH), and hydrochloric acid (HCl) were purchased from Sigma-Aldrich Chimie (St Quentin Fallavier, France). All aqueous solutions were prepared in distilled water.

7.3.2. Ternary complexes preparation

Imidazole-acetate buffer (5 mM, pH 7.0) was prepared by solubilizing weighed amounts of imidazole and acetic acid in distilled water and then adjusting the pH to 7.0. Concentrated stock LYS solution (7.142 g/L), CAS-LMP mixture solutions (total concentration: 7.142 g/L, ratio 1:1, 1:2 and 2:1) were prepared by dispersing each powder in imidazole-acetate buffer (5 mM, pH 7.0) separately and stirred for at least 1 h with a magnetic stirrer to make sure them totally soluble. The solution pH was then adjusted by using HCl (1.0 M) or NaOH (1.0 M) to pH 7.0. According to the ratio between LYS and CAS-LMP, calculated volumes of the two stock solutions were mixed and diluted with imidazole-acetate buffer (5 mM, pH 7.0) to get a final solution with 0.7142 g/L LYS and 0 – 1 g/L CAS-LMP (CAS-LMP:LYS ratio: 0 – 1.4).

7.3.3. Turbidity measurement

The turbidity of the ternary complexes at pH 7.0 were measured by using an UV/Vis spectrophotometer (photoLab® 7600 UV-VIS series, WTW, Weilheim, Germany) at 600 nm in plastic cuvettes (1 cm path length). The pure LYS solution (0.7142 g/L) was used as zero blank. Every data was obtained by at least two separated samples with three measurements.

7.3.4. Zeta potential

The zeta potential (ζ -potential) of ternary complexes was determined at 25 °C using a Zetasizer Nano ZS90 (Malvern Instruments, Malvern, UK). If necessary, the samples were diluted with pH 7.0 imidazole-acetate buffer to avoid the effects of multiple scattering. All measurements are performed in triplicate. The mean ζ -potential (ZP) values (\pm standard deviation (SD)) were obtained from the instrument.

7.3.5. Particle size distribution

Particle size distributions of ternary complexes were assessed by a laser diffraction instrument (Mastersizer 3000, Malvern Instruments, Malvern, UK). To avoid multiple scattering effects, the complexes were injected into the measurement chamber where they were diluted with imidazole-acetate buffer (5 mM, pH 7.0) prior to the measurements. The complexes

were stirred continuously throughout the measurement to ensure the samples were homogeneous. The volume mean particle diameter ($D [4,3]$) was calculated by the software from three injections of three separate samples with five readings per sample.

7.3.6. Isothermal titration calorimetry (ITC)

The heat change of the interaction between CAS-LMP and LYS were measured using an isothermal titration calorimeter (VP-ITC, MicroCal, Northampton, MA) with a reaction cell volume of 1.4214 mL. The LYS solution and CAS-LMP mixture solution were prepared by using the same buffer (5 mM imidazole-acetate buffer, pH 7.0) and degassed while stirring for 5-10 min before being loaded. The LYS solution (0.714 g/L) was loaded into the calorimetric cell equilibrated at 25 °C and titrated by adding a 3 μ L initial injection and 28 successive 10 μ L injections of CAS-LMP mixture solution (5.0 g/L) while continuously stirring the solution at 307 rpm. Each injection lasted 20 s, and there was an interval of 200 s between successive injections. Control titrations were performed to obtain the heat of dilution by injecting the CAS-LMP mixture solution into imidazole-acetate buffer, so corrected raw data was acquired by subtracting the heat of dilution data from the raw data. Data analysis was performed with Origin 7.0 software (MicroCal LLC). The Gibbs free energy was calculated from the equation $\Delta G = \Delta H - T\Delta S$. Measurements were carried out in triplicate, and the results are reported as the mean and standard deviation.

7.3.7. Lysozyme activity evaluation

The LYS activity of the ternary complexes was assayed by monitoring the reduction of optical density at 450 nm (OD_{450}) due to the lysis of *M. lysodeikticus* cells by lysozyme at 25 °C. Briefly, in a 1 cm cuvette, 2.9 mL of the *M. lysodeikticus* suspension ($OD_{450} = 1$) in 5 mM imidazole-acetate buffer adjusted to pH 7.0 and 0.1 mL of the enzyme solution (prepared at the same pH) were mixed quickly, and the reduction in the absorbance was recorded using an UV/Vis spectrophotometer (photoLab® 7600 UV-VIS series, WTW, Weilheim, Germany) until reaching a plateau. Lysozyme activity was calculated from the slope of the initial linear portion of absorbance versus time curve. The hydrolytic activity of the lysozyme solution can be calculated using [equation \(7.1\)](#) below (one unit was 0.001 change in absorbance in one minute):

$$Activity (U/ml) = \frac{S}{0.001 \times V} \quad (7.1)$$

where S is the slope of the initial linear portion of absorbance versus time curve and V is the volume of lysozyme solution (0.1 mL).

7.3.8. Statistical analysis

All measurements were measured at least in duplicate. Means and standard deviations were calculated and differences between means were determined with Fishers Least Significant Difference (LSD) test at $p < 0.05$ significance level (Statgraphics Centurion XV).

7.4. Results and discussion

7.4.1. Turbidity of ternary complexes

With adding CAS-LMP mixtures at different mass ratios (1:2, 1:1 and 2:1) to LYS from ratio 0.2 to 1.4, the turbidity evolution curve of ternary complexes was shown in [Fig. 7.1](#) (the concentration of LYS was kept constant at 0.714 g/L in the complex system). When LMP was the major part in CAS-LMP mixture (1CAS-2LMP), the turbidity of ternary complexes increased sharply from 0.50 ± 0.08 at CAS-LMP/LYS ratio 0.2 to 2.38 ± 0.03 at CAS-LMP/LYS ratio 0.6, and decreased sharply to 1.09 ± 0.12 at CAS-LMP/LYS ratio 1.0, then the decreasing trend slowed down to the final turbidity value as 0.69 ± 0.11 at CAS-LMP/LYS ratio 1.4. When CAS/LMP mass ratio is 1:1 in the mixture, the turbidity increased sharply from 0.47 ± 0.14 at CAS-LMP/LYS ratio 0.2 to 2.48 ± 0.01 at CAS-LMP/LYS ratio 0.6, and then decreased slowly to 1.32 ± 0.20 at CAS-LMP/LYS ratio 1.4. When CAS is the major part in CAS-LMP mixture (2CAS-1LMP), the turbidity of ternary complexes increased slowly from 0.35 ± 0.02 at CAS-LMP/LYS ratio 0.2 to 1.82 ± 0.12 at CAS-LMP/LYS ratio 0.8, and then the turbidity was almost constant with some fluctuations. At low CAS-LMP/LYS ratio (0.2), higher proportion of LMP in ternary complexes possessed higher absorbance. Conversely, at high CAS-LMP/LYS ratio (1.4), the higher proportion LMP in ternary complexes, the lower the absorbance of ternary complexes. As CAS/LMP ratio increased from 1:2 to 2:1, the turbidity evolution curve changed from a sharp peak to a slowly increased plateau. These results were in accordance with our previous work ([Bayarri et al., 2014](#)), an obvious peak can be observed during the turbidity evolution curve with adding LMP to LYS, the turbidity reached maximum at LMP/LYS ratio of 0.28. In addition, for heteroprotein binary complexes of CAS/LYS, the turbidity of CAS/LYS complexes was maximal at CAS/LYS ratio 1.0. Therefore, compared with the same amount of CAS, LMP could combine with more LYS at pH 7, which could be further confirmed by the zeta-potential value of LMP that is more negative than CAS.

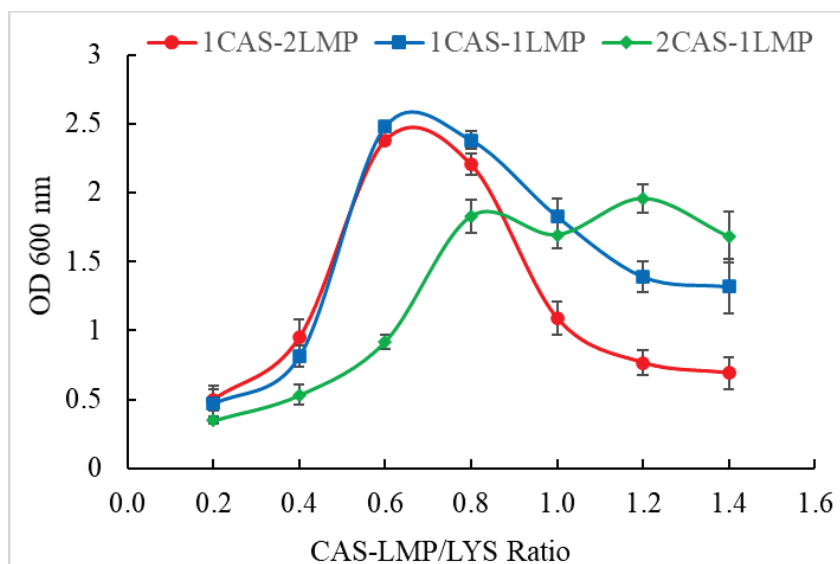


Figure 7.1. Optical density at 600 nm (OD600) of ternary complexes as a function of CAS-LMP/LYS ratio (the concentration of LYS is constant at 0.714 g/L in the complex system, the ratio of CAS-LMP mixtures is 1:2, 1:1 and 2:1).

7.4.2. Isothermal titration calorimetry (ITC)

The complexation behavior between CAS-LMP mixtures and LYS at pH 7.0 was investigated by ITC through detecting the heat change during the titration of CAS-LMP mixture solution with LYS solution, as shown in Fig. 7.2. With injection of CAS-LMP mixtures at different mass ratios (1:2, 1:1 and 2:1), the interactions between CAS-LMP and LYS was an exothermic process. It could be consumed that the released heat was from the neutralization process between negatively-charged CAS-LMP mixture and positively-charged LYS. Similar results also could be found for the interaction between lysozyme and pectin ([Antonov et al., 2020](#)) or sodium caseinate in our previous work. This result reveals that the interactions between CAS-LMP and LYS are mainly driven by electrostatic force. In addition, it can be observed that, the greater the proportion of LMP in the CAS-LMP mixture, the more the heat released and the faster the interaction process ended. In detail, for the first injection, around 1.30 kcal heat was released by injecting 1 g of 1CAS-2LMP mixture, around 1.15 kcal heat for 1 g of 1CAS-1LMP mixture and around 1.03 kcal heat for 1 g of 2CAS-1LMP mixture. With injection number increase, the released heat of each injection decreased. LYS was saturated with CAS-LMP at ratio 0.6 for 1CAS-2LMP and 1CAS-1LMP cases, and for 2CAS-1LMP case, the saturation point was found at CAS-LMP/LYS ratio 0.8. This result is corroborated to the detected maximal turbidity at each composition.

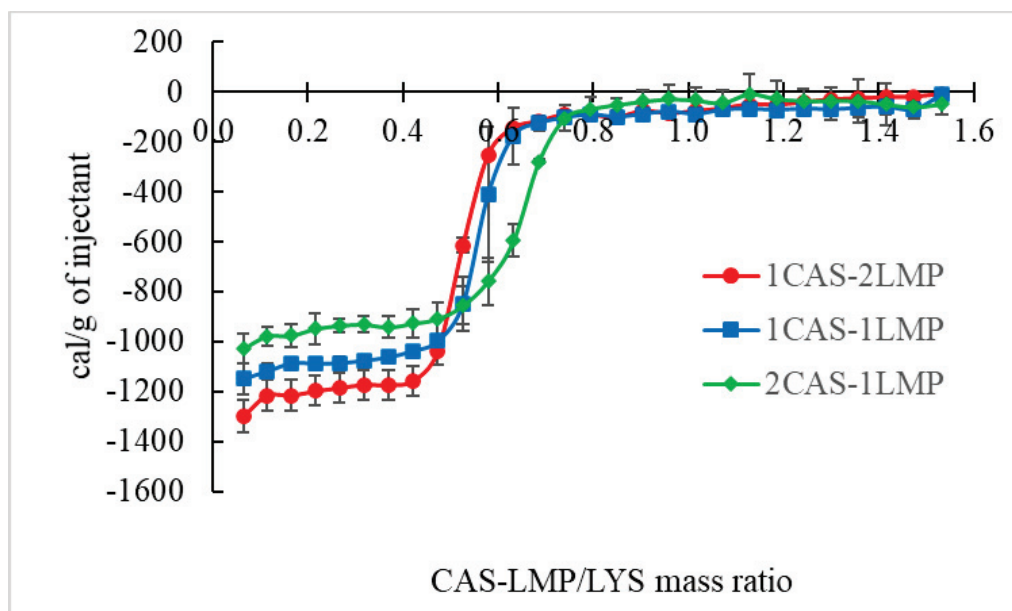


Figure 7.2. The ITC graphics of interaction between LYS and CAS-LMP mixtures at different CAS:LMP ratios (1:2, 1:1 and 2:1).

7.4.3. Zeta-potential of ternary complexes

As shown in Fig. 7.3, the zeta-potential of ternary complexes decreased with adding CAS-LMP mixtures at different mass ratios (1:2, 1:1 and 2:1) to LYS from ratio 0.2 to 1.4. According to our previous work (Wang et al., 2019), at pH 7.0, the zeta-potential value of LMP (-40 mV) is more negative than CAS (-20 mV). Therefore, the zeta-potential of ternary complexes changed more quickly when higher proportion of LMP in CAS-LMP mixtures. Basically, the zeta-potential value decreased with increasing proportion of LMP at all CAS-LMP/LYS ratios. At CAS-LMP/LYS ratio 0.2, the ternary complexes were almost neutrally-charged. According to CAS-LMP mixture composition, 1CAS-2LMP and 1CAS-1LMP cases were similar, the zeta-potential of ternary complexes significantly decreased with increasing CAS-LMP/LYS ratio from 0.2 (around 0 mV) to 0.6 (around -30 mV), after that, the decrease trend slowed down. Among the three tested cases, the 2CAS-1LMP case was significantly different from the other two cases, and showed the less change of the zeta-potential of ternary complexes with increasing CAS-LMP/LYS ratio. It was due to the less negative charges of CAS than which of LMP.

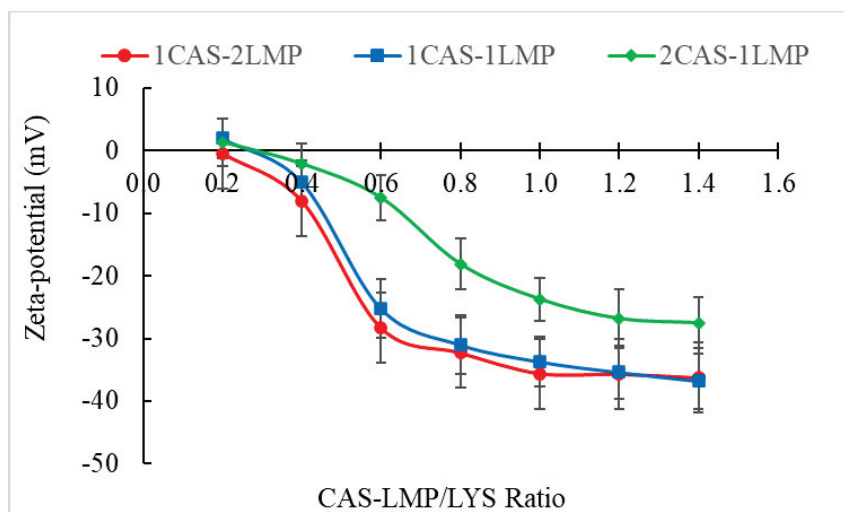


Figure 7.3. The zeta-potential of ternary complexes as a function of CAS-LMP/LYS ratio (the concentration of LYS is constant at 0.714 g/L in the complex system, the ratios of CAS-LMP mixtures are 1:2, 1:1 and 2:1).

7.4.4. Particle size of ternary complexes

The particle size results of ternary complexes were corroborated with previous results. As shown in Fig. 7.4, after adding the 1CAS-2LMP mixture to LYS, the particle size of ternary complexes significantly decreased from $55.54 \pm 0.87 \mu\text{m}$ at CAS-LMP/LYS ratio of 0.2 to $10.84 \pm 1.85 \mu\text{m}$ at CAS-LMP/LYS ratio of 0.6, and was almost constant after CAS-LMP/LYS ratio of 0.6. Similarly, for the 1CAS-1LMP case, the particle size of ternary complexes significantly decreased from CAS-LMP/LYS ratio 0.2 (but a higher value as $100.24 \pm 5.48 \mu\text{m}$) to 0.6 ($14.56 \pm 1.58 \mu\text{m}$) and was kept constant in a low value. The turning point at CAS-LMP/LYS ratio 0.6 was also observed in Fig. 7.1-7.3, which indicated the saturation of the binding sites in LYS with CAS-LMP molecules. Different from previous two cases, for the 2CAS-1LMP case, there was a maximum particle size ($86.87 \pm 1.33 \mu\text{m}$) observed at CAS-LMP/LYS ratio 0.4. Basically, the complexes would possess the maximum size when their surface charges were completely neutralized. In addition, LYS needs more CAS-LMP mixture to form neutrally-charged ternary complexes when CAS took higher proportion in CAS-LMP mixtures, which could be confirmed in Fig. 3. Therefore, the CAS-LMP/LYS ratio at which the particle size of ternary complexes was maximum would shift from higher CAS-LMP/LYS ratio with the increase of the CAS proportion in CAS-LMP mixture.

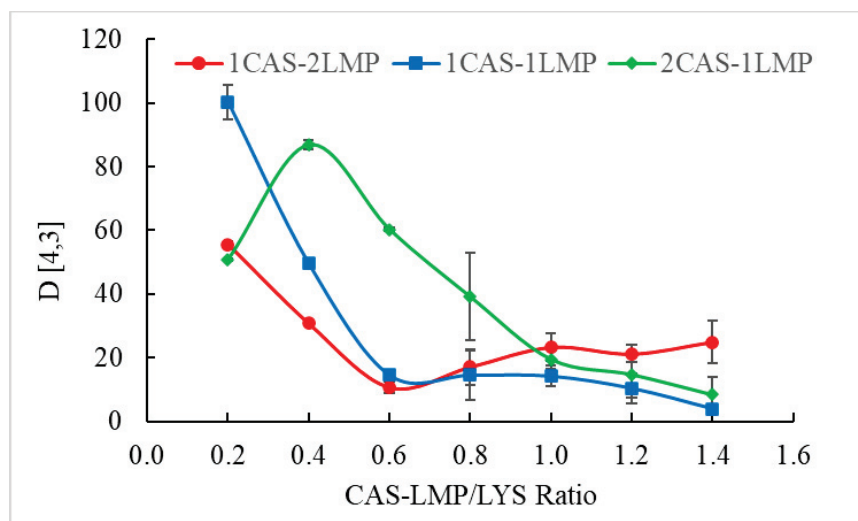


Figure 7.4. The particle size of ternary complexes as a function of CAS-LMP/LYS ratio (the concentration of LYS is constant at 0.714 g/L in the complex system, the ratios of CAS-LMP mixtures are 1:2, 1:1 and 2:1).

7.4.5. Activity of ternary complexes

The LYS activity of ternary complexes is shown in Fig. 7.5. As expected, LYS would lose its activity after binding with CAS-LMP mixture. Like our previous studies, after adding anionic biopolymers like CAS and LMP ([Bayarri et al., 2014](#)), the activity of LYS would firstly decrease to quite a low activity and recover with the continued addition of anionic biopolymers until a constant value. Carboxymethylcellulose was also found to affect the affinity between lysozyme and liposome, which caused the reduction of LYS activity ([Wang et al., 2020](#)). As shown in Fig. 7.5, the composition of CAS-LMP mixture had a significant impact on the activity of LYS in ternary complexes. The minimum activity of LYS in ternary complexes were different for three test cases. The minimum activity for the 2CAS-1LMP case was lowest (762 ± 47 U/mL), compared to the other two cases, which was found at CAS-LMP/LYS ratio 0.8. The LYS activity for the 1CAS-1LMP case was less affected, had a minimum value as 3129 ± 417 U/mL at CAS-LMP/LYS ratio 0.4, and recovered to 5121 ± 390 U/mL at CAS-LMP/LYS ratio 0.6. With the continued increase of CAS-LMP/LYS ratio, the LYS activity for the 1CAS-1LMP case was constant at around 5000 U/mL, which was significantly higher than the other two cases (around 3000 U/mL).

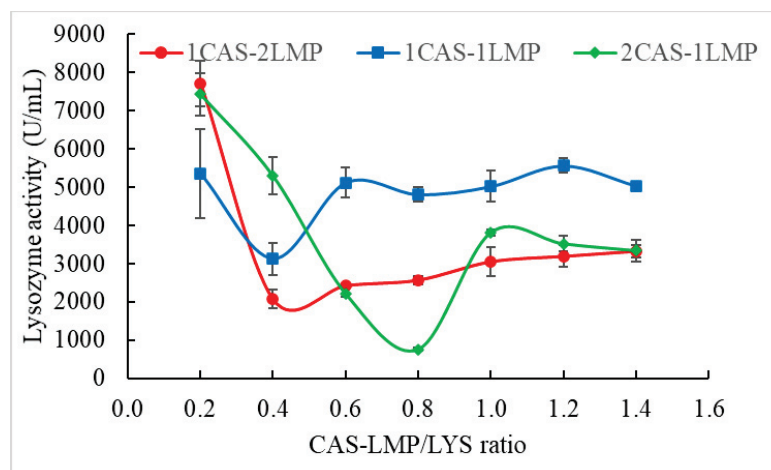


Figure 7.5. The activity of ternary complexes against *Micrococcus lysodeikticus* membranes as a function of CAS-LMP/LYS ratio (the concentration of LYS is constant at 0.714 g/L in the complex system, the ratios of CAS-LMP mixtures are 1:2, 1:1 and 2:1).

7.5. Conclusion

The present study investigated the formation of ternary complexes between CAS-LMP mixture (with different ratios) and LYS at pH 7.0. Depending on the CAS-LMP ratio, the ternary complexes had a different turbidity evolution curve as a function of CAS-LMP/LYS ratio, the higher the proportion of LMP, the faster the turbidity of ternary complexes increased; the higher the proportion of CAS, the slower the turbidity of ternary complexes decreased. This result indicates that both CAS and LMP participated in the interactions with LYS. ITC result showed that the interactions between CAS-LMP and LYS was mainly driven by electrostatic forces. LYS could be combined with more CAS-LMP as the proportion of CAS increased in CAS-LMP mixtures. In addition, the zeta-potential results showed that, with increasing CAS-LMP/LYS ratio from 0.2 to 1.4, the surface charge of the ternary complexes changed from nearly neutral to highly negative. As a consequence, the particle size of the ternary complexes also decreased. Finally, the LYS activity of ternary complexes would show a trough during the increase of CAS-LMP/LYS ratio, due to the coverage of active sites. With the continued increase of CAS-LMP/LYS ratio, the LYS activity of ternary complexes would gradually return to a stable level, due to the structural change of the ternary complexes. Among the three tested cases with different CAS-LMP ratios, the 1CAS-1LMP case had higher LYS activity. The present work provided useful information about the complexation behavior between CAS-LMP and LYS, and the subsequent effects on LYS activity, which could facilitate the potential application of LYS in dairy products containing thickeners like pectin for food preservation or the formed ternary complexes for the encapsulation of bioactive compounds.

References

- Antonov, Y. A., Zhuravleva, I. L., Celus, M., Kyomugasho, C., Lombardo, S., Thielemans, W., Hendrickx, M., Moldenaers, P., & Cardinaels, R. (2020). Generality and specificity of the binding behaviour of lysozyme with pectin varying in local charge density and overall charge. *Food Hydrocolloids*, 99, 105345.
- Ba, C., Fu, Y., Niu, F., Wang, M., Jin, B., Li, Z., Chen, G., Zhang, H., & Li, X. (2020). Effects of environmental stresses on physiochemical stability of beta-carotene in zein-carboxymethyl chitosan-tea polyphenols ternary delivery system. *Food Chemistry*, 311, 125878.
- Bayarri, M., Oulahal, N., Degraeve, P., & Gharsallaoui, A. (2014). Properties of lysozyme/low methoxyl (LM) pectin complexes for antimicrobial edible food packaging. *Journal of Food Engineering*, 131, 18-25.
- Croguennec, T., Tavares, G. M., & Bouhallab, S. (2017). Heteroprotein complex coacervation: A generic process. *Advances in Colloid and Interface Science*, 239, 115-126.
- Dai, L., Sun, C., Wei, Y., Zhan, X., Mao, L., & Gao, Y. (2018). Formation and characterization of zein-propylene glycol alginate-surfactant ternary complexes: Effect of surfactant type. *Food Chemistry*, 258, 321-330.
- de Kruif, C. G., Weinbreck, F., & de Vries, R. (2004). Complex coacervation of proteins and anionic polysaccharides. *Current Opinion in Colloid & Interface Science*, 9(5), 340-349.
- Eghbal, N., & Choudhary, R. (2018). Complex coacervation: Encapsulation and controlled release of active agents in food systems. *LWT - Food Science and Technology*, 90, 254-264.
- Liu, F., Ma, C., McClements, D. J., & Gao, Y. (2016). Development of polyphenol-protein-polysaccharide ternary complexes as emulsifiers for nutraceutical emulsions: Impact on formation, stability, and bioaccessibility of β -carotene emulsions. *Food Hydrocolloids*, 61, 578-588.
- Oliveira, A. L., von Staszewski, M., Pizones Ruiz-Henestrosa, V. M., Pintado, M., & Pilosof, A. M. R. (2016). Impact of pectin or chitosan on bulk, interfacial and antioxidant properties of (+)-catechin and β -lactoglobulin ternary mixtures. *Food Hydrocolloids*, 55, 119-127.
- Ormus, S., Oulahal, N., Noël, C., Degraeve, P., & Gharsallaoui, A. (2015). Effect of low methoxyl (LM) pectin complexation on the thermal and proteolytic inactivation of lysozyme: A kinetic study. *Food Hydrocolloids*, 43, 812-818.
- Wang, J., Dumas, E., & Gharsallaoui, A. (2019). Low Methoxyl pectin / sodium caseinate complexing behavior studied by isothermal titration calorimetry. *Food Hydrocolloids*, 88, 163-169.
- Wang, L., Li, L., Xu, N., Sun, W., Ding, B., Xu, W., & Li, Z. (2020). Effect of carboxymethylcellulose on the affinity between lysozyme and liposome monolayers: evidence for its bacteriostatic mechanism. *Food Hydrocolloids*, 98, 105263.
- Wang, M., Fu, Y., Chen, G., Shi, Y., Li, X., Zhang, H., & Shen, Y. (2018). Fabrication and characterization of carboxymethyl chitosan and tea polyphenols coating on zein nanoparticles to encapsulate β -carotene by anti-solvent precipitation method. *Food Hydrocolloids*, 77, 577-587.
- Wu, D., Ensinas, A., Verrier, B., Cuvillier, A., Champier, G., Paul, S., & Delair, T. (2017). Ternary polysaccharide complexes: Colloidal drug delivery systems stabilized in physiological media. *Carbohydrate Polymers*, 172, 265-274.
- Yang, J., Mao, L., Yang, W., Sun, C., Dai, L., & Gao, Y. (2018). Evaluation of non-covalent ternary aggregates of lactoferrin, high methylated pectin, EGCG in stabilizing beta-carotene emulsions. *Food Chemistry*, 240, 1063-1071.
- Yang, W., Xu, C., Liu, F., Sun, C., Yuan, F., & Gao, Y. (2015). Fabrication mechanism and structural characteristics of the ternary aggregates by lactoferrin, pectin, and (-)-

- epigallocatechin gallate using multispectroscopic methods. *Journal of Agricultural and Food Chemistry*, 63(20), 5046-5054.
- Yi, J., Huang, H., Liu, Y., Lu, Y., Fan, Y., & Zhang, Y. (2020). Fabrication of curcumin-loaded pea protein-pectin ternary complex for the stabilization and delivery of betacarotene emulsions. *Food Chemistry*, 313, 126118.

CHAPTER 8

GENERAL DISCUSSION, CONCLUSION AND PERSPECTIVES

8.1. General discussion and conclusion

Complex coacervation between proteins and polysaccharides has been investigated and applied in practice for several decades. Overall, the two oppositely-charged biopolymers commonly consist of an anionic polysaccharide and a positively-charged protein. In this situation, the solution pH should be lower than the isoelectric point of the protein. In the opposite situation, complex coacervates could consist of a cationic polysaccharide (like chitosan and its derivatives) and a negatively-charged protein, therefore, the solution pH should be higher than the isoelectric point of the protein. Considering that chitosan is only soluble at acidic pH, the pH range for the formation of complex coacervates with a cationic polysaccharide and a protein is normally limited between pH 4.0 and pH 6.5, which could limit its application. Besides that, the availability and function of biopolymers are also important factors. Therefore, choosing a proper pair of proteins and polysaccharides is important for complex coacervation.

In our work, sodium caseinate (CAS) and low methoxyl pectin (LMP) were chosen as the studied models in complex coacervation between proteins and polysaccharides, because this biopolymer system can well reflect the phenomena that exist in the complexation between proteins and polysaccharides. Through observing the phase behavior, we found that pH affects the form of CAS/LMP mixtures. During pH shift from neutral pH to acidic pH, co-soluble mixtures will aggregate to form soluble complexes, and the complexes further become insoluble. Through measuring zeta-potential of each biopolymer, the charge of CAS changes from negative to positive with pH decreasing, due to the protonation of amino groups of the protein. Furthermore, the results from isothermal titration calorimetry (ITC) revealed that there are no interactions between CAS and LMP at neutral pH, weak interactions were observed in soluble complexes and strong ones were observed in insoluble complexes. Besides the effect of pH, increasing ionic strength can shield the electrostatic interactions between CAS and LMP, which is in accordance with other literatures. Importantly, temperature plays an important role during the formation of complexes between the two biopolymers. Our results showed that higher

temperature enhances the interaction intensity, which is not fit with the common opinion that temperature has no significant effect on electrostatic forces. We assume that increasing temperature could change the structure of biopolymers, which exposes more charged sites for electrostatic bonding. In summary, we have identified the optimum conditions for CAS/LMP complexation.

For the encapsulation of hydrophobic molecules, preparation of an emulsion is indispensable. The application of complex coacervates in emulsion preparation can follow two strategies: stabilization of emulsions by protein/polysaccharide complexes formed in advance, and stabilization by protein firstly followed by adding polysaccharide (Layer-by-Layer method). Inherited from previous research, the complexation between CAS and LMP is strongest at pH 3.0, both emulsion preparation strategies are operated at this pH with the same CAS concentration (5 g/L). The emulsions stabilized by complexes formed in advance and layer-by-layer method were characterized by measuring zeta potential, dynamic viscosity, serum index, and particle size distribution. The results showed that, at low LMP concentrations, complexes-stabilized emulsions were more stable than LBL-stabilized ones, while at high LMP concentrations, LBL-stabilized emulsions showed better stability.

Otherwise, spray-drying is the most common technique for preparing microcapsules. However, the shearing forces in the atomization step and the heat exchange during the dehydration process have a significant impact on the protein/polysaccharide complexes. Therefore, we have investigated the influence of atomization (spraying step) and heat treatment (during the dehydration step) on the molecular interactions between CAS and LMP. To study these two steps separately, we utilized the spraying system in the spray-drier without heating. To simulate the heating process, we heated the sample solutions in a water bath at a temperature corresponded to outlet air temperature. We have to admit that the effect of heating process during the dehydration step was not totally the same with the heating process in water bath. However, it is an original test, we didn't find a better way. The results showed that the spraying step had a significant effect on the charge and the size of the complexes. In fact, the application of the atomization resulted in the dissociation of CAS/LMP aggregates especially for high LMP concentrations. Importantly, through the analysis of the surface hydrophobicity of CAS, our results indicated that complexation with high concentrations of LMP is able to protect the structure of the protein against heat denaturation.

Besides the theoretical results, from a practice point, we chose citral as a typical hydrophobic active molecule to be encapsulated with our previous studied CAS/LMP system, and obtained microcapsules encapsulating citral through spray-drying. To validate the

protection mechanism of high LMP concentrations during the spray-drying process, we prepared the emulsion stabilized by CAS alone (Monolayer emulsion) as control. Combined with our previous results concerning the higher stability of Layer-by-Layer stabilized emulsions than complexes stabilized emulsions at high concentrations of LMP, we chosen Layer-by-Layer (LBL) method as the emulsion preparation strategy. After spray-drying, we obtained the final product as spray-dried microcapsules encapsulating citral. As we expected, higher encapsulation efficiency was found in microcapsules prepared with LBL method at both the two tested proportions of citral. The antimicrobial tests of spray-dried microcapsules further confirmed the importance of the addition of LMP.

For the encapsulation of hydrophilic active molecules, lysozyme (LYS) was chosen as the studied model. Therefore, we also investigated the heteroprotein complex coacervation between CAS and LYS. Considering the optimum pH of LYS activity is neutral, all the complexes were prepared at pH 7.0. We have investigated the interactions within heteroprotein complexes through turbidity, particle size, zeta potential and ITC analysis. Our results showed that the CAS/LYS ratio had a highly effect on the formed CAS/LYS complexes, especially at CAS/LYS ratio 1.0. With CAS/LYS ratio increase to 1.0, the heteroprotein coacervates dissociated to small particles (from $\sim 100\ \mu\text{m}$ to $\sim 1\ \mu\text{m}$), this was accompanied by a trough of LYS activity. We assumed that at this special CAS/LYS ratio, the hydrolytic active site of LYS was fully covered by CAS. Therefore, the heteroprotein coacervates at CAS/LYS ratio 1.0 were further spray-dried in the presence of maltodextrins. The release of LYS encapsulated in microcapsules was controlled through adding calcium ions, the activity of LYS was restored to more than 80% of its initial activity. This result proved that the formed heteroprotein coacervates can protect LYS against the heat stress during spray-drying operation, which could facilitate the encapsulation of LYS.

In the final part, inspired by the previous work, we continued to investigate the interactions between LYS and CAS-LMP co-soluble mixtures at pH 7.0, and ternary complexes composed of CAS, LMP and LYS were prepared. According to our previous researches, both CAS and LMP could interact with LYS at pH 7 through electrostatic forces, there are no interactions between CAS and LMP. Therefore, we designed ternary complexes by adding CAS-LMP co-soluble mixtures to LYS, and studied the effect of CAS/LMP ratio in CAS-LMP mixtures on the complexation between LYS and CAS-LMP mixtures. Our results showed that the ternary complexes were formed through electrostatic forces. With adding negatively-charged CAS-LMP mixtures to LYS, the ternary complexes would dissociate into small particles as the negative charges increasing, however, higher proportion of CAS in CAS-LMP mixtures could

slow this process. Through measuring the LYS activity of ternary complexes, the ternary complexes prepared by CAS-LMP mixtures with the same proportion of CAS and LMP possessed the most stable LYS activity with adding CAS-LMP mixtures. This work provided useful information about the complexation behaviors between CAS-LMP and LYS, and the subsequent effects on LYS activity, which could facilitate the potential application of LYS for dairy food contained thickeners like pectin or the formed ternary complexes for the encapsulation of bioactive compounds.

In summary, complex coacervation between proteins and polysaccharides was investigated to understand the role of each biopolymer in these interactions. These specific complexation behaviors were applied for encapsulating bioactive molecules, including hydrophobic and hydrophilic molecules.

8.2. Perspectives

There are some aspects for further exploration in future works:

- 1) Some other hydrophobic bioactive molecules can be encapsulated by our studied encapsulation systems, and studies can be focused on the effect of encapsulated compounds on the properties of emulsions, microcapsules or films.
- 2) The emulsion stability as effected by encapsulated compounds and environmental stress such as pH, ionic strength and heating can be explored.
- 3) The chemical stability of citral in microcapsules can be further explored by chemical analysis, especially for the effect of environmental conditions (like temperature, moisture...) during the storage in different environments.
- 4) Some other techniques like CD, NMR, FTIR, X-ray, DSC can be applied for studying the complexation between biopolymers and encapsulated molecules.
- 5) The release behavior of encapsulation systems in different environments, like food/drug matrices, simulated gastrointestinal tract (GIT) system, or food packaging... can be explored.